

Enlightening cities: Design for natural rhythm

A framework for measuring the impact of facade- and city lighting design on circadian rhythm

MSc Architecture, Urbanism & Building Sciences; Building technology

Maartje Damen

Enlightening cities: Design for natural rhythm

A framework for measuring the impact
of facade- and city lighting design on
circadian rhythm

By

Maartje Damen

To obtain the degree of Master of Science
In Architecture, Urbanism and Building Sciences
Track Building Technology
At Delft University of Technology,
To be defended 28th of October 2024

Student number: 4716736
Architectural Engineering and Technology;
Climate design & 3D geoinformation

Thesis committee:
Nima Forouzandeh Shahraki, Climate design
Eleonora Brembilla, Climate design
Giorgio Agugiaro 3D Geoinformation
Monica Veras Morais, Delegate examiner

© 2024 Maartje Damen.

Cover picture: Amsterdam city centre, visualized at night. Noticeable is the high amount of artificial lighting, placed close to buildings and windows. (Frank Doorhof, 2015)

Preface

I would like to express my gratitude towards the people that helped me make this thesis project possible. I want to thank Eleonora and Giorgio, for their expertise and their insightful perspectives during this process. I want to thank Nima, who has been such a dedicated supervisor for this project and whom I could ask for help, feedback or a brainstorm session, and who was also there when I had trouble seeing the bigger picture. Thank you for your encouraging words.

Furthermore, I want to thank Olga and Sylvia, not only for your help and good advice when commencing this thesis project next to my rowing career, but also for the years before, where you have always helped me find a way to perform successfully in both of these parts in my life.

Lastly, I would like to thank the people close to me: Thanks for getting me away from my laptop every now and then, chatting in the kitchen over a cup of coffee, finding new, better study places or providing a place of comfort.

With handing in this work, I will not only look back on a successful career as an athlete, but also as an architecture and a building technology student: having been able to join the creative, the intellectual, and the physical in such a formative part of my life is something I would wish for everyone; it has been a rollercoaster, it has been such a gift.

Abstract

As living in urban environments increases, the impact of city design on the health of individuals becomes more relevant. Cities have shown to negatively affect individuals' circadian health. This thesis investigates the influence of façade and city lighting design on indoor circadian lighting availability, addressing the increasing prevalence of circadian disruption in cities caused by poor daylight access and excessive artificial light exposure.

The research introduces a workflow that evaluates how façade designs and urban lighting choices affect circadian light exposure within homes based on open data sources. By creating a tool capable of simulating these effects for individual floor levels on an urban scale, the study provides a method to assess and optimize architectural and urban design for circadian health with public information in a large-scale manner.

The results aim to bridge the gap between available 3D urban data and practical applications, offering design strategies that improve indoor circadian lighting availability and contribute to healthier urban living environments.

Key findings prove the misalignment of indoor circadian lighting availability with human needs in cities, and show the importance of window size, floor level and façade orientation in mitigating circadian disruption caused by the urban context. Next to that, it shows the negative impact city lighting has on indoor circadian health, for which design suggestions are done

Nomenclature

List of figures

Figure 1-1 the wavelengths (Blume et al., 2019).....	14
Figure 1-2 Seasonal variation in dim-light melatonin onset (DLMO), sleep timing, and their phase angle relationship. Legend: DLMO (gray), sleep onset (blue), sleep offset (green), day length (yellow) (Zerbini et al., 2021)	15
Figure 1-3 circadian sensitivity over a 24-hour cycle (Andersen et al., 2012).....	16
Figure 2-1 Uncertainties related to context variability and space properties integrated in a relationship map between measurable (scientific) parameters and design elements (Andersen et al., 2012).....	22
Figure 2-2 The four nodes affecting the receipt of circadian light from a daylight source (Ghaeili Ardabili et al., 2023).	23
Figure 2-3 factors impacting the circadian lighting availability	23
Figure 2-4 variation in transmittance between two windows with similar T_{vis} (Ardabili et al., 2023)	25
Figure 2-5 spectral power distribution for three CIE daylight illuminants, alongside photopic ($V(\lambda)$) and circadian ($C(\lambda)$) sensitivity curves (Andersen et al. 2012)	27
Figure 2-6 Key-value pairs for CityJSON (CityJSON specifications, 2019)	30
Figure 2-7 explanation Levels of Detail (LoD) (Biljecki et al., 2016).....	31
Figure 2-8 facade steps from google Streetview (top), façade masks (middle) to LoD 3.1 (Eijgenstein, 2020)	31
Figure 3-1 factors impacting the circadian lighting availability	37
Figure 3-2 Examples of facade masks (eijgenstein, 2020)	39
Figure 3-3 Buildings with available façade information (own source)	40
Figure 3-4 Left: clustering of the windows, based on upper and lower window boundary. Right: estimated floor & ceiling levels.....	40
Figure 3-5 Left: building centre & retrieved street-point vector. Right: facades visible from the projection-plane.....	41
Figure 3-6 selection of window plane, per floor level (level 3 selected)	42
Figure 3-7 the street-point vector forms the basis for a projection plane;	42
Figure 3-8 SPD artificial light inputs, normalized by the area under curve (A.U.C.).....	46
Figure 3-9 Normalized spectral efficiency curves for photopsin, melanopsin, and neuropsin and the 9-channel divisions (Jung et al., 2023).....	46
Figure 3-10 Spectral electric light source definition; the LARK SPD, the melanopic coefficient and the resulting SPD distribution, normalized (own source).....	47
Figure 3-11 Test building with no building context, in context LoD 1.2 and in context LoD 2.2 (top to bottom).....	48
Figure 3-12 Spectral distributions relevant for m-EDI post-processing (data LARK, visualisation own source)	49
Figure 3-13 LARK 9-bin irradiance calculation to Melanopic EDI (own source).....	50
Figure 4-1 Building context on a high (2.2) level of detail added	51
Figure 4-2 Surface water, green areas & street lighting positions, translated from GIS to Rhino	51
Figure 4-3 Examples of facades with lack of window information (Eijgenstein, 2020)	53
Figure 4-4 The three facade mask with a high warning count, due to low level heights and negative WWR (Eijgenstein, 2020 with adaptations)	53
Figure 4-5 comparison of original facade pictures with the façade masks, displaying retrieved window boundaries and estimated floor levels (Eijgenstein, 2020 with adaptations).....	55
Figure 4-6 large-scale floor level splitting.....	56

Figure 4-7 Floor level splitting returned similar results for the large-scale assessment as for the 5-buildings	58
Figure 4-8 Selection of window plane, per floor level (level 3 selected).....	58
Figure 4-9 Split level buildings, visualized side by side with google maps 3D image (google, 2024)	59
Figure 4-10 Single floor test (left) single building test (right), visualised in their urban context (bottom).....	60
Figure 4-11 LARK post processing.....	61
Figure 4-12 Consistency tests of radiance 9-channel calculation (top: consistency test of daylight. Bottom: consistency test of artificial light)	62
Figure 4-14 The impact of various IES inputs on the circadian lighting availability	63
Figure 4-14 The impact of weighing factors on circadian lighting availability	63
Figure 4-15 m-EDI result variations for different SPDs	64
Figure 4-16 Sky visualisations.....	65
Figure 4-17 Comparison in daylight availability measurements for two contextual levels of detail (LoD1.2, LoD2.2)	67
Figure 4-18 Correlation between WWR and m-EDI (average of all measurements for a year per floor level).....	67
Figure 4-19 Design factors potentially affecting circadian lighting results	68
Figure 4-20 Visualisation of ALAN simulated for the selected buildings.....	69
Figure 5-1 Four versions of boundary reconstruction are needed to find correct window placement for different façade orientations	77
Figure 5-3 Extracting window boundaries shows good results.	77
Figure 5-2 When using the make2D algorithm a false façade edge is taken into account.....	77
Figure 5-5 invalid geometry	78
Figure 5-6 measurement point outside of the building	78
Figure 6-1 factors impacting the circadian lighting availability	83
Figure 7-1 selected streets: Willemstraat, Haarlemmerdijk, Boomstraat, Eerste Boomdwarsstraat (Google, 2023)	89

List of tables

Table 1 Table 1 WELL metric for melanopic light intensity in living environments	19
Table 2 WELL metric for circadian emulation in living environments.....	19
Table 3 Prescribed interior reflectance values (EN 17037, 2018 and Koster, 2020)	24
Table 4 Urban geometrical and geographical information, source overview	38
Table 5 IES electric light source photometric specifications.....	45
Table 6 Building selection and window construction visualised (google maps, 2024 and own source)	57
Table 7 single building test: impact of IES light source and weighing factors	63

Abbreviations

Abbreviation	Measurement Unit	Definition	
3DBAG			3D Building model dataset based on Dutch cadastral data used for urban modelling and analysis in the Netherlands
AHN		Actueel Hoogtebestand Nederland	a detailed elevation dataset of the Netherlands
ALAN		Artificial Light At Night	used in studies of light pollution and its effects on the environment and human health
API		Application Programming Interface	a set of protocols for building software applications
AUC		Area Under Curve	A technique used to standardize and evaluate different data distributions in analysis.
BAG		Basisregistratie Adressen en Gebouwen	the Dutch national database of addresses and buildings
BGT		Basisregistratie Grootchalige Topografie	a topographical mapping system used in the Netherlands
BREP		Boundary Representation	a mathematical method used in 3D modeling
CAD		Computer-Aided Design	software used for precision drawings or technical illustrations
CBTmin	°C	Core Body Temperature minimum	often used in circadian rhythm studies
CCT	Kelvin (K)	Correlated Colour Temperature	used to describe the colour appearance of light
CIE		International Commission on Illumination	setting standards for light and colour
CityGML			A 3D city model data format used for urban planning and simulations
CityJSON			JSON encoding for CityGML data used for simplifying 3D city models
CityObjects			3D objects within a city model used in CityGML and CityJSON
CLA		Circadian Light Administration	a measure of light's biological effects on human rhythms
CS		Circadian Stimulus	a measure of light's effectiveness in stimulating the circadian system
CSV		Comma-Separated Values	a text format for storing tabular data
DF	Ratio (0-1)	Daylight Factor	a metric for assessing indoor daylight availability

DHI	Watts per square meter (W/m ²)	Diffuse Horizontal Irradiance	solar radiation received indirectly
DLMO	Time (h)	Dim Light Melatonin Onset	the time when melatonin levels rise in dim light
DNI	Watts per square meter (W/m ²)	Direct Normal Irradiance	solar radiation received directly from the sun
DXF		Drawing Exchange Format	a CAD file format for data interoperability
EDI	lux (lx)	Equivalent Daylight Illuminance	a measure of daylight's biological effects
EML		Equivalent Melanopic Lux	measuring light's impact on melanopic photoreceptors
EN		European Norm	a standard from the European Committee for Standardization
EPSG		European Petroleum Survey Group	code for identifying coordinate reference systems
FSI	Ratio (0-1)	Floor Space Index	also called Floor Area Ratio used in urban planning
GeoJSON			A format for encoding geographic data structures using JSON
GIS		Geographic Information System	for gathering and analysing spatial data
HSV		Hue Saturation Value	a colour model describing colour characteristics
IES		Illuminating Engineering Society	an organization setting lighting standards
ipRGCs		Intrinsically photosensitive Retinal Ganglion Cells	Cells influencing circadian rhythms
IWEC		International Weather for Energy Calculations	weather data for building energy simulations
LIDAR		Light Detection and Ranging	a method of remote sensing for Earth surface analysis
LoD		Level of Detail	referring to the complexity in 3D modeling and representation
m-EDI	lux (lx)	Melanopic Equivalent Daylight Illuminance	measuring melanopic stimulation
NEN			Dutch Standardization Institute developing standards in the Netherlands
NEN-EN			Dutch and European standards applied in the Netherlands and Europe
OGC		Open Geospatial Consortium	creating open standards for geospatial data
OpenCV		Open-Source Computer Vision	a library for real-time computer vision tasks
PDOK		Publieke Dienstverlening Op de Kaart	a Dutch geodata service providing access to geographic data
QGIS		Quantum Geographic Information System	an open-source GIS platform

R-CNN		Region-based Convolutional Neural Network	used in machine learning for image recognition
RGB		Red, Green Blue	a colour model for electronic displays
RhinoCityJSON		A plugin for Rhino to work with CityJSON data	used in 3D urban modeling
SCN		Suprachiasmatic Nucleus	the brain region controlling circadian rhythms
SI		International System of Units	the modern metric system of measurement
SPD		Spectral Power Distribution	representing light's power as a function of wavelength
SpectralDB		A database for storing spectral data	used in lighting simulations
Tvis	Ratio (0-1)	Visible Transmittance	the fraction of visible light transmitted through a material
WELL		WELL Building Standard	a certification system for promoting health in built environments
WFR	Ratio (0-1)	Window-to-Floor Ratio	comparing window area to floor area in daylighting
WFS		Web Feature Service	serving geographic features over the web
WMS		Web Map Service	serving map images over the web
WWR	Ratio (0-1)	Window-to-Wall Ratio	comparing window area to wall area in buildings

Table of Contents

Preface	4
Abstract	5
Nomenclature	6
List of figures	6
List of tables.....	7
Abbreviations	8
1. Introduction	14
1.1. Perceiving circadian light.....	14
1.1.1. Impact of architectural design on lighting availability	16
1.2. Research gap & problem definition.....	17
1.3. Research questions	17
1.3.1. Objectives	17
2. Theoretical framework: Quantifying the impact of the built environment on circadian health.....	18
2.1. How can we quantify circadian health impact?.....	18
2.1.1. Designing for light: Rules & regulations	18
2.1.2. Measuring circadian lighting impact.....	20
2.2. Factors affecting circadian light availability in existing buildings	22
2.2.1. Recipient.....	24
2.2.2. Interior spatial and spectral characteristics.....	24
2.2.3. Windows optical characteristics	25
2.2.4. Façades: light blocking, orientation	25
2.2.5. Urban context reflectance	26
2.2.6. Urban building context	26
2.2.7. Light source	26
2.3. Calculating light in urban context: implementation of knowledge in lighting analysis tools 28	
2.3.1. Lighting analysis tools	28
2.3.2. The preparation of a digital Modelling for lighting simulation	29
2.3.3. Urban context Data in Rhino Grasshopper	29
2.3.4. Digital building models on urban scale	30
2.3.5. Other factors in the lighting simulation.....	32
2.4. Summary and synthesis of findings	33
3. Methodology.....	36
3.1. Phase 1: Preparing urban geometrical and geographical information.....	37
3.1.1. Data pipeline.....	38
3.1.2. 3D building data.....	38

3.1.3.	Conclusion	39
3.2.	Phase 2: Extraction of building window and floor level information from façade pictures	40
3.2.1.	Clustering algorithm	40
3.3.	Phase 3: Window boundary reconstruction in 3D environment	41
3.3.1.	Preparation of analysis volumes	41
3.3.2.	Floor-level splitting	41
3.3.3.	Systematic façade element selection	41
3.3.4.	Relative window placement	42
3.4.	Phase 4: Lighting modelling	43
3.4.1.	Model preparation	43
3.4.2.	Daylight	44
3.4.3.	Artificial light	45
3.4.4.	LARK circadian lighting simulation	46
3.4.5.	Simulation scenarios	47
3.5.	Running the simulation	48
3.5.1.	Test runs	48
3.5.2.	Iterative running	48
3.5.3.	Calculating m-EDI	49
4.	Results	51
4.1.	Phase 1: geo information data preparation	51
4.1.1.	Description of output files	52
4.2.	Phase 2: Façade masks to dataset	52
4.2.1.	Performance of the façade clustering algorithm	52
4.2.2.	Description of output files	54
4.3.	Phase 3: 3D window reconstruction by projection	54
4.3.1.	Description of output files	58
4.4.	Phase 4: Lighting modelling	60
4.4.1.	Consistency tests	61
4.4.2.	Lighting inputs	62
4.4.3.	The role of the design factors on circadian lighting availability	66
4.4.4.	General circadian lighting results	68
5.	discussion	70
5.1.	Interpretation of results	70
5.1.1.	Design factors affecting circadian lighting availability	72
5.1.2.	What design recommendations can be derived from the assessment of the impact of façade design and lighting design on circadian health in urban context?	73
5.2.	limitations	74

5.2.1.	Phase 1.....	74
5.2.2.	Phase 2.....	75
5.2.3.	Phase 3.....	77
5.2.4.	Phase 4.....	78
5.3.	future research	79
5.4.	design implications	80
5.4.1.	urban planning	80
5.4.2.	architectural design.....	80
5.5.	Scientific implications.....	81
6.	Conclusion	82
6.1.	Problem summary.....	82
6.2.	Key findings	82
6.2.1.	Design factors affecting circadian health	82
6.2.2.	Simulating the impact of façade design and urban lighting design.....	83
6.2.3.	Design recommendations based on impactful design factors in urban context 83	
7.	Appendices	85
7.1.	Workflow building preparation (phase 1, 2, 3).....	85
7.2.	Workflow circadian lighting analysis (phase 4).....	86
7.3.	Material library	87
7.4.	Example result phase 2	88
7.5.	Test simulation setup	89
7.6.	Results per building	Error! Bookmark not defined.
8.	Bibliography	94

1. Introduction

Space scarcity in urban environments affect the quality of living that is feasible within these areas. One of the implications regards the reduction of daylight availability in indoor environments. Circadian rhythm, the body's internal clock regulating sleep-wake cycles, is highly influenced by light exposure. This scarcity has significant health implications, as exposure to natural daylight is crucial for regulating circadian rhythms and supporting overall well-being. Inadequate daylight has been linked to sleep disturbances, mood disorders, and metabolic issues.

Additionally, the widespread use of artificial light, especially at night, can disrupt the body's internal clock, a phenomenon known as chronodisruption. This misalignment, caused by excessive artificial light exposure, has been associated with sleep disorders, cardiovascular problems, and other health risks. Addressing these challenges and providing design implications through urban planning could promote healthier living environments. For this, the understanding of the impact of light on human wellbeing must be understood, and after that, the impact of the urban environment on this availability will be researched.

1.1. Perceiving circadian light

What we perceive as light is not based on a fundamental physical meaning but is the receptivity of the human eye for electromagnetic radiation. The human eye has evolved to optimize the use of solar radiation: The visual band of the electromagnetic spectrum is also the band of wavelengths that are the strongest in the solar radiation that reaches the Earth. (Tregenza & Wilson, 2011) The visual band is a combination of Photopic vision and Scotopic vision: The three types of cone opsins (cyanolabe, chlorolabe, erythrolabe) providing photopic vision (daylight) and the rod opsin providing scotopic vision (dim light). A more recent breakthrough is the discovery of intrinsically photosensitive retinal ganglion cells (ipRGCs), containing the fifth photopigment melanopsin. These ipRGCs mediate most effects of light on the circadian clock, receiving information from the melanopsin photopigment and from the rod and cone

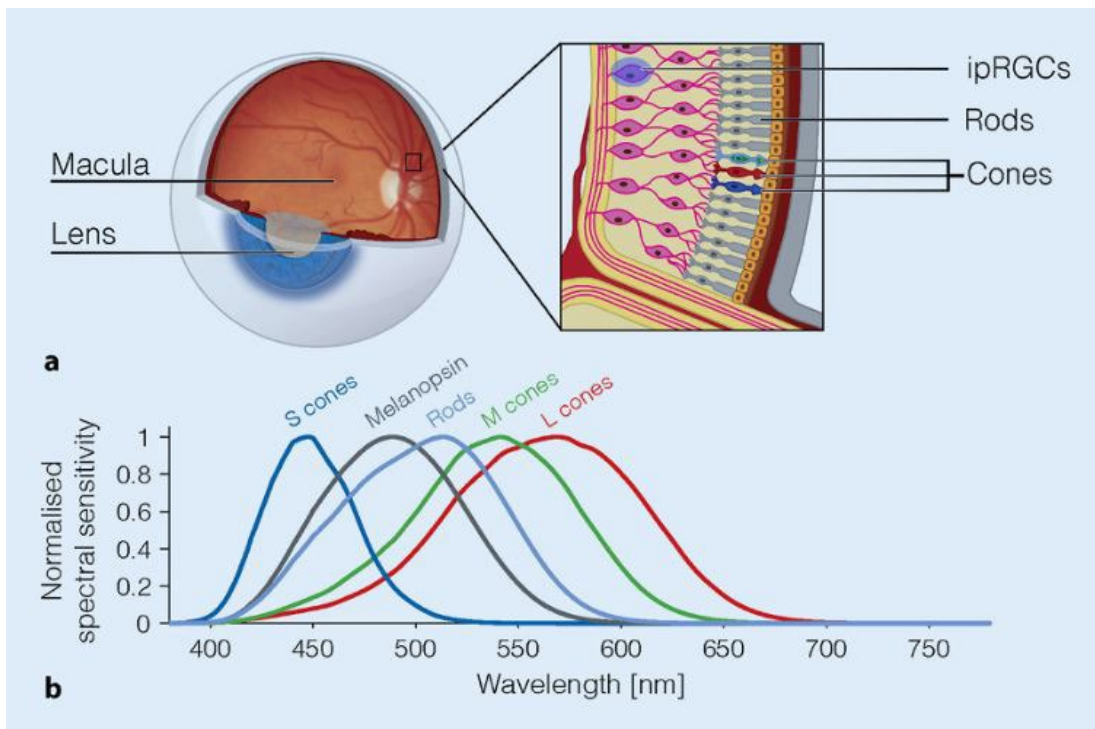


Figure 1-1 the wavelengths (Blume et al., 2019)

receptors, integrating information regarding the light environment. As is shown in the picture, melanopsin is most sensitive to the absorption of the shorter wavelengths within the light spectrum. These ipRGCs receive this sum of light information and communicate this with the suprachiasmatic nuclei (SCN). The SCN is considered the central "body clock", in mammals: Our circadian pacemaker. (Blume et al., 2019)

A strong connection has been found between the non-visual effects of light, health, and well-being. A lack of stimuli can negatively affect physical and mental health, interrupting the human body's circadian rhythm and leading to issues such as depression and sleep disruption (Anaraki et al., 2023). Circadian rhythm is not only founded in the availability of circadian light, but other factors also that affect this are found in biological and lifestyle processes:

- Biological processes: body temperature, blood pressure, hormone secretion, gene expression, and immune functions.
- Lifestyle processes: eating habits, work schedules, travel, social engagements etc.

(Cable et al., 2021)

For healthy circadian rhythm, the circadian phase is to be as consistent as possible, as the evolution of humans have taken place predominantly in areas with stable diurnal patterns of light and dark (Beute & Aries, 2023). This availability of daylight over the year in a more instable pattern as the Netherlands could have considerable implications. (Wirz-Justice et al., 2021).

Especially the long-term effects of circadian lighting availability are hard to define, but the direct impact of light on circadian rhythm has been captured by researchers with phase response curves (Xu et al., 2022). By gathering the information of phase change during the 24-hour time period, the fluctuation in responsivity to certain types of light over the course of 24 hours are being understood.

For the circadian phase, markers such as the lowest core body temperature (CBTmin; Andersen et al., 2012) and dim light melatonin onset (DLMO; Ohashi et al., 2023)) are being used to define the start of a 24 hour cycle, and define the responsivity of the body to circadian light on the biological rhythm. At certain points in time, the body is more sensitive for certain

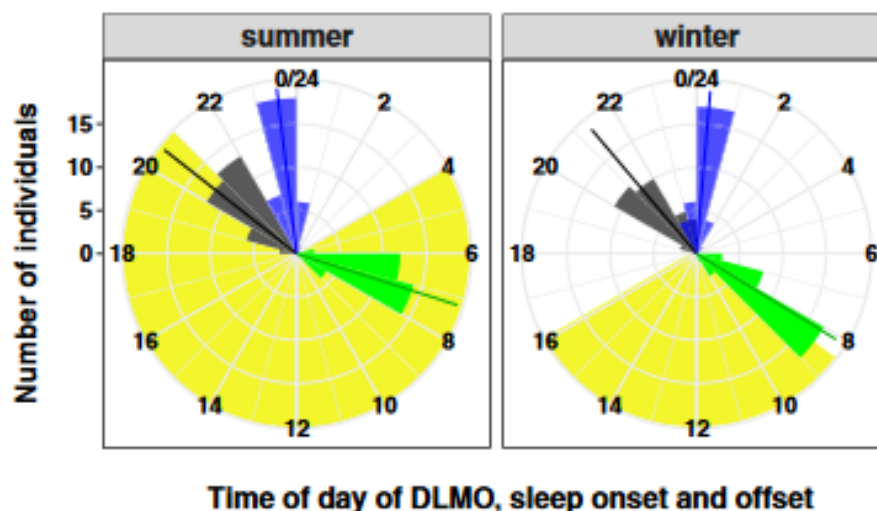


Figure 1-2 Seasonal variation in dim-light melatonin onset (DLMO), sleep timing, and their phase angle relationship. Legend: DLMO (gray), sleep onset (blue), sleep offset (green), day length (yellow) (Zerbini et al., 2021)

wavelengths, and this weighed to the availability of light results in positive or negative phase change.

Zerbini et al. (2021) studied the relationship between the photoperiod (daytime) and DLMO, and found that the relationship with DLMO (visualised in Figure 1-2) is much stronger with mid-day than it is with the day-to-night transition (twilight). Thus, both the amount of daylight available mid-day as the consistency of daylight availability in day-night transitions are of significance for a healthy circadian entrainment.

Morning exposure to light within the melanopic spectrum advances the circadian phase, while evening exposure delays it. Additionally, mid-day circadian light availability has been found to promote more consistent night-time sleep.

1.1.1. Impact of architectural design on lighting availability

The availability of circadian lighting is shown to be affected by design: Urban planning strategies significantly determine the possibility to receive solar irradiation in buildings (Lopez et al., 2016), window size and availability has been proven to negatively affect sleep duration, sleep disturbances and sleep impairments (Ghaeili Ardabili et al., 2023), and high levels of artificial light have been found to correlate with later weeknight bedtime in humans when exposed to it at night (Paksarian et al., 2020). These disruptions could be a serious contributor to some of the bigger health concerns of our times (Gaston & Sánchez De Miguel, 2022)

Designers carry the responsibility to design cities that not only minimize impact on environmental damage, but also to minimize health and emotional consequences on its inhabitants. By integrating circadian health principles into urban planning and building design, they can help mitigate the adverse effects of disrupted sleep and light exposure, contributing to the overall well-being and quality of life for city inhabitants. Thus, taking circadian health into consideration is essential.

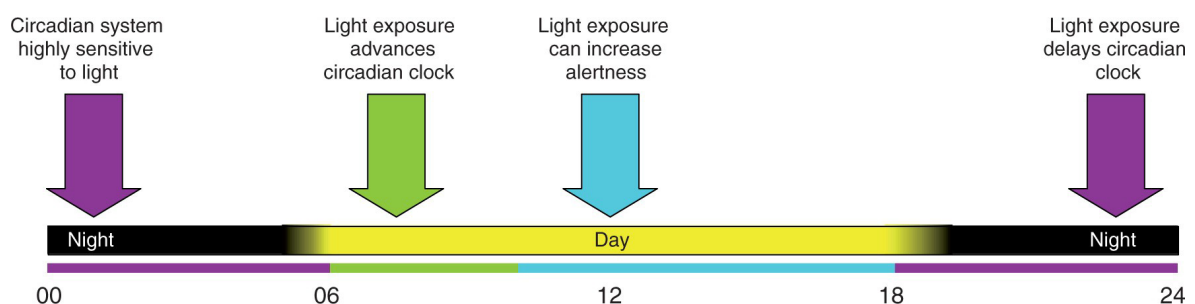


Figure 1-3 circadian sensitivity over a 24-hour cycle (Andersen et al., 2012)

1.2. Research gap & problem definition

Despite the well-known health benefits of natural daylight, current architectural and urban design practices often neglect circadian lighting requirements. This oversight has led to increased circadian disruption, particularly in urban environments, where natural daylight is frequently blocked, and artificial light at night (ALAN) is overabundant. This gap can be attributed to both a lack of regulatory measures and insufficient understanding of the biological effects that circadian lighting has on individuals. Additionally, the implications of inadequate circadian lighting, resulting from urban design and architecture, are often overlooked.

Existing tools for circadian lighting analysis lack sufficient integration into design workflows, and there is a clear disconnect between scientific knowledge and its application in urban contexts. The challenge lies in bridging this gap to allow for the comprehensive evaluation of lighting design's impact on circadian health. Bridging this gap is essential for creating healthier living environments, as it enables designers to implement evidence-based strategies that not only enhance daylight availability but also mitigate the adverse effects of ALAN. By prioritizing circadian health within urban planning, we can foster spaces that support the physiological needs of inhabitants and contribute to a higher quality of life in our cities.

1.3. Research questions

This thesis will aim to answer the question: **What is the impact of façade design and lighting design on circadian health in urban context?**

This will be done by answering the following questions:

1. *What factors are to be taken into consideration for modelling the impact of urban context on circadian light availability in existing buildings?*
2. *How can the impact of façade design and lighting design on circadian health in urban context be simulated?*
3. *What design recommendations can be derived from the assessment of the impact of façade design and lighting design on circadian health in urban context?*

1.3.1. Objectives

Building on the principles of climate design and 3D geoinformation, this thesis seeks to integrate the objectives of creating healthy, comfortable buildings with the development and implementation of open data and open-source solutions for 3D city modeling. With the focus on circadian health, this results in the following objective for this thesis: **To assess the impact of façade design and urban context on the exposure of circadian lighting for individuals in their home environment, on an urban-scale level.**

This main objective is divided into sub-objectives. The sub-objectives are:

- To understand the current methodologies of circadian lighting analysis, and how these are implemented in regulatory practices;
- To create a workflow in Rhino Grasshopper to build a link between the 3D BAG 3D building information, GIS knowledge of the environment and circadian light simulation models;
- To find a method of implementing window information in the available 3D environment for analysing indoor circadian lighting availability;
- To simulate the impact of outdoor artificial light at night (ALAN) on indoor environments on circadian health;
- To recommend design strategies for façade design and urban decision making that can help improve circadian health in urban context.

2. Theoretical framework: Quantifying the impact of the built environment on circadian health

This study aims to develop a method capable of assessing the impact of façade design and urban context on circadian lighting exposure for individuals in their home environment, on an urban scale.

This chapter presents a literature review. First, it evaluates methods for quantifying circadian lighting availability. Then, it explores factors within the built environment that influence this availability. The findings will inform the identification of key actors addressed by this research and help refine the scope by highlighting gaps in existing knowledge. Lastly, the chapter reviews existing methods used to answer similar research questions. This review serves as a foundation for selecting an appropriate method to address the research question.

2.1. How can we quantify circadian health impact?

2.1.1. Designing for light: Rules & regulations

To regulate the amount of daylight availability in homes, laws translated to sets of regulations, collected in the NEN (Nederlandse (*Dutch*) Norm) for Dutch regulations, and the EN (European Norm) for the European regulations.

These norms consider daylighting performance in the NEN 2057 (2011) and the EN 17037 (2018). Since 1-1-2024 all building-related laws have been centralized in the environment and planning act, (Besluit Bouwwerken Leefomgeving 2024). The BBL makes a diversion between existing build and new construction, where existing build is considered based on the NEN 2057 and the concept is that new construction will be adhering to the norms of EN 17037 from no earlier than January 2026 (Rijkswaterstaat, 2024). Until then, the NEN 2057 will keep being in use. The norms do not specialize towards the need for circadian lighting, and can be summarised as the following for living environments:

NEN 2057 ((Rijkswaterstaat, 2024a):	EN 17037(Rijkswaterstaat, 2024b):
Window-to-floor ratio (WFR): 10% Minimum of 0.5m ² window	Illuminance of 300lx for a minimum of 50% of occupied space under a CIE overcast sky. Illuminance of 100lx for a minimum of 95% of occupied space under a CIE overcast sky.

Although the knowledge regarding circadian lighting design is shown to be quite extensive, there is only one regulation that includes the availability of circadian lighting in its building certification. This certificate by the International WELL Building Institute (IWBI) designed the WELL certificate with the mission 'to improve human health and well-being in buildings and communities across the world' (IWBI, 2022).

The scientific background is based on the research of Brown et al. (2022), who based their recommendations on the m-EDI circadian light metric. The translation of the recommendations to the certification are as follows in the version of q4 2020 for living environments:

During the daytime, 200 or more equivalent melanopic lux as measured facing the wall in the centre of the room 1.2 m above the finished floor. The lights may be dimmed in the presence of daylight but are able to independently achieve these levels.
During the nighttime, lights provide not more than 50 equivalent melanopic lux (to the extent allowable by code) as measured 0.76 m [30 inches] above the finished floor.

Table 1 Table 1 WELL metric for melanopic light intensity in living environments

With this metric, WELL states that these EML requirements are achieved with use of artificial lighting and lack the focus for need of natural lighting from outdoor. It is especially remarkable that the measurements are executed facing the centre wall, away from the window. This might be done to account for a more stable availability of circadian light, and a simplification of the measurement method making it feasible for simple assessment over the course of one day. By taking interior lighting into account, it will be more feasible to reach the high EML levels, as the variation in length of day in various latitudes of the world during a year is strong.

Where Brown et al. (2022) had explicit suggestions regarding the timeframes at which circadian lighting should be available, the WELL q4 2020 metric abstracts this to 'daytime' and 'nighttime'. For the work-place requirement, WELL does state a timeframe, requiring 200 lux between 9:00 AM to 1:00 PM for every day of the year.

The height suggested by Brown et al. (2022) is based on seating height (1.2m) and in this paper they recommend the lighting values to be reached by daylight alone. The orientation is not made explicitly, but this would suggest that an orientation towards the window would be necessary. WELL uses orientation towards the wall, but assumed is that this is done because of the requirement that artificial lighting alone can produce the needed lighting values.

Next to circadian lighting availability, a metric is posed for circadian emulation. With circadian emulation is meant the imitation of subtle changes found natural lighting, to modulate the intensity of activity, levels of alertness and preparation for sleep (*Circadian Emulation | WELL Standard*, n.d.).

In all bedrooms, the lighting system or a standalone device should: Gradually increases light (as measured at the bed, viewing the light) from 0 to at least 250 equivalent melanopic lux over the course of 15 minutes or longer.
In all bedrooms, bathrooms, and residential rooms with windows, the lighting system meets the following requirements: <ul style="list-style-type: none"> - If lights are turned on in the interval spanning "wake time" and 2 hours before "bedtime", they provide a maintained average of at least 250 equivalent melanopic lux. - If lights are turned on in the interval spanning 2 hours before "bedtime" and "wake time", they provide a maintained average of 50 equivalent melanopic lux or less.

Table 2 WELL metric for circadian emulation in living environments

2.1.2. Measuring circadian lighting impact

Based on the knowledge that has been gathered regarding non-visual biological impact of light, multiple metrics have been proposed to simulate the impact of circadian lighting on the human, and three of them have been leading in the field: The Equivalent melanopic lux, (EML), melanopic equivalent daylight D65 illuminance (m-EDI), and circadian stimulus (CS) (Li et al., 2022). All metrics aim to reflect the circadian effectiveness of a light exposure condition and are obtained with the spectral power distribution and the illuminance of the light that reaches the cornea. The spectral power distributions of (day)light could be measured in real-life, but they also have been effectively captured by low-dimensional models with the CIE as frontier (Spitschan et al., 2016).

2.1.2.1. CS

The Circadian Stimulus metric is designed by Rea et al. (CS2021). One of the more distinctive differences between the CS metric and the m-EDI metric is the way of processing the signals of different channels (LMS—cones, rods and ipRGCs): Where other metrics assume additivity of the nonvisual pathways, CS consider subadditivity, meaning that considering the contributions of various pathways is not simply adding their values. Next to this, the CS model is based on the exposure time and the visual field, and has been proven to be a trustworthy method for evening and nighttime lighting design (Khanh et al., 2023).

Based on various studies, humans need a Circadian stimulus of the eye of more than 0.3 during the daytime hours and especially during the early part of the day, to improve circadian entrainment and sleep quality (Cai et al., 2018). During the evening hours, a low CS (<0.1) is required to maintain a healthy circadian rhythm (Li et al., 2022).

2.1.2.2. EML

Where the CS leans on the sub-additivity of the five different receptors in the retina, the equivalent melanopic lux (EML) metric is based on the understanding that the non-visual biological impact of light should be based on just the signals of the ipRGCs, expressing the effect of the melanopsin pigments alone. The EML metric is embraced by the WELL Building institute, which base their circadian lighting design recommendations for various types of spaces on this.

2.1.2.3. m-EDI

This metric, melanopic equivalent daylight illuminance (m-EDI) is developed by the CIE (2018). Just as the EML, the m-EDI has its fundamentals in the absorption spectrum of melanopsin. It differs from the EML as it expresses the amount (illuminance) of the CIE standard illuminant D65. The two metrics are closely related and can be converted with the coefficient of 0.9063 from EML to m-EDI.

Brown et al. (2022) concluded a recommendation of m-EDI levels (at the eye measured at the vertical plane at seating height (1.2m)) of 250 lx during daytime, and they advise that during evening hours (18.00-21.00) the maximum m-EDI on the eye should not exceed 10lx, and during nighttime (21.00-8.00) complete darkness is recommended: a maximum m-EDI of 1lx (Khanh et al., 2023).

throughout the daytime, the recommended minimum melanopic EDI is 250 lux at the eye measured in the vertical plane at approximately 1.2 m height (i.e., vertical illuminance at eye level when seated). If available, daylight should be used in the first instance to meet these levels.

2.1.2.4. Comparison of metrics

Although various metrics have been developed, there is not one that stands out above the rest regarding feedback from the literature. Khanh et al. (2023) compared the values from the various metrics and concluded that with ‘*acceptable accuracy from an engineering point of view.*’ These metrics for m-EDI and CS can be converted with the following linear formulas:

$$mEDI = 0.6792 \cdot CLA_{2021}(\sim CLA, 2.0) - 8.3139$$

(For all spectra between 2201 K and 17815 K) (Khanh et al., 2023)

The spectra between $3710K < CCT \leq 17, 815K$ are considered the range in which most buildings and rooms will have their lighting situations by daytime, and thus a more accurate formula is derived for this range:

$$mEDI = 0.5924 \cdot CLA_{2021}(\sim CLA, 2.0) + 55.5$$

(3710K < CCT ≤ 17, 815K, Neutral and cold white light) (Khanh et al., 2023)

And the correlation between m-EDI and EML has been defined by Li et al. (2022). This correlation is strong, as the fundamentals of both metrics are similar, and is expressed as:

$$mEDI = 0.9063 \cdot EML$$

Thus, although variations are found within the methods of these metrics, for measurement purposes their accuracy is comparable, and not only the results are convertible: there can also be leaned upon the suggested recommendations for corneal illumination from one metric to the other.

The other two are similar, where the m-EDI differs by the EML as the m-EDI is directly correlated to illuminance, and thus fits within the International System of Units (SI). For all metrics, regulations have been proposed with values that would suggest good availability of circadian lighting for humans, where the measurements from Brown et al. are most extensive.

2.2. Factors affecting circadian light availability in existing buildings

In the streamline from light source to corneal illumination, many factors play a role in the receptivity of circadian light, where the relative positioning from light source to recipient is the foundation. To translate the impact of urban design on circadian lighting availability, individual factors of impact are described and their role in urban design is considered.

Scientific parameters defined by Andersen et al. (2012) that are relevant to incorporate non-visual effects in lighting simulations and their relation to design parameters are shown in Figure 2-1. Intensity, spectrum, duration, timing, and contrast of circadian light are recognised. For each factor that will be described, the design parameters associated with this factor will be stated.

Next to these scientific parameters, design parameters are explored to explore the full range of factors that impact circadian lighting availability. Ardabili et al. (2023) classified four nodes, affecting the receipt of circadian light from a daylight source. These nodes are visualised in Figure 2-2, being:

1. The daylight source;
2. The facade element;
3. The interior space;
4. The recipients of indoor circadian lighting.

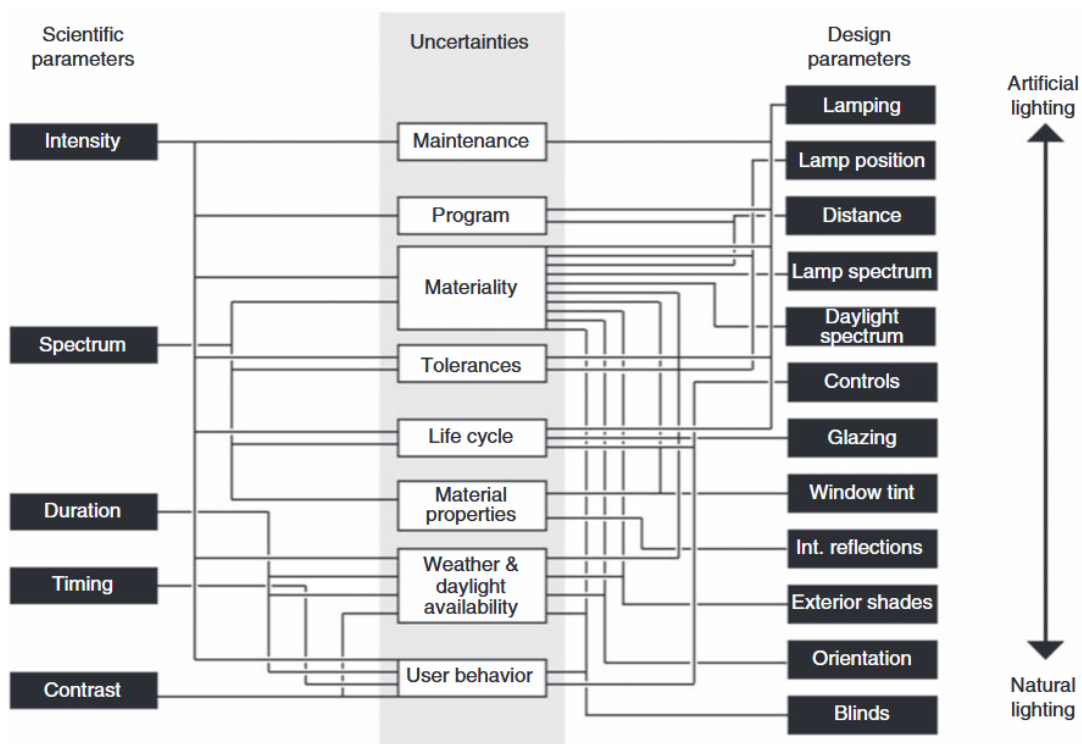


Figure 2-1 Uncertainties related to context variability and space properties integrated in a relationship map between measurable (scientific) parameters and design elements (Andersen et al., 2012)

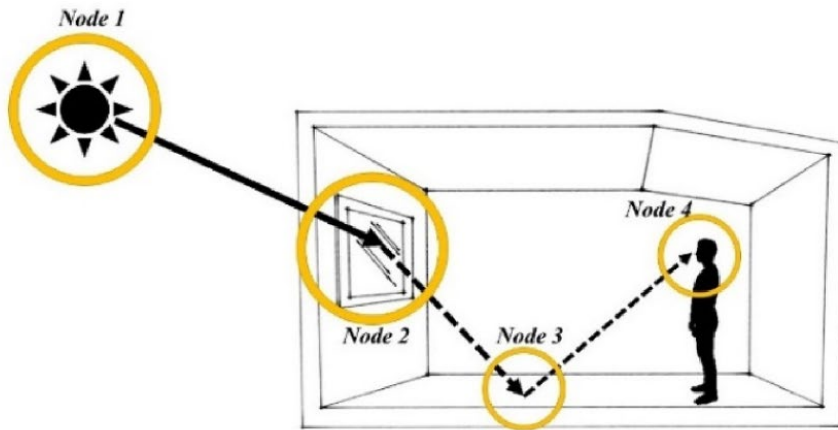


Figure 2-2 The four nodes affecting the receipt of circadian light from a daylight source (Ghaeili Ardabili et al., 2023).

As follows from the introduction, urban design significantly determines the possibility to receive solar irradiation in buildings (Lopez et al., 2016), and thus the factors that affect lighting before the light source meets the façade are explored. Distinguished are:

1. The urban building context, which effects the lighting availability when the ratio between building height and street width is high, and so-called urban canyons are formed. (Islam & Subasinghe, 2022)
2. Contextual reflectance, with the known effect of indoor reflectance (Ghaeili Ardabili et al., 2023), the effect of outdoor reflectance values is explored.
3. Artificial lighting in urban context, as artificial light is known to affect circadian health (Gaston & Sánchez De Miguel, 2022), the effect of outdoor artificial lighting is explored.

These factors have been organised on the scale from light source to recipient and are visualised in Figure 2-3. The role that each of these sources plays in influencing the receptivity to indoor circadian availability is explored in the following paragraphs. Finally, the target groups that can impact each factor are explored.

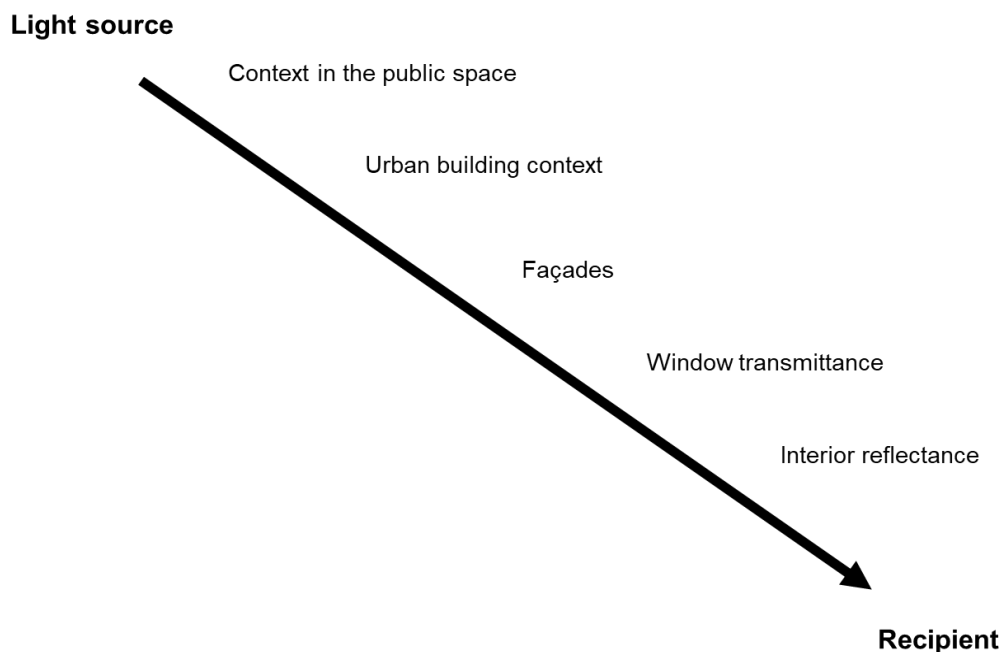


Figure 2-3 factors impacting the circadian lighting availability

2.2.1. Recipient

As follows from the introduction of this thesis, the effect of circadian lighting is strongly related to human receptivity. This concerns timing, lighting sensitivity and relative positioning to the light source. Shown is that morning stimuli advance the phase, daytime stimuli help for consistency in the circadian period and night-time stimuli result in postponement of the cycle. (Ohashi et al., 2023; Zerbini et al., 2021). This circadian effect is not consistent for everyone. Mechanisms behind individual variation for circadian lighting sensitivity include differences occurring within the retina and variations in the intrinsic circadian clock (Chellappa, 2020). About 75 percent of the population have an intrinsic circadian period of more than 24 hours, requiring a daily morning stimulus to entrain the 24-hour light-dark cycle, and 25 percent of population require an evening stimulus to delay the intrinsic circadian period for the entrainment of a pattern (Czeisler et al., 1999). As last, behavioural variations between individuals strongly affect the need for circadian lighting in specified timeframes. As is stated in the introduction, the positioning of an individual within a home will strongly affect the receptivity to circadian light, as this affects the relative positioning to the light source.

2.2.2. Interior spatial and spectral characteristics

The corneal illuminance is strongly impacted by the room surface reflectance. The contribution to the corneal illuminance from inter-reflected light indoors can significantly surpass that from the direct incident light, as has been found by Cai et al. (2018).

In a simulation environment, three sets of reflectance values derived from the EN 17037 (2018) have been tested on their impact on a daylight factor (DF), which has shown a direct correlation with up to 25% increase of daylight factor, both for the upper and lower reflection values derived from EN 17037 in comparison with a representative set of values that lay in between these reference values (Table 3). Even within the limits of the regulatory values, the interior reflectance thus can modify the daylight availability drastically. In a study analysing educational spaces for optimal circadian stimulus by Acosta et al. (2019), it has been found that to reach a circadian stimulus (CS) of at least 0.3 during the morning, a difference in Window-to-wall ratio (WWR) of 15 to 30% was needed to reach these levels in a setting with dark inner surfaces, and it is concluded that the environment reflectance is one of the most influential variables.

The interior spatial and spectral characteristics are influenced by interior design choices, mainly relying on the owner of a house.

	lower bound		higher bound
Ceiling	0.70	0.88	0.90
Interior walls	0.50	0.54	0.80
Flooring	0.20	0.36	0.40

Table 3 Prescribed interior reflectance values (EN 17037, 2018 and Koster, 2020)

2.2.3. Windows optical characteristics

The properties of the glazing also have a strong impact on the available lighting in indoor setting. (Ghaeili Ardabili et al., 2023) executed a systematic review on the impact windows on human circadian health and found that the optical properties of glazing systems (spectral transmittance and reflectance) influence the spectral power distribution (SPD) of the available light trespassing from outside to the recipient inside. A high visible transmittance (T_{vis}) will often directly positively affect the circadian lighting trespassing, but multiple studies found cases in which glazing with high visible transmittance are inefficient at meeting circadian lighting thresholds. This can be found in the variation in transmittance for different wavelengths, that are associated with different levels of circadian sensitivity in humans. This variation is showcased in Figure 2-4, where two windows show dramatically different spectral transmittance features in the melanopic transmittance range. As the spectral transmittance is a weighing factor for the different wavelengths of the available light spectrum passing through, the impact of the corneal illuminance of circadian light is correlated with this distribution in the melanopic realm.

For circadian lighting, there is no commonly used indicator in the fenestration field found. It has been posed that an accurate representation of transmitted circadian light can be achieved using radiometric quantities or melanopic transmittance. The actors that can influence the circadian health in indoor buildings are architects and building professionals, who have the option to choose for glazing that aligns with the spectral response for circadian health. A standardised indicator is suggested by Ardabili et al. (2023) to enable architects and building professionals to easily improve their building design for circadian health. With this design measurement, the spectral properties of incident light can be adjusted to allow circadian stimuli to pass through as effectively as possible.

2.2.4. Façades: light blocking, orientation

The review study from Ghaeili Ardabili et al. (2023) found seven experiments that showed the correlation between windows and their effects on wellbeing, where a significant correlation was found between windows and sleep duration, sleep related disturbances and impairments.

The impact of façades on the availability of urban light availability can be split into three study variables: The window to wall ratio (WWR), the window placement and the orientation of the

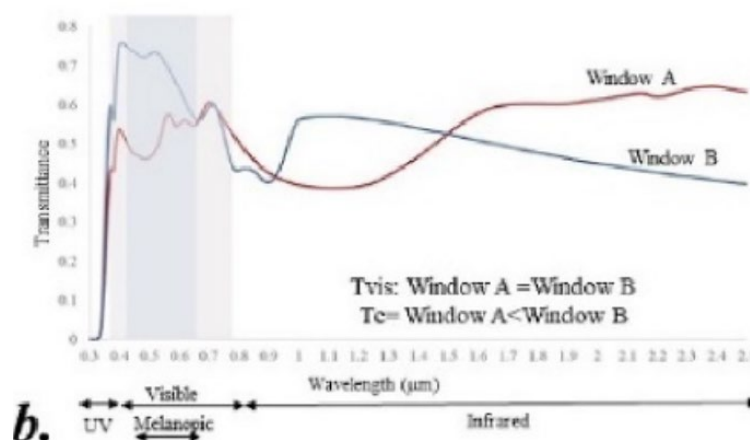


Figure 2-4 variation in transmittance between two windows with similar T_{vis} (Ardabili et al., 2023)

façade. With daylight being directional, orientation of the façade defines the time of day at which the amount of daylight is highest. Acosta et al. (2019) showed that for different locations (London, Paris, Madrid), a higher ratio is needed for north-facing facades, where 50% of the tests require a WWR difference of 15%, 12.5% requires a difference of 30% and 37.5% of the findings show no effect by orientation.

Façade design plays a crucial and long-lasting role, making proper design essential. It is influenced by both urban planners, who determine the orientation of buildings, and architects, who make key decisions about window placement and sizing. Their roles are vital because the façade's design directly affects daylight exposure.

2.2.5. Urban context reflectance

Outdoor reflectance, much like indoor reflectance, potentially plays a role in lighting distribution and the resulting circadian impact. The reflectance database Spectral DB (2024) shows that variations in reflectance between materials such as brick and natural elements like grass and water are big, and that for each material the difference between melanopic and photopic reflectance is different. For instance, between brick ($V(\lambda) = 18.38\%$, $M(\lambda) = 17.03\%$, SpectralDB, 2024), grass ($V(\lambda) = 11.96\%$, $M(\lambda) = 7.47\%$, SpectralDB, 2024) and water ($V(\lambda) = 10\%$, UTwente, 2024) differences in photopic and melanopic reflectance are remarkable. Even within one type, for example brick, these reflectance values differ strongly: A selection of brick reflectance values from SpectralDB are:

- Dark Brick: $V(\lambda) = 4.3\%$, $M(\lambda) = 4.0\%$
- Red Brick: $V(\lambda) = 18.4\%$, $M(\lambda) = 8.6\%$
- Res Hall Brick: $V(\lambda) = 35.3\%$, $M(\lambda) = 28.5\%$
- Light Yellow Brick: $V(\lambda) = 58.3\%$, $M(\lambda) = 43.6\%$

These variations in reflectance values between materials, and the discrepancy between visible reflectance and melanopic reflectance, highlight the complexity of light distribution in built environments.

2.2.6. Urban building context

Within the urban environment, the lighting availability within a building is highly context related. In English law, the 'rights to light' have been settled for ages, with the regulation that 'sufficient light according to the ordinary notions of mankind' has been the official measure in Great Britain (*Rights to Light*, n.d.). This availability of light follows from density, based on building height, building depth and the direct road profile. How these relate can be summarised with measures like Maximum Ground Coverage or Floor Area Ratio (also known as FSI) (Islam & Subasinghe, 2022), but also sky view factor is tested as a measure for designing urban plans that keep daylight availability in mind (López et al., 2016).

2.2.7. Light source

For humans, various light sources are impacting the living environment of the individual. Within the outdoor built environment, we can distinguish between natural light and artificial light, and between direct and indirect forms of lighting. As described by the introduction, three scientific parameters related with the light source are distinguished, being intensity, spectrum and timing.

2.2.7.1. Natural light

All light sources hold their own spectral power distribution (SPD): the distribution of (normalized) power of a luminant as a function of its wavelengths. Humans have been evolutionary optimized for the spectral characteristics of natural light in a stable diurnal pattern.

The changes in natural light are related to how we behave and arrange our lifestyles and day to day rhythm. Cai et al. (2018) show that the mid-day daylight spectrum is relatively efficient in providing circadian stimulus, as only 233 lx corneal illuminance of this daylight spectrum (Cie D65) is needed for a similar circadian stimulus as a 4000K FL11 fluorescent lamp at 575 lx. Figure 2-5 demonstrates the efficiency of the circadian sensitivity for three representative daylight illuminants. The dynamic changes of daylight due to latitude, time of day, time of year and the nature of the physical environment result in strong variations in intensity and SPD over time (Münch et al., 2020).

Next to that, the intensity and spectral changes of the natural light are heavily affected by weather conditions. Daylight has a broad, continuous spectral power distribution (SPD), and is strongly dynamic in intensity (illuminance) with variations from 20 000 to 100 000 lx on a sunny day, to 3000 lx in rain and 1000 lux during civil twilight (Wirz-Justice et al., 2021). Compared with starlight (~0.001 lx) and moonlight (~0.2 lx) on a clear night sky the ambient illumination is between 1 000 000 and 100 000 000 times brighter by day than by night (Spitschan et al., 2016). Acosta et al. (2019) found that the variations in typical weather conditions play a bigger role than latitude in promoting a good circadian stimulus.

Next to daylight, various studies have been conducted to test whether moonlight has impact on the natural rhythm of humans, and although Cordi et al. (2014) imputed positive correlation in earlier studies mainly on the effect of the lunar cycle on publication bias, more recent study ((Casiraghi et al., 2021) found that a synchronisation of nocturnal sleep timing with the lunar cycle in all of their participants, and Yousfi et al. (2024) compared this pattern with 17 other studies and concluded that the lunar cycle does appear to have a substantial impact on sleep patterns and melatonin production in humans. This impact mainly appears on nights before the full moon: moonlight availability in the early dusk hours caused delayed sleep onset and shortened sleep duration.

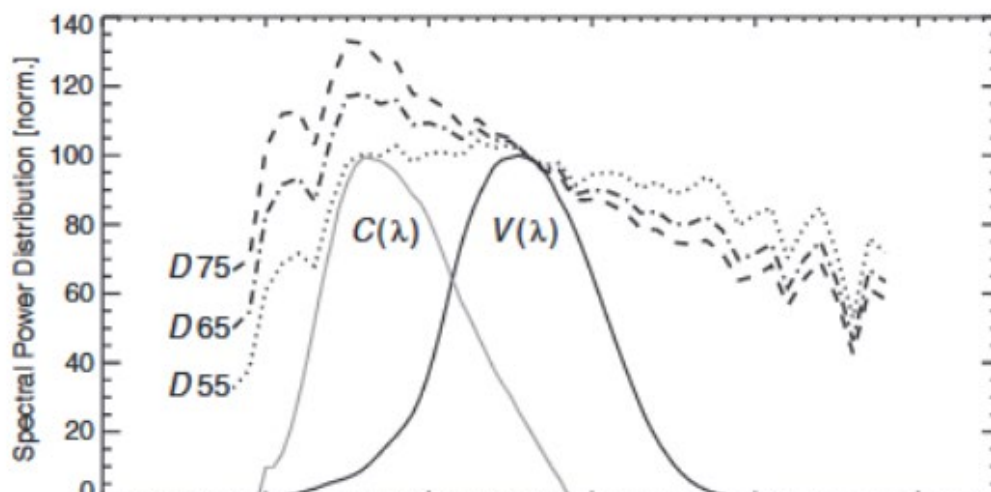


Figure 2-5 spectral power distribution for three CIE daylight illuminants, alongside photopic ($V(\lambda)$) and circadian ($C(\lambda)$) sensitivity curves (Andersen et al. 2012)

2.2.7.2. Artificial light

Artificial light provides a consistency in SPD and intensity. It provides humans a consistent light source, with which counteraction of daylight scarcity in buildings happens, improving vision in daylight-scarce areas and times of day. Individuals have a certain degree of control on the artificial light that they take in in indoor environments, but they are also subject to the direct

artificial light sources that are integrated into our urban context, and the light pollution that follows from this artificial light. Especially when the natural light dims, the aspect of artificial light receptance on the cornea emerges. This may have led to our circadian balances being disrupted, and for humans to be able to become more nocturnal (Ohashi et al., 2023).

Various studies have been conducted on the impact of artificial light at night. High levels of outdoor ALAN (Artificial light at night) have been found to correlate with later weeknight bedtime in adolescents, and adolescents with lower levels of ALAN had longer weeknight sleep duration, adjusted for several sociodemographic and area-characteristics (Paksarian et al., 2020).

More generally, the nighttime exposure to artificial lighting has been argued to have impact on multiple dimensions of human health, including immune function, risks of vector-borne diseases, various forms of cancer, obesity and mood disorders. Artificial light at night could therefore be a serious contributor to some of the bigger health concerns of our times (Gaston & Sánchez De Miguel, 2022). In The Netherlands, guidelines for street lighting are based on the measured illuminance at street level in the NPR 13201. With higher lamp placement, an increase in luminance will thus be necessary for reaching adequate street level illuminance.

With the knowledge of spectral sensitivity to circadian light, an uprising field in artificial lighting design arose: designing with spectral tuning. Souman et al., (2018) demonstrated that it's possible to reduce the shorter wavelengths, which have high melanopic sensitivity, without altering the illumination level or colour temperature. This is done by designing a reduction in spectral power between wavelengths of 450 and 500 nm with and an enhancement of spectral power at even shorter wavelengths.

2.3. Calculating light in urban context: implementation of knowledge in lighting analysis tools

With these design suggestions, measurements could be done to assess the quality of indoor circadian lighting availability in urban context. The tools as described in paragraph 2.1.3 have been designed for circadian lighting analysis. In this paragraph, research methods and data sources are assessed that relate to circadian lighting assessment and provide relevant information for implementation of the defined factors impacting circadian health.

A study that includes the urban context in daylighting studies is executed by Koster (2023). In this study, the impact of urban context on both daylight availability and circadian lighting availability is conducted. The study uses made up case studies of new building designs. For this setup, building properties are available, and a variation of representative urban densities is assessed.

Research connecting circadian lighting analysis and actual urban data for all the factors of impact on the urban scale, including the impact of artificial lighting, has not been executed. A big bottleneck for this large-scale analysis is lack of building-specific knowledge.

2.3.1. Lighting analysis tools

The circadian daylight analysis tools that are available and working at the initialisation model development process are Lark Spectral Lighting (Jung et al., 2023) and ALFA ((Solemna, n.d.).

Both LARK and ALFA are software that work within the Rhino environment, but ALFA has its own interface within Rhino, where LARK works as a plugin for grasshopper, allowing for easier parametric workflows.

Pierson et al. (2023) did a validation study for the simulation tools LARK and ALFA, and found that under daylighting conditions, more than 12% of the m-EDI results derived from ALFA-simulated data are overestimated by 50% or more, whereas this is found to be below 3% of the m-EDI derived from Lark-simulated data.

A disadvantage of LARK that is found is the lack of good spectrally accurate model of the sky. In these conditions, the impact of the sky irradiance is much greater than the sky spectrum on the accuracy of the simulation, leading to a range of error of about 20% in m-EDI. A disadvantage of ALFA is found in the overestimation of the irradiance on clear sky days, whilst generating larger errors for days with overcast and rainy skies.

Next to LARK and ALFA a new circadian lighting analysis tool is being developed for the Rhino Grasshopper environment. This plugin called Circalight (Aguilar-Carrasco et al., 2023), and it resembles the workflow of LARK. It has not been validated, nor is it available for use yet, so this tool is being kept out of consideration for this research.

Pierson et al. (2023) concluded that Lark leads to more accurate indicators associated with melanopic responses, but that the analysis tool takes about three times as long for processing.

2.3.2. The preparation of a digital Modelling for lighting simulation

All impactful factors, as outlined in the previous section, should be digitized and collected into a single environment before circadian lighting availability can be accurately simulated. Based on the aim of this thesis, the data used to implement all factors needs to be openly available. If possible, the data source with the largest coverage of information will be opted for maximizing scalability. With the availability of circadian lighting tools in Rhino Grasshopper, it is relevant to determine the possibilities of implementation of all factors in this program.

2.3.3. Urban context Data in Rhino Grasshopper

To process large-scale urban datasets in Rhino Grasshopper, they need to be correctly imported into the program. Tsai et al. (2023) demonstrate various methods of processing various data formats and distribution methods to correctly carry out data acquisition and alignment. Ideally, a method to have the data available through OGC APIs, such as WMS and WFS, would be carried out to minimize number of actions required within the workflow. It has been shown that his workflow is feasible within the Rhino Grasshopper environment for CityGML filetypes with a corresponding WFS API by writing Grasshopper python components; for many other filetypes, grasshopper plugins allowed for workflows that enabled data retrieval. Within all workflows tested, the alignment of different datasets posed challenges, as inconsistencies among dataset coordinate systems posed challenges regarding proper alignment. With variations in importing methods, discrepancies can arise and should be monitored appropriately.

As a simple method to read 2d geoinformation (GIS) data in Rhino Grasshopper has not been developed, but translation from two-dimensional formats to CAD-programs, including Rhinoceros, is shown effective.

2.3.4. Digital building models on urban scale

In the field of 3D geoinformatics, the most accurate set of large-scale building models is the 3DBAG (2024). Models of this typology are stored in the data model CityGML, encoded in the file format CityJSON (Ledoux et al., 2019). This CityJSON format is used for 3D BAG, as it allows for efficient file sizing. Objects within a CityJSON file are called city objects, and each object is a collection of at least the following members:

- One member with the name "type", whose value must be "CityJSON";
- One member with the name "version", whose value must be a string with the version (X.Y) of CityJSON used.
- One member with the name "CityObjects". The value of this member is a collection of key-value pairs, where the key is the ID of the object, and the value is one City Object. The ID of a City Object must be unique (within one CityJSON Object).
- One member with the name "vertices", whose value is an array of coordinates of each vertex of the city model.

(CityJSON Specifications, 2019)

A CityJSON file can be up to 6 times smaller than a CityGML file due to its semantic labelling and referencing with the key-value pairs. This structure is visualized in Figure 2-6.

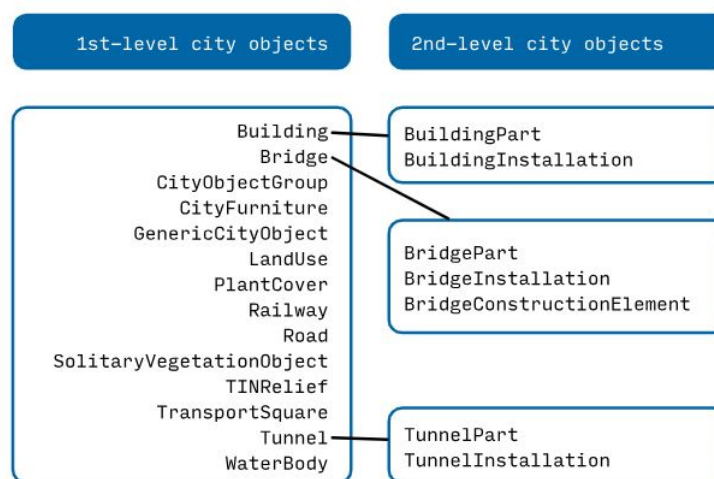


Figure 2-6 Key-value pairs for CityJSON (CityJSON specifications, 2019)

3D BAG has developed 3 levels of detail for each city object, in line with proposed extension of the field standard by Biljecki et al. (2016). This extension suggests a Level of Detail (LoD) specification in 16 levels presented in Figure 2-8, being LoD1.2, LoD1.3 and LoD2.2. The differences between each level of detail are visualized in Figure 2-6.

For lighting calculations, the level of detail available is insufficient. This lack of 3D information is a field-wide challenge. Within the Netherlands, there are two main pathways in development for generating this information that aim to connect their workflow to the 3D BAG: The pathway based on point cloud information (Vliet, 2024), and the pathway that is picture based

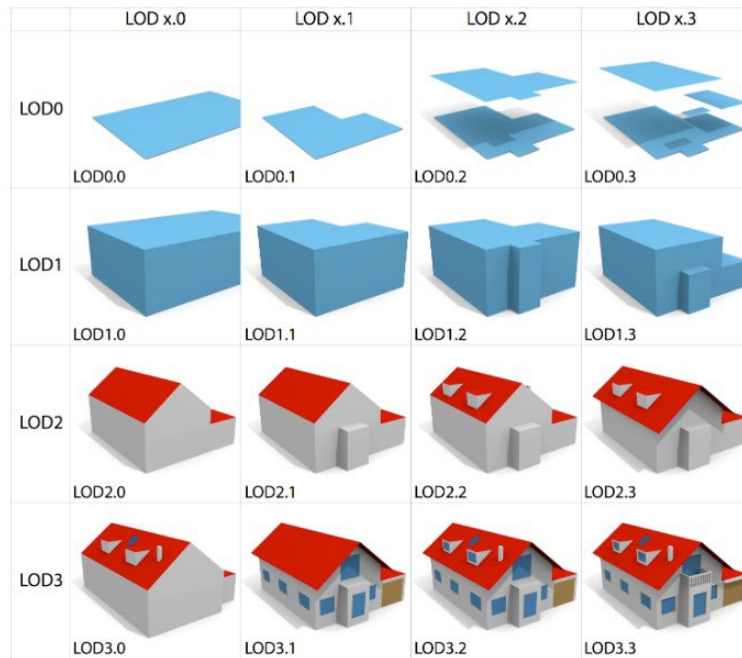


Figure 2-7 explanation Levels of Detail (LoD) (Biljecki et al., 2016)

(Eijgenstein, 2020) (van Asten, 2021). Both pathways have benefits, but both paths also have the drawback of lacking a consistent open-source data-foundation. For point-cloud information, the source that most accurately describes 3D information is the Digital Elevation Model ‘AHN’ (Current Elevation Dataset of the Netherlands), which is a point-cloud model acquired through airborne laser scanning (3DBAG, 2024). This makes that vertical building information is limited, and an additional source of information is needed. For the picture-based pathway, street imaging is available through google and thus façade-information is acquired on large scale more easily. The drawback for this method is that this data is not openly available. Eijgenstein (2020) used this method to extract a dataset of dataset of 910 façade pictures and door- and window information, as can be seen in Figure 2-7. This workflow is promising for the façade elements that are visible from the street, but steps are still needed to be taken, as the implementation of façade elements is not done systematically. As the 3DBAG building elements are not just single façade elements, Eijgenstein opted to place the opening geometry in front of the wall surface, without integrating this into the building. This points towards a big knowledge gap, where this building manipulation could be executed in an iterative manner for improving the Level of Detail in large-scale datasets, and thus allowing for large-scale circadian lighting analyses.



Figure 2-8 facade steps from google Streetview (top), façade masks (middle) to LoD 3.1 (Eijgenstein, 2020)

2.3.5. Other factors in the lighting simulation

Following from the literature, variations within window transmittance can be quite high. Although this impacts the results significantly, there is no large-scale information about the window typology for buildings. Other information that potentially relate with the transmittance of windows are:

- Building year: The building year of a dwelling can give an indication of the status of the window, but the accuracy is assumed to be quite low. For Amsterdam, it is officially considered a defect to have single glass panes in Amsterdam (Rechtbank Amsterdam, 10559878 CV EXPL 23-8728, 2024), so for a minimum requirement, there can be looked at local rules and regulations. It can be assumed that most façades have been upgraded somewhere in the past. Renovation information is not available on city-level scale.
- Energy label: In The Netherlands, the energy label that belongs to the building reflects directly on the energy efficiency. Window typology is part of this assessment. This could be a good method to get a better indication of window type, but a direct correlation between energy label and window type is not existent.

2.4. Summary and synthesis of findings

Correctly timed lighting availability is essential for human health. Humans have predominantly evolved in areas with stable diurnal patterns through the year, and it is found that fluctuations on daily and seasonal scale in daylight availability correlate with various mental health disorders (Gaston & Sánchez De Miguel, 2022). Next to the equatorial distance from stable diurnal patterns, the impact of urbanisation affects the circadian health in surplus of artificial light at night, as in shortage of natural light.

The impact of ALAN has shown associations with various mental health disorders and disruptive sleep patterns. A correlation between windows and sleep duration, sleep-related disturbances and impairments suggest that outdoor ALAN might have an impact on this, but further knowledge is lacking.

To model and quantify the impact of light on circadian rhythms, several metrics have been developed, including CS, EML and m-EDI. These metrics help quantify the effectiveness of light exposure in supporting circadian health and can be used to provide guidelines for both natural and artificial lighting in various environments.

WELL is the only regulation metric that is being in place. This metric took some abstractions from the circadian lighting suggestions, probably based on ease of use, and thus the origin of the WELL metric is needed as an addition for a more accurate baseline. The only timeframe that is suggested within the WELL building standard is in place for the workplace requirements. This information would still be a useful reference, as home offices and staying at home also require a good wake-time stimulant. This combined with the suggestions by Brown et al. (2022), calculated from m-EDI to EML, form the following metric:

21.00-8.00	8.00-18.00	18.00-21.00
<1 lm m-EDI	≥250 lm m-EDI	<10 lm m-EDI
<~ 1 EML	≥ ~ 280 EML	<~ 10 EML

Urban factors like building density, façade orientation, façade design and street lighting placement significantly affect indoor daylight availability. All factors that follow from literature to have the potential to affect the circadian lighting availability have been visualized in Figure 2-3. The role of designers, urban planners and policymakers differ for each factor. Intensity, spectrum, duration, timing and contrast of circadian light are the scientific parameters recognised. These are all affected by design parameters that alter the streamline from source to corneal illumination. The factors, their effect, the actor and the scientific and simulation parameters related have been summarized in the following table:

Factor:	Effect on circadian light:	Actor:	Scientific parameter(s) associated:	Simulation parameters
1. Recipient	Human receptivity relates to relative positioning and light sensitivity. Although a consensus of circadian lighting needs is defined (Brown et al., 2022), individual variations are correlated with variations within the retina and with the intrinsic circadian period.	Recipient.	Intensity, spectrum, timing, duration, contrast	Position in space
2. Indoor characteristics	Indoor characteristics have shown to be able to affect the circadian light measurements with a deviation of 13-30%. (Acosta et al., 2019)	Recipient, interior designer	Intensity, spectrum	Spectral reflectance
3. Window characteristics	For window characteristics, no common indicator is in use in the fenestration field. This makes that the impact of different windows is to be tested or simulated based on the spectral transmittance of each window. Visual transmittance, a factor with a range from 0-1 is commonly used. Single glazing has a value in the range of 0.9, where all values lower than that are plausible for different window types, with blacked-out windows at $T_{vis}=0$. Variations in window characteristics show big differences in the transmittance of circadian light for consistent T_{vis} values. (Ghaeili Ardabili et al., 2023)	Homeowner, architect	Intensity, spectrum	Spectral transmittance
4. Façade	The effect of façade design on circadian health is found in multiple factors; Window-to-Wall ratio, relative window placement and orientation of the façade. It is found that orientation plays a role in the amount of daylight that is measured, with differences from 0% up to 30%. (Acosta et al. (2019)	Architect, policy maker	Intensity, timing, duration, contrast	Spatial positioning
5. Outdoor reflectance	As the impact of indoor reflectance is shown to impact the circadian lighting availability with up to 30%, the variations in outdoor materiality are expected to also play a significant role in the circadian measurements indoor, as comparing measured reflectance	Architect, urban planner, policy maker	Intensity, spectrum	Spectral reflectance

	(SpectralDB< 2024) for different materials show high variations in both photopic as melanopic reflectance values.			
6. Urban building context	It is shown that the urban building context affect the daylight availability in cities, especially when building height is high, and street profiles are small. A standard factor has not been found in the literature. (Islam & Subasinghe, 2022)	Urban planner, policy maker	Timing, duration, contrast	Spatial positioning
7. Light source: Natural light	The amount of daylight is shown to be quite variable, where variations from mid-day to civil twilight affect with factors of 3-100, depending on weather conditions. Next to timing, these weather conditions strongly affect daylight availability, with variations from 100 000 lx to 3000 lx under different weather circumstances. (Wirz-Justice et al., 2021)	-	Intensity, spectrum, timing, duration, contrast	SPD, Luminous flux
Light source: Artificial light	Artificial light is a consistent light source, only affected by the SPD and intensity of the light source. It is shown to be possible to keep the intensity and colour temperature of a light source but still reducing the melanopic impact, by altering the spectral distribution. (Souman et al., 2018)	Urban planner, policy maker	Intensity, spectrum, timing, duration, contrast	SPD, luminous flux, spatial positioning

Although this potential effect of most factors is quantified, It is unknown how occupants of existing buildings are affected by the impact of urban context on circadian lighting availability in The Netherlands. Urban planning and building design should prioritize natural light access to support overall well-being, and the effect of artificial light at night should be taken into consideration. This could be done by developing a simulation tool that compares indoor circadian lighting availability with the above-mentioned metric by Brown et al. (2022). This has not been executed, and to answer this need, the implementation of 2d façade information should be taken into a 3d large scale model for improving the Level of Detail in large-scale datasets, and thus allowing for large-scale circadian lighting analyses to answer the research question of this thesis.

3. Methodology

In this chapter, all research methods and steps to answer the research question and sub-questions are covered. With the interdisciplinary focus of this research, a consistent methodology for transitioning between scales is designed and grouped into research phases. To explain this decision-making process, an introduction of these scales is described first, whereafter an explanation of and reasoning behind the specific methods for each individual research phase are provided.

The focus of this study is to find a method of implementing geo-information for climate design studies in an indoor environment, with the focus on circadian lighting. For generating information regarding circadian lighting availability, a 3d environment that approaches the real-world setting is a requirement. For this, the Thus, the first goal is set as:

Enhancement the accuracy and usability of the current 3D models for circadian lighting analysis, with the development of a method to enrich existing 3D data by incorporating precise information about window and floor levels.

The second goal is aimed on retrieving the circadian lighting information of buildings for which this enhancement has been successful, being described as:

The execution of a large-scale circadian lighting analysis that delivers results with a level of accuracy that closely approximates real-world conditions for individual homes and floor levels.

This will return the information that forms the fundamentals of the final aim, being:

The retrieval of design recommendations for positively affecting circadian health.

This will be done by focussing on the variation in factors that are under the control of the designer, so measurable differences will be able to be traced back to a concise set of design factors. The parameters considered constant for clarification of the results are the position of the recipient, the indoor characteristics and the window characteristics. In addition to this, detailed representations of the 3D environment that fall outside of the capacity and scope of this study include, but are not limited to:

1. Small, static urban objects (street furniture)
2. Moving urban objects (with artificial light)
3. Moving urban objects with predictable flows (busy roads, with artificial light)

This workflow is designed with the fundamental concept that the tool is executable and scalable for any input location. In practice, the assessed locations are limited due to availability of input data and the feasibility within the scope of the thesis. The results will show a proof of concept.

Due to the various tools and programs that are in use, a classification of four phases is made to keep the workflow understandable. For each phase, a set of outputs are generated that can

be passed on to the following phase, resulting in the final daylight analysis results after phase 4.

- Phase 1: preparing urban geometrical and geographical information
- Phase 2: extraction of building window and floor level information from façade pictures
- Phase 3: Window boundary reconstruction in 3D environment
- Phase 4: simulation and analysis of per-floor non-visual effects of light

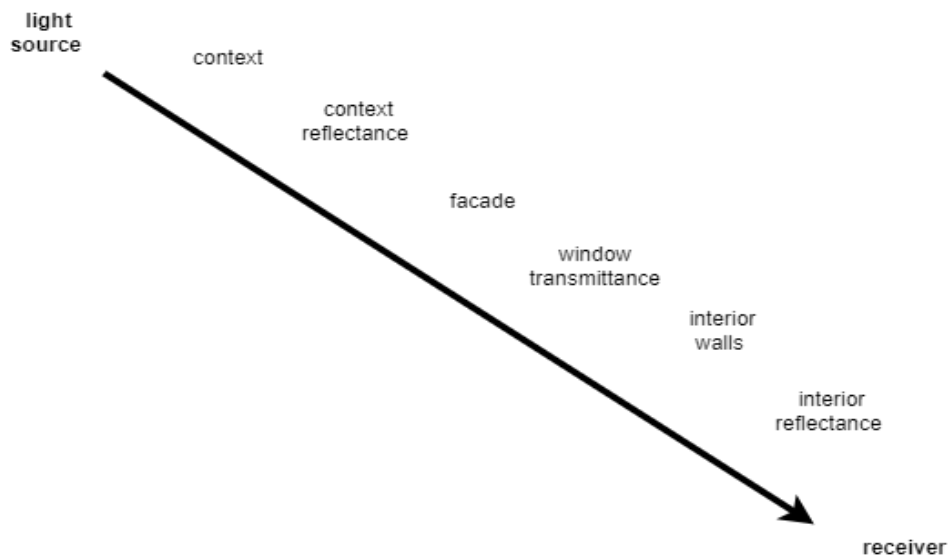


Figure 3-2 factors impacting the circadian lighting availability

3.1. Phase 1: Preparing urban geometrical and geographical information

For a scalable analysis tool, all sources are to be gathered systematically, taking into consideration the geoinformation is reaching adequate level of accuracy, adequate level of detail, and that the information is retraceable for a broad audience. The foundational geometrical source for this thesis is 3D BAG; a dataset containing 3D building models of the Netherlands in multiple levels of detail (3D.bk.tudelft, 2024). This dataset is fully automated based on height source information provided by AHN (a LiDAR-based height map of the Netherlands) and BAG (basic registration of Addresses and Buildings of the Netherlands). Both sources are easily accessible and designed for smooth implementation with other sources in the public domain. The building codes associated with each building, generated by BAG have been embraced by 3D BAG, but for multiple other mapping tools as well. one of these is the BGT: Basic registration of large-scale Topography. This geo-basic registration administers the furnishing of all physical objects (Buildings, roads, water, greenery) in a digital mapping tool, with accuracy levels of 20cm (Koninkrijksrelaties, 2018).

Next to surface information, street lighting information is taken into consideration for analysing its impact on inhabitants. This information is not available on a national scale, thus for this thesis the street lighting information from the municipality of Amsterdam is used.

Joining these large-scale sources with accurate lighting modelling analyses, the level of accuracy is highly relevant, as well as the actualisation of the sources. In Table 4 the used

sources are summarised. The level of detail that is shown is in line with the field standard LoD specification of 16 levels, presented by Biljecki et al. (2016).

Table 4 Urban geometrical and geographical information, source overview

Source	Citation	Use	Data format	Level of Accuracy	Level of Detail
BAG	National Georegister, 2024	Mapping, address information	WFS	-	-
3DBAG	3DBAG, 2024	3D modelling	CityJSON	30cm	1.1, 1.2, 2.2
BGT	PDOK, 2024	Context surface reflectance	GeoJSON	20cm	-
Data.amsterdam	Gemeente Amsterdam, 2024	Street lighting positions	GeoJSON	20cm	-
Data.amsterdam	Gemeente Amsterdam, 2024	Street lines for origin of façade mask picture	GeoJSON	30cm	-

3.1.1. Data pipeline

The tool chosen for lighting analysis followed from the literature is LARK and will be elaborated in phase 4. As LARK is a Grasshopper-based tool, all sourced geometries are to be imported to Rhino Grasshopper.

All the 2-dimensional model geometries are placed on the XY plane, with an exception for the street lighting points. Thus, no height differences are included in terrain patches. For the 3D Building data, alignment of the bottom plane is done with the XY plane as well, so that gaps and inconsistencies with the terrain are prevented. It is expected that height differences will not affect the result considerably, due to the limited height differences in Amsterdam. This could be assumed for most places in the Netherlands, but height impact can affect daylight analyses considerably, so for other locations this should be a serious point of concern.

The lighting points are placed at a height of 4 meters from the XY plane. Due to lack of data, this height is considered a constant in the simulation.

3.1.2. 3D building data

The current level of detail that is available in large-scale building information stops with building shape: The source that allows for generating geospatial analysis most accurately on large scale for the Netherlands is the Digital Elevation Model 'AHN' (Current Elevation Dataset of the Netherlands), and with this information vertical building information is limited. For accurate daylighting calculations, façade information and interior partitioning (floor level and interior walls) are highly relevant, and thus this project endeavours to improve 3D information with façade and floor level information.

According to the literature research, two pathways of retrieving façade information are being explored in the Netherlands: The picture-based pathway and the point-cloud-based pathway. Limitations and benefits are discussed previously, and for this thesis, the picture-based pathway is chosen. C. Eijgenstein (2020) extracted façade pictures, associated with the BAG building IDs from panoramic images. With Mask R-CNN², a deep convolutional neural network, these pictures have been parsed into colour-segmented masks. These masks mark out segment information in four categories: walls, sky, doors and windows. Each category is displayed with a distinguished colour as shown in Figure 3-2. This mask information forms the basis of phase 2.



Figure 3-3 Examples of facade masks (eijgenstein, 2020)

Before implementing the mask-information, the correct association between mask and 3d building should be made. For each mask, the following additional data is found in the naming of the image:

- The BAG Building ID;
- A value representing the distance in meters from the capture location of the panoramic image to the centre point of the façade location (in 2D).

These file names allow bridging between the masks and the BAG GIS information as well as the 3DBAG 3D building information. To check which masks are available, Python is used. a GeoJSON file is created by filtering the full BAG GeoJSON dataset using the building IDs found in file names within the mask file directory.

3.1.3. Conclusion

Based on the availability and limitations of data for the model, a test location is chosen. The limits can be described as following:

1. 3D BAG is being used as the source for 3D building models, which limits the area to the Netherlands.
2. Context of the public space is available for all municipalities in the Netherlands, based on the Basic Registration of Large-scale Topography (BGT), that are collected and shared by PDOK (2024).
3. For this model, the picture-based pathway from Eijgenstein is being used, as the data availability is the highest at the moment of developing this research. The façade information that is available corresponds with the 3D BAG data format. The dataset limits the area to the city centre of Amsterdam.
4. For Amsterdam, street lighting information (placement and type of fitting) is available within the data.amsterdam (Gemeente Amsterdam, 2024) database.

From the available data, the biggest limitation is the availability of façade information. With this limitation in mind, a single building tile as subdivided by 3DBAG is picked (10-430-716). This tile has a good coverage of façade elements, street profiles and street orientations.

3.2. Phase 2: Extraction of building window and floor level information from façade pictures

3.2.1. Clustering algorithm

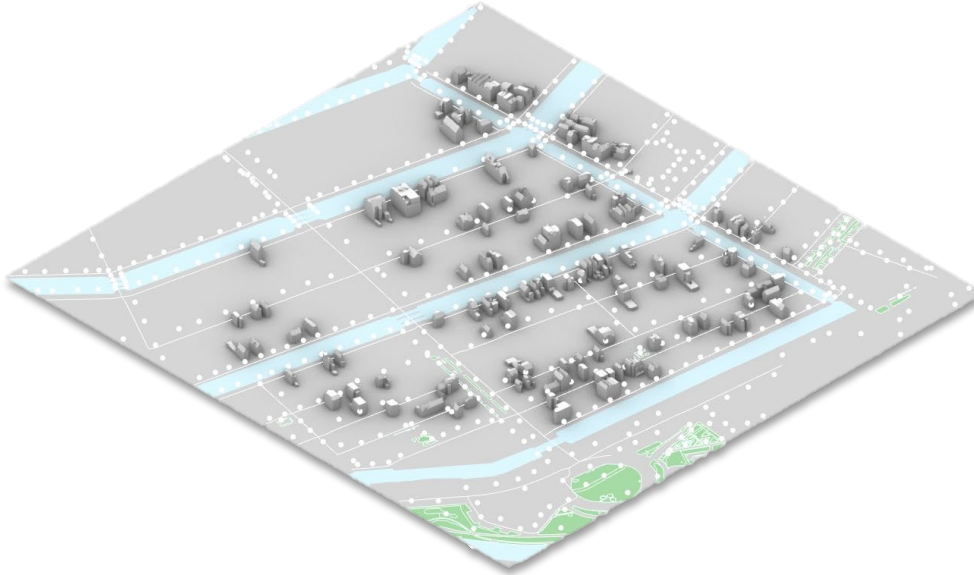


Figure 3-4 Buildings with available façade information (own source)

The façade masks are imported into Python, where the OpenCV library is utilized to interpret the available masks. The mask images, as shown in Figure 3.2, are converted from RGB to HSV colour space to enhance colour segmentation, after which the window shapes are extracted. These shapes are then simplified into orthogonal square elements, based on the assumption that most windows are placed orthogonally within their frames. This assumption enables a more streamlined calculation process. The window clusters are detected based on these orthogonal boundaries. Each window cluster is defined as a list of windows with overlapping vertical extents. Assumed is that if windows have overlapping vertical extends, a floor level cannot be placed in between them. Therefore, all windows with overlapping heights are considered to belong to a single floor level. The data that is retrieved for further analysis is:

- Floor level height estimation;
- Window positioning per floor;
- Façade information per floor: window area, wall area, Window-to-Wall-Ratio (WWR).

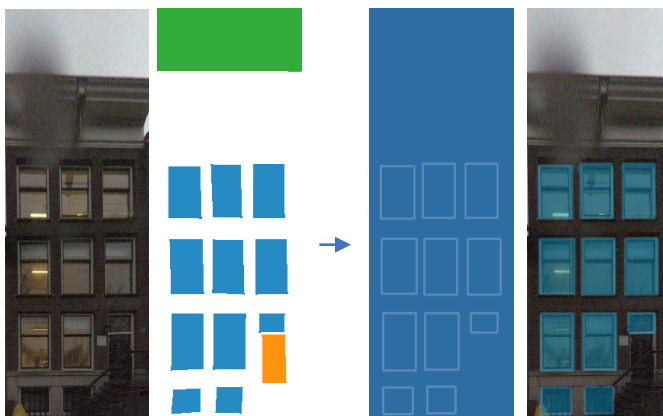


Figure 3-4 Preparations for the clustering algorithm

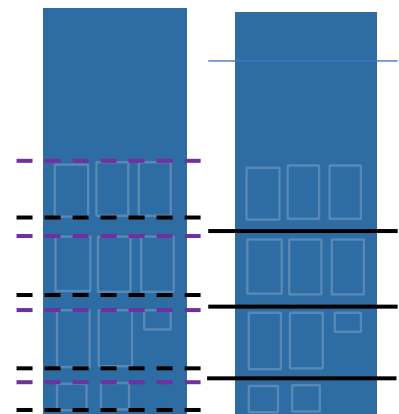


Figure 3-5 Left: clustering of the windows, based on upper and lower window boundary. Right: estimated floor & ceiling levels

3.3. Phase 3: Window boundary reconstruction in 3D environment

For this phase, the window data derived from the masks is integrated into the 3D environment. Since window placement is traceable from open data sources and is crucial for lighting analysis, improving its accuracy in 3D significantly enhances large-scale daylight studies.

The workflow begins by dividing the buildings into individual floor levels. Windows are subsequently reconstructed in relation to these floor segments, enabling parallel lighting analyses across multiple floors using Rhino Grasshopper, thereby optimizing the process efficiency.

3.3.1. Preparation of analysis volumes

The semantics from the CityJSON structure provide attribute information for each building and building element. With the building ID known, a sift can be made between buildings of which façade information is available, and buildings of which we have no façade information available.

For simplicity of this workflow, the CityJSON structure is simplified and only the building information is considered. Two levels of detail are retrieved: The LoD 2.2 and the LoD 1.2. As the buildings in LoD 1.2 will merely be used for context, these won't be filtered by their façade information availability. This results in three Rhino layers: LoD 1.2 unfiltered, LoD 2.2 with façade information and LoD without façade information. For all buildings, their building ID is captured in the title of the geometry.

3.3.2. Floor-level splitting

For each building, the 3D building element is segmented based on the estimated floor heights from phase 2. It is closed to ensure a watertight volume. This watertight surface model is the requirement needed for lighting analyses.

3.3.3. Systematic façade element selection

With this algorithm, the facade elements that are oriented towards the street, and are thus the facade elements that have the biggest chance of being compatible with the facade mask are selected. For this, the street dataset from Amsterdam.data (Gemeente Amsterdam, 2022) is used. This dataset provides multiline geometries which are translated from Geopackage to DXF in QGIS, so they can be imported and read as line segments in Rhino Grasshopper.

First, from the centre of the building, the closest point on the street network is calculated. This point approaches the position from which the rectified façade images are taken. A two-point

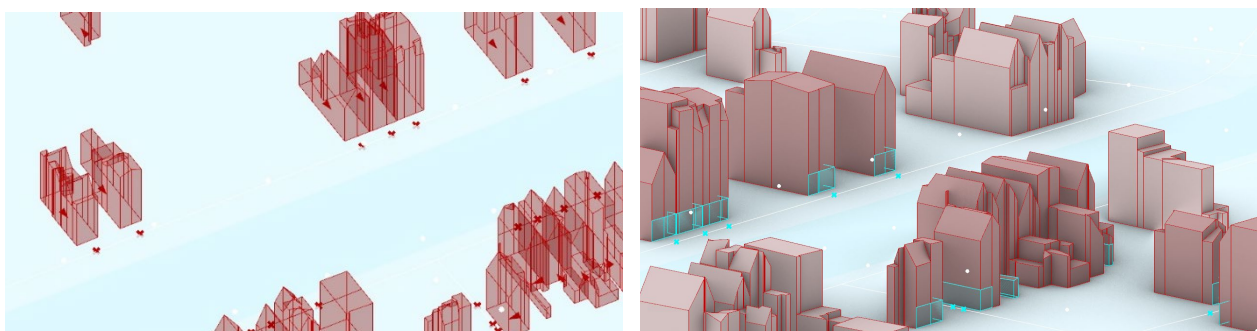


Figure 3-6 Left: building centre & retrieved street-point vector. Right: facades visible from the projection-plane

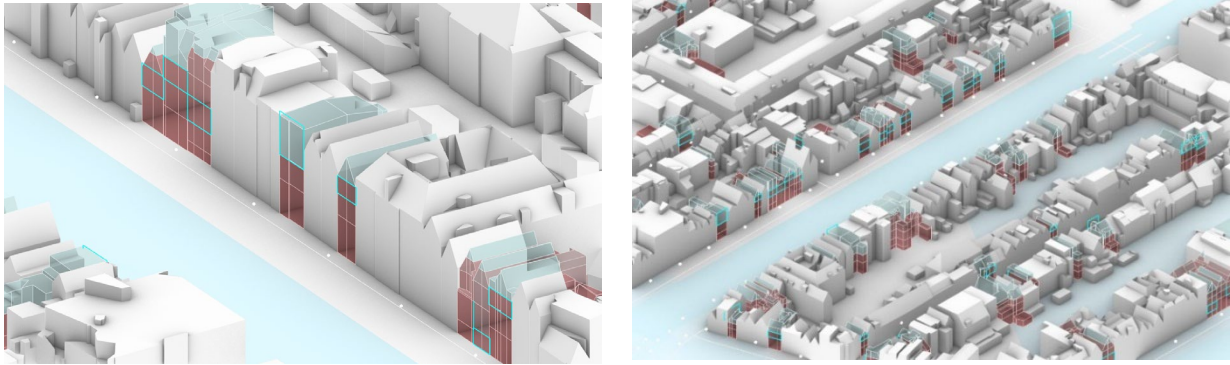


Figure 3-7 selection of window plane, per floor level (level 3 selected)

vector from the building centre and this closest point is taken as an approximation of the direction in which the façade information is generated. There will from this point on be referred to the 'street-point vector', when mentioning this vector. street point and the vector form the projection plane.

Onto this plane, all façade elements are projected. By projecting all geometries onto this plane, a distinction can be made between elements that are 'hidden' behind other elements, and elements that are on the front, and are thus can be visible from the position of which the façade image is taken. These elements are used for the relative window placement.

By including all façades that are visible from the position, not only the façade elements that are perpendicular to this sight line are visible, but also façade elements that fall within the 90° angle and that are not obstructed by other façade elements.

3.3.4. Relative window placement

For the placement of windows, the bounding box of all projected facades is used as the relative placement for the windows in the 3D space. With the 2D information of all window shapes (lower corner X,Y, Height & width) of specific floor level, the window boundaries get projected onto the plane as is shown in Figure 3-8. These then get projected onto the 3D geometry with the street-point vector, resulting in 3D placement of window boundaries.

The original façade elements get split by the projected window lines and all building elements are grouped based on their type. Separated are ceiling, floor, walls and windows. This is done to assign optical properties each type for the lighting modelling.

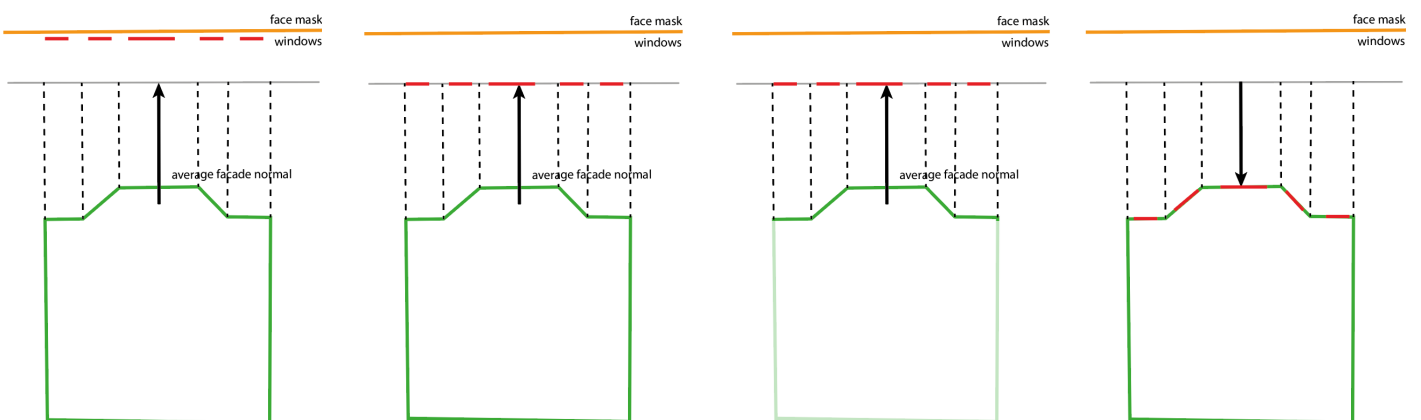


Figure 3-10 the street-point vector forms the basis for a projection plane;

The windows boundaries are projected onto this plane;

The facades that are visible from this plane are grouped;

The window boundaries are projected onto the façade elements that are visible.

3.4. Phase 4: Lighting modelling

Based on the information from the literature review and the lack of availability for a valid licence for the use of ALFA, the decision to opt for LARK as a lighting modelling environment is made.

For keeping the simulation relatively light and scalable, the simulation will be running for one position for each floor that has been retrieved from the façade masks. The measurement orientation is pointed horizontally, in the direction of the window. The calculations will be executed for 16 points in time, with 4 markers for each season and 4 markers per day. Next to this, an electric lighting simulation will be executed separately, resulting in 17 values per floor per building. These values can then be related to the circadian lighting suggestions that followed from the literature review.

The LARK modelling environment has a series of requirements that are to be specified, before accurate measurements can be made. In the following paragraphs, there will be elaborated on these.

3.4.1. Model preparation

3.4.1.1. Recipient

For the sensor placement of the simulation, it is relevant to look to the method of sensor placement with which the results are to be compared. Based on the literature review, a seating height of 1.2 and an orientation towards the daylight origin can be picked. WELL considers placement in the centre of the room, but as indoor wall information is lacking, each building is assumed to have a front room and a back room, and thus the sensor will be placed at $\frac{1}{4}$ of the building depth with its orientation towards the window.

3.4.1.2. Interior reflectance

As there is no specific information on interior reflectance values for individual buildings, this model must take this out of consideration, and consistent values will be taken for all buildings. EN 17037 suggests reflectance values for interior surfaces, and Koster (2023) analysed the impact of these reflectance values on daylight simulation results. For this thesis, the reflectance values are retrieved from this thesis, being:

The materials that are used within the modelling environment are retrieved from SpectralDB (2024) and are summarised in Appendix 7.3. ⁴

Surface	Reflectance value
Ceiling	0.88
Interior walls	0.54
Flooring	0.35

3.4.1.3. Window transmittance

Following from the literature, variations within window transmittance can be quite high. Although this impacts the results significantly, there is no large-scale information about the window typology for buildings. As both options investigated in the theoretical framework do not result in reliable assumptions, double glazing will be used for all buildings. Although this would not represent variation in window transmittance, it would make the reliability of comparing the results on other variables more reliable.

Further elements in the urban context that should be considered for the model is the optical properties of the public space. For retrieving accurate optical properties of the surrounding buildings, ground, roads, greenery and water bodies are specified. The materials that are used for this are summarized in appendix 7.3. For the reflectance of water, a simplification is used. The complexity of accurately modelling water surface reflectance (Ma et al., 2019), falls out of the scope of this thesis, and based on simplified reflectance values stated by ITC, University of Twente (2024.), a material from the SpectralDB (2024) library with a high similarity in spectral reflectance has been chosen.

All contextual elements and the specific building volumes are imported and joined with their corresponding materials, in a 9-channel simulation.

3.4.2. Daylight

For simulation of natural light, the Lark model relies on Honeybee. An approximation of all light emitted by the sun is categorised by direct and diffuse natural light and is calculated based on the local sun positioning, with Spectral power distribution (SPD) CIE d65 spectrum for overcast sky and CIE ASTM for direct sunlight. The placement on the geographical coordinate system is used as an input, with a level of accuracy of four decimals. For the scope of this thesis, these values can be considered a constant. Four points in time have been considered, to compare the impact over the seasons: summer solstice, winter solstice, autumn equinox and spring equinox. To simulate a representative situation, it is opted to look for a clear sky simulation. Koster (2023) Executed an analysis of the weather file IWEC Amsterdam and retrieved four dates that approached a clear sky simulation near the seasonal extremes), being 04-01, 26-3, 07-06 and 29-9, with variations in date difference with the actual seasonal extremes being $d=15$, $d=6$, $d=14$, $d=8$ respectively.

For this simulation, for each of the four dates, four timestamps will be tested that are considered relevant for circadian entrainment. Sky values vary throughout the day, and thus using the weather file to select appropriate measurements would lead to a possible variation of 16 test dates. To minimize the high variation that might arise from selecting dates purely based on weather file data, a more controlled approach is taken. By using the Tau Clear Sky simulation model, the dates of seasonal extremes (20-3, 21-6, 22-9 and 21-12) can be picked to ensure uniformity across the simulation. For each of the dates and times, Direct Normal Irradiance (DNI) and Diffuse Horizontal Irradiance (DHI) is retrieved for calculation of Gendaylit. Gendaylit is a Radiance program that produces a Radiance scene description based on these two (DNI and DHI) inputs, date and time, over the visible spectral range. The simulation type run is illuminance (lux).

The strong variation in SPD that occurs with natural light is not included in this model. This is due to a lack of accessible simulation options. This might strongly affect the simulation results, especially around dusk and dawn, and will be remarked in the discussion.

3.4.3. Artificial light

The scientific parameters that are associated with the light source are intensity, spectrum, timing, duration and contrast. Within the model, the factors that form the input of the light source are:

- The spatial configuration of the light source;
- The SPD: the spectral power distribution of the light source;
- SPD α -opic weighing factor.

For artificial street lighting information, specific streetlighting information available (data.amsterdam, 2024) is insufficient to execute accurate impact analyses. Thus, to simulate the effects of artificial light on indoor circadian lighting, three test simulations will be conducted with various luminous intensities and Spectral Power Distributions (SPD's), representative for streetlight.

A consistent height in lamp positioning is set at 6m, and to approach good accuracy, the wattage- & luminous flux values that are associated with lamps within 10% of this height are approached with .IES files for analysis (see Table 5).

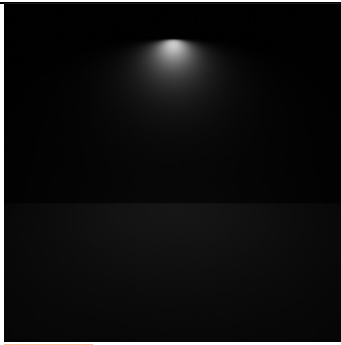
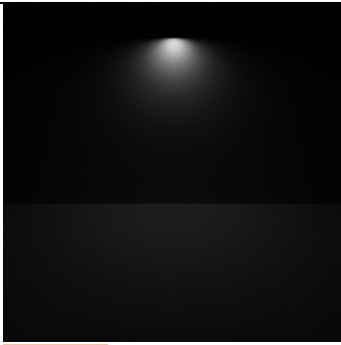
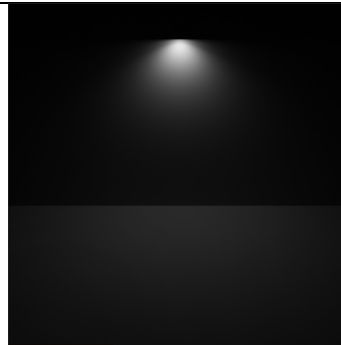
	IES file 1	IES file 2	IES file 3
	Low intensity	Medium intensity	High intensity
Spatial distribution, visualised			
Luminous flux (lm):	886 lm	2174 lm	3612 lm
Wattage (W):	16 W	32 W	48 W
Source:	IES library (2024)	IES library (2024)	IES library (2024)

Table 5 IES electric light source photometric specifications

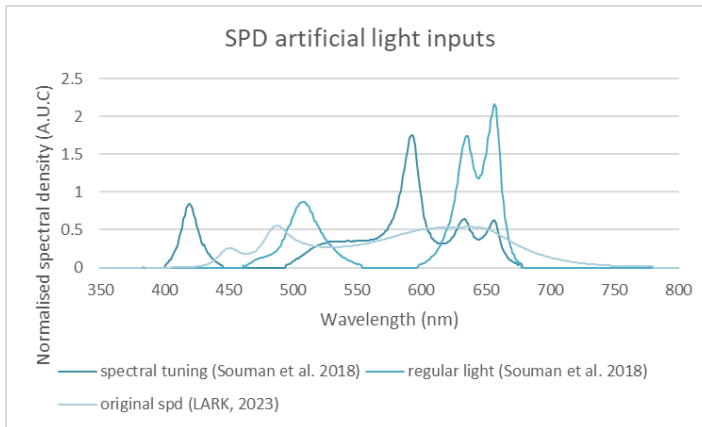


Figure 3-12 SPD artificial light inputs, normalized by the area under curve (A.U.C.)

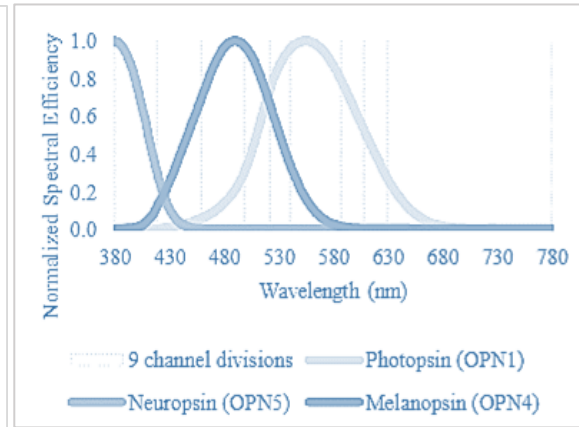


Figure 3-13 Normalized spectral efficiency curves for photopsin, melanopsin, and neuropsin and the 9-channel divisions (Jung et al., 2023)

These files contain the information for light distribution and intensity but are to be analysed with a representative SPD. For this, three different SPD's are retrieved: The SPD that LARK spectral lighting provides with the software (CCT=3500K) and two SPD's derived from Souman et al. (2018), with a consistent CCT (2700K) but with strong variations in SPD (. These SPD's have been chosen, as Souman et al. (2018) proved a difference of 50% in melatonin suppression when measuring participant's reaction to a light with an SPD with low power in the melanopic sensitivity range. These SPD's will be tested to simulate the effectivity of spectral tuning for minimizing the effect of circadian disruption by artificial light without reducing the artificial lighting availability on streets. These SPDs were selected to assess the effectiveness of spectral tuning in minimizing circadian disruption caused by artificial light, while maintaining adequate lighting levels for street illumination. Souman et al. (2018) demonstrated a 50% difference in melatonin suppression in participants when comparing lights a regular SPD with an SPD with low power in the melanopic sensitivity range, while keeping power and Correlated Colour Temperature (CCT) consistent.

The SPD is translated to 9 colour channels, and different methods for weighing the channels are executed. No weighing will be compared with the proposed method in the LARK template file, where each colour channel is weighted by the inverse photopic coefficient defined by Jung et al. (2023) and scaled by the numerical integration of the sum of all weighted values. A second weighing follows the method of Jung et al. (2023), where each channel is multiplied by the melanopic coefficient described. The weighed spectral electric light source definition in 9 channel divisions on the LARK input SPD is visualized in Figure 3-9.

For implementation of the artificial light sources, luminaire placement is retrieved from the 2d spatial placement as distributed by Gemeente Amsterdam (2024) and set at 6m height. Direction is set to point towards street level. No light loss is considered (LLF=1).

The Honeybee luminaire component is used to create a Radiance representation of the photometric data for further calculations, gathering luminaire zone, IES light distribution and colour space (CIE 1931) for the three RGB colour channels within the 9-channel simulation, written to a file.

3.4.4. LARK circadian lighting simulation

The simulation elements are based on the LARK 9 channel simulation. The components that are used for the circadian lighting simulation are simplified and visualised in Figure 3-8.

Two sets of input parameters have been tested for a single floor, and with the second set of parameters, the consistency of results has improved considerably. The first set of settings, as provided with the LARK calculation template (quality 0 -ab 2 -ad 512 -as 256 -ar 128 -aa 0.100 -lw 0.0001) has been tested for four different electric light inputs. Strong variations were found (1218lm: 0.07, 0.09, -6.51, 0.12, 0.16; 2174lm: 0.74, 0.37, 1.16, 3.01, 0.51; 3428lm: 0.81, 0.96, 0.38, -0.48, 0.57) and even negative values followed from these inputs. With the settings as described by Jung et al. (2023) (-ab 6, -ad 1024, -as 500, -ar 100, -aa 0.1, -lw 0.0001), the calculation time surpassed the capabilities of the hardware. With the assumption that this is due to the amount of ambient bounces (-ab 6), the final set of settings derived from these two metrics (quality 2 -ab 2 -ad 1024 -as 256 -ar 128 -aa 0.1 -lw 0.0001) returned values that approached expectations more steadily. To check for consistency of the results, 10 runs are executed, and the results are compared for each of the 9 colour channels. This has been done both for the electric light (3428lm) and the daylight setting.

3.4.5. Simulation scenarios

As both the availability of light around dusk and dawn and the mid-day and night exposure to light is affecting circadian health, four timestamps have been chosen that align with these findings (02.00, 8.00, 13.00, and 19.00) To retrieve an answer for the variation within a year, the four seasonal extremes have been used: the 20th of march, the 21th of June, the 22nd of September and the 21 of December. For these 16 timestamps, a daylight analysis has been executed. Next to this, a seventeenth analysis is done for measuring the impact of electric city lighting. It is opted to assess this separately from the daylight measurements, so the impact of both light sources can be compared.

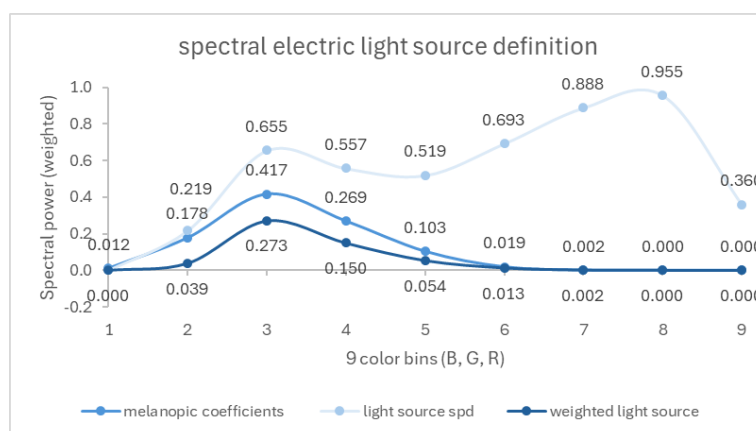


Figure 3-14 Spectral electric light source definition; the LARK SPD, the melanopic coefficient and the resulting SPD distribution, normalized (own source)

3.5. Running the simulation

3.5.1. Test runs

For checking the accuracy of the simulation, test runs are executed for a simplified simulation setup. For this, a single building measurement is taken, at the timestamp where the availability of daylight is assumed to be the highest (21st of June 13.00hr). The context is simplified to the concrete ground level, without water, greenery or context buildings.

Before executing the full run, the simplified simulation setup is used to compare the results for the effect of LoD 1.2 and LoD 2.2. It is presumed that the setup with LoD 1.2 will return slightly lower values, as due to the uniform heights for each volume, the LoD 1.2 results in higher volumes than the more detailed variant.

To validate the accuracy of the lighting, a run is executed with the light source 1 meter above the measurement point. The measured lux should be in the order of magnitude of 1/12th of the illuminance value (lm);

$$lux = \frac{lm}{(4\pi * d^2)}$$

And to compare this with the m-EDI, an estimated reduction factor of 0.5 to 1 is expected to account for the melanopic/photopic ratio. The measurement direction towards the window and the Lightsource orientation with aim downwards might also affect the returned m-EDI value in a reductive manner.

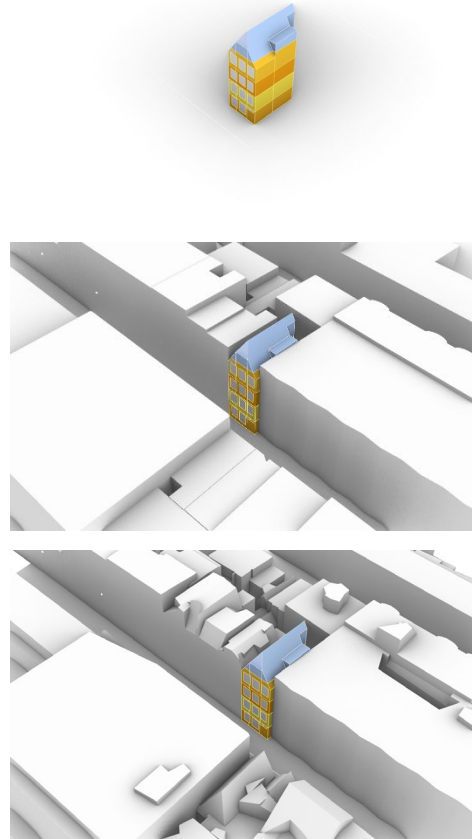


Figure 3-15 Test building with no building context, in context LoD 1.2 and in context LoD 2.2 (top to bottom)

3.5.2. Iterative running

This workflow is set up with the concept of scalability, thus multiple options for scaling the 3d calculations and the measurements to a large-scale execution have been explored. The workflow for executing these calculations is based on three steps:

1. Designing the workflow for a single building
2. Scaling the workflow to a predetermined set of buildings: this step allows for proof of concept, and it highlights weaknesses and errors.
3. Executing the workflow to a large-scale building dataset. This step proves scalability and allows for large-scale analyses and correlations with different design factors.

This scalability is tested with multiple methods, where computation time and complexity of data structures form the biggest challenge. To simplify complexity of data structures, a system where multiple inputs can be calculated in parallel by using the same code for the single building seems the most straightforward and thus appealing way. Other options that are explored are by making use of the data tree structure that grasshopper allows, using Python with Rhino inside or using the Grasshopper Pollination tool to run large scale.

3.5.3. Calculating m-EDI

The final calculation of m-EDI has been described by Cie (2020), and consists out of multiple steps to translate the LARK 9-bin irradiance calculations to a single melanopic EDI value. These steps are visualised in Figure 3-13, where the blue elements encompass a spectral distribution, and the white elements encompass a value. All distributions retrieved from the LARK (2023) post-processing tool are visualised in Figure 3-14.

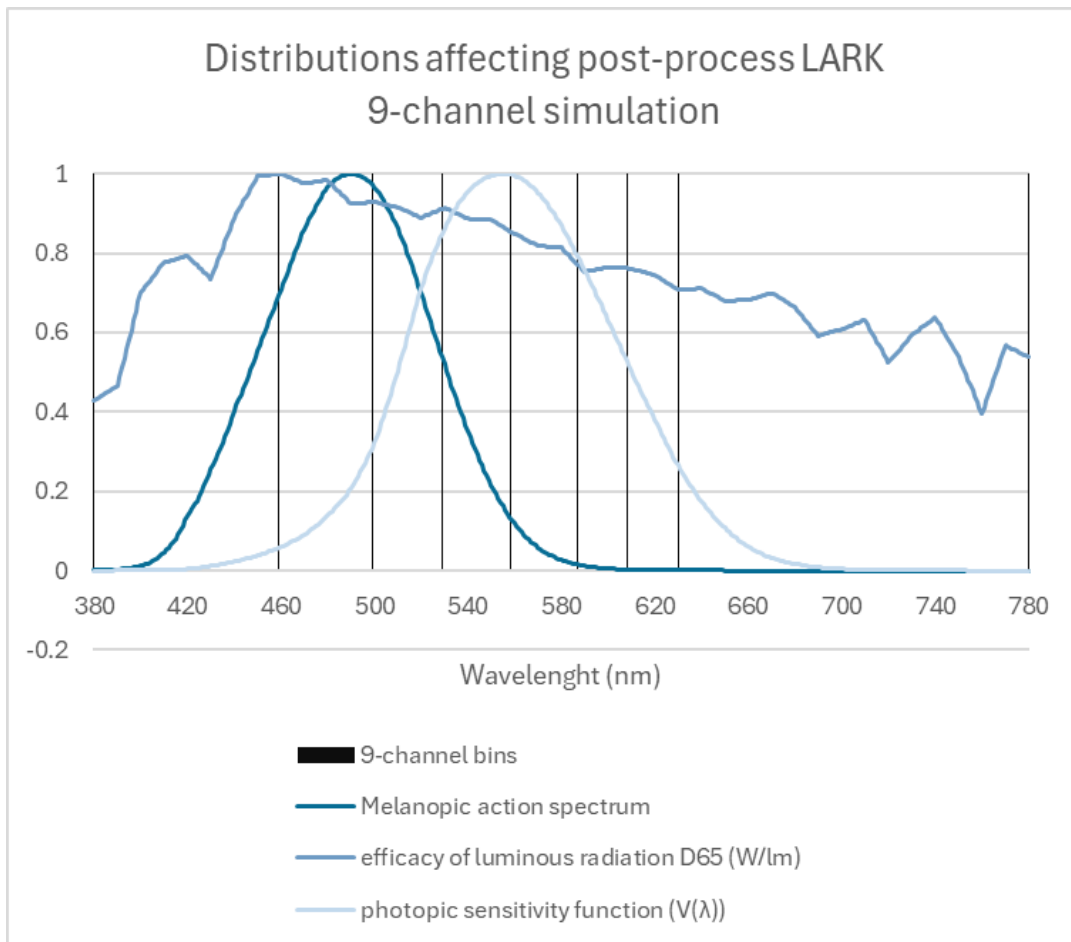


Figure 3-16 Spectral distributions relevant for m-EDI post-processing (data LARK, visualisation own source)

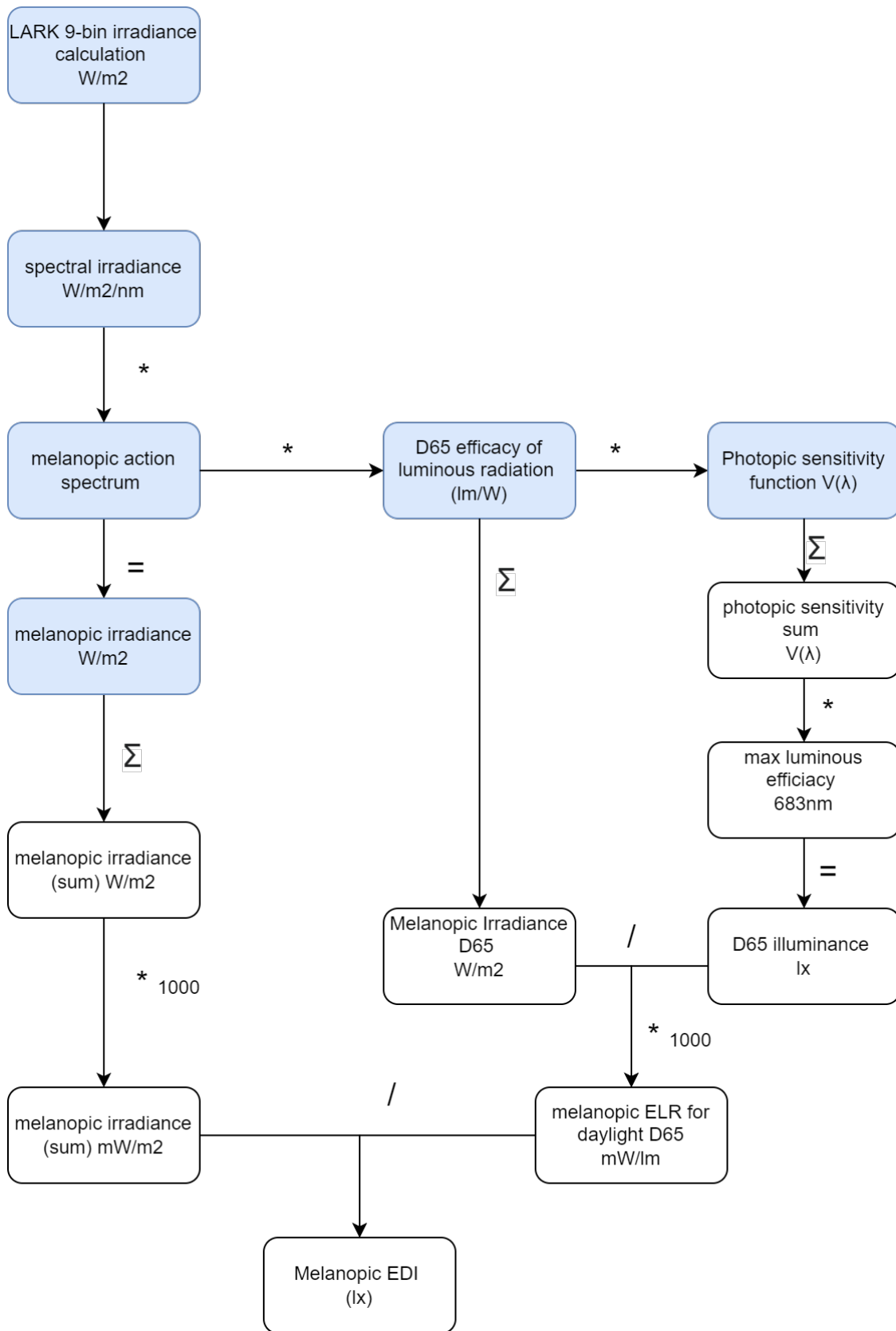


Figure 3-19 LARK 9-bin irradiance calculation to Melanopic EDI (own source)

4. Results

In this chapter, the results of the 3D reconstruction of the façade information and the lighting analysis are presented and key observations are provided. The chapter is subdivided into the four phases that have been distinguished in the methodology section with a partial result for each phase leading up to the next, and the results posed in the last phase.

4.1. Phase 1: geo information data preparation

For the city of Amsterdam, a single tile is picked and all geometries are stored in a 3D model (Rhinceros .3dm), as is visualised in Figure 4-1.. For the two-dimensional geometries, an extended buffer of 100m is added around the tile borders.

The building selection for which the lighting calculations are executed is made by consciously picking buildings that are not close to the edge of the analysis site and are oriented in the

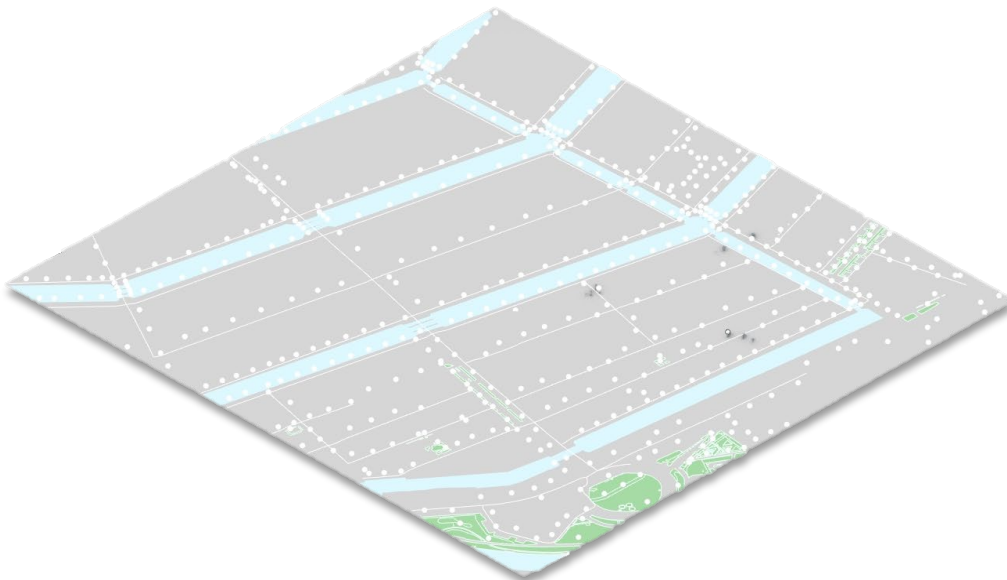


Figure 4-4 Surface water, green areas & street lighting positions, translated from GIS to Rhino

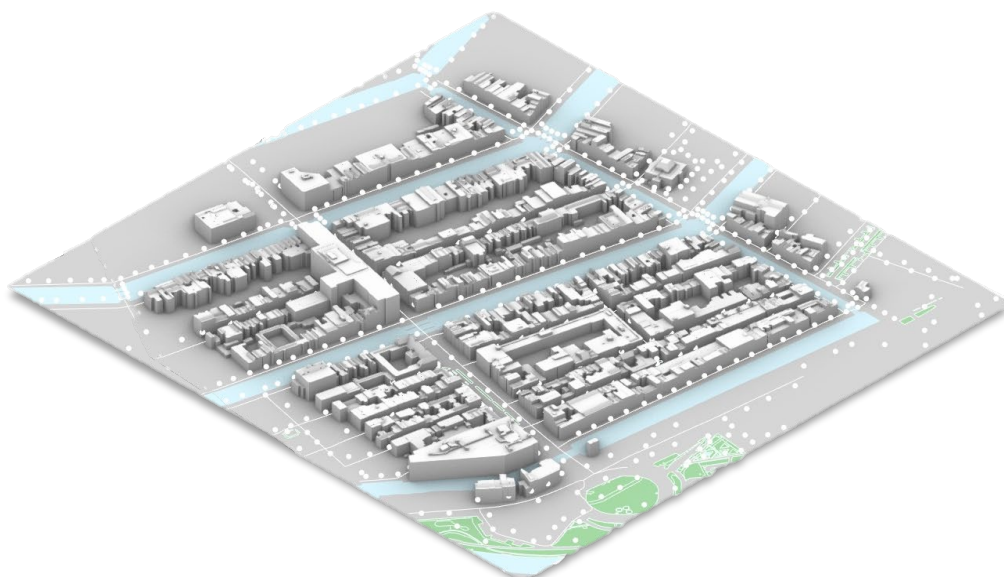


Figure 4-2 Building context on a high (2.2) level of detail added

direction of the contextual buildings, thus minimising the impact of available context on the lighting analyses.

Although the methodology of translation between filetypes has not been found feasible to automate, the relative placement fully matches that of the original datasets, and thus this won't impact the analysis results.

4.1.1. Description of output files

This phase results in a building tile with the simplified context, as described in the methods. The components of context include:

- Waterways
- Vegetation
- Lighting points
- Ground surface
- Building blocks LoD 1.2 (3D BAG)
- Building blocks LoD 2.2 (3D BAG), discretised:
 - a. With façade information
 - b. Without façade information

The building selection for quantitative analysis is a subset from the discretised building blocks in LoD 2.2 with the façade information available.

In this 3D model, street representations by line segments are included, as they are relevant for façade selection in phase 3. These lines are excluded from the lighting calculations.

All elements are saved within a single 3D model. For further retrieval within the lighting analysis environment each cluster of elements is grouped in a layer for easy application of material information in the Rhino Grasshopper environment.

4.2. Phase 2: Façade masks to dataset

For all available 810 façades and their façade masks, as retrieved from C. Eijgenstein (2020), the window information and associated floor level information are retrieved as described in the methodology. From the 810 files, 14 files returned no window information (depicted in Figure 4-3), and are thus filtered for further processing. The robustness of these masks will be covered in the discussion.

4.2.1. Performance of the façade clustering algorithm

For the 796 façades, 2752 floors have been identified based on the clustering algorithm as elaborated in the methodology. For these floors, a warning is posed when the value of the floor height is below the minimum legal floor height in the Netherlands, found at 2.2m for living spaces in the Netherlands (bouwbesluit, 2012). These warnings have been found to often occur more than once for individual buildings, where the buildings in Figure 4-3 show some of the errors. Next to these buildings with high warning count, 53 buildings turned out to have a floor level height less than 2.2m on their ground floor. For Amsterdam, this is no peculiarity, as souterrains are a common building feature in the city centre. Thus, the façade clustering plausibly returned accurate segments, but due to the nature of the building design results are misleading. It is to be noted that a good lighting analysis for these floor levels will return invalid results. 3DBAG lacks information regarding underground building components. A false

assumption of the ground floor height is made, and the relative sensor placement becomes inaccurate.

Three floors returned negative WWR values. As WWR values should not exceed the 0-1 range, these cases were not included in the case-study list. The façades that return negative floor height are visualised in Figure 4-3. As has been found in the CSV-output, the floor level that returns negative floor height values are initialised based on a window that lays below the floor level one iteration previous.

As is the case for the façade masks shown in Figure 4-3, the shape of the top floor is often inadequately estimated, resulting in wall areas that end up far above the assumed reality. An improvement to approach WWR results would be to subtract the green area from the estimated wall. For the window placement, this information is not relevant. For accurate WWR values, the presence of parapet gables in Amsterdam already impacts the accuracy that can be reached for the estimation of the wall area, especially for top floors. Thus, it is opted not to improve these estimations further.



Figure 4-5 Examples of facades with lack of window information (Eijgenstein, 2020)

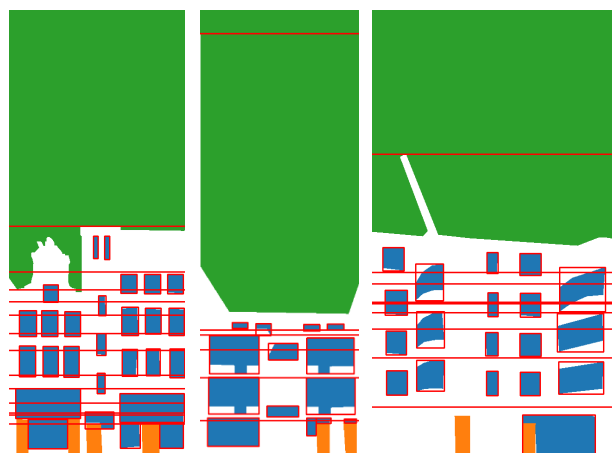


Figure 4-8 The three facade mask with a high warning count, due to low level heights and negative WWR (Eijgenstein, 2020 with adaptations)

4.2.2. Description of output files

For this phase, the following two output files are generated:

*.csv: a CSV file with all extracted façade information that is relevant for further analysis, containing the following columns:

- **Window count (n)**: the number of windows on this floor level. This information would be relevant for generating windows within Grasshopper, using the Honeybee 'glazing based on ratio' component.
- **Indices (n)**: From the list of all windows that are retrieved from the façade mask, this list comprises the indices of the windows that correspond to this floor level. This information is an extra measure so the window boundaries will be retrieved correctly in Grasshopper.
- **Window boundary (px, px)**: These values represent the highest top and the lowest bottom of all windows that are within the floor level. These are the basis for floor-level separation, as the top and bottom value will not share overlap with other windows within this mask, and thus a floor level separation is possible.
- **Window placement (px ,px, px, px)**: the window boundaries that are retrieved and that belong to this façade piece. The pixels represent the X and Y position of the bottom corner & the width and height of the window, respectively.
- **Average window height (px)**: the average of the heights for all windows on this floor level. This information would be relevant for generating windows within Grasshopper, using the Honeybee 'glazing based on ratio' component.
- **Floor level (px)**: The number of pixels that indicate where the floor level is estimated to be. Relative to the top of the picture (900px).
- **Ceiling level (px)**: the number of pixels that indicate where the ceiling level is estimated to be.
- **Floor height (px)**: the number of pixels that indicate the difference between ceiling level and floor level.
- **Average sill height (px)**: This information would be relevant for generating windows within Grasshopper, using the Honeybee 'glazing based on ratio' component.
- **Window area (px * px)**: the sum calculated area of all windows found.
- **Wall area (px * px)**: the calculated wall area.
- **Window-to-wall ratio (WWR) (n)**: The ratio between window area and total wall area.
 - o $WWR = W_iA/W_aA$

*.png: the façade mask as provided by Eijgenstein (2020), enriched with:

- A visualisation of the perpendicular window boundaries;
- Floor level estimations.

The data found in these CSV files is used for window implementation in the next step. The enriched façade mask images are solely generated to provide visual feedback of the effectiveness of the model.

4.3. Phase 3: 3D window reconstruction by projection

A method has been conducted to reconstruct the 2-dimensional windows to 3-dimensional objects, with the aim for scalability. For the development of this method, a single building has been used as a test object. With this proof of concept, the scalability is tested with six buildings,

allowing for good traceability of warnings and errors, and thus allocating the vulnerabilities within this workflow. As last, the workflow is tested for the full set of 3D data.

The six buildings that were chosen are all positioned outside of the direct influence of trees, and cover façade orientations in four directions. Within the analysis plot, a variation in street width has been opted where possible, but with the limited typological variations of the area, a wide coverage in variation has not been found.

The 3D buildings are all retrieved from 3DBAG. As the RhinoCityJSON (2022) plugin allows for reading both the CityJSON objects as the attributes that are associated with these. Within 3DBAG, the Building IDs as found in BAG are one of the attributes: The individual buildings have been saved with their Building IDs as object name, so that automation of assigning the correct façade element (with the corresponding building ID saved in the picture title) with the 3D building became feasible. The found façade masks for the 6 allocated geometries have been shown in Figure 4-4. As can be seen, the floor level automation returns favourable results: for these 6 façade masks, all but one floor is positioned on reasonable heights. The first floor for the façade associated with building ID 363100012180112 shows some overlap with the window. This could be due to the high difference in the window heights on the floor below this; the floor positioning is executed with the average window position as an input, and thus all floor level estimates with high variation of window heights below them are estimated slightly lower than reasonable. For further recommendations, an approach using the top window height would be suggested.

The floor level splitting returned successful for all three scales. The floor level splitting for all building elements is shown in Figure 4-6 and Figure 4-7.

A limit that has been found for generating window placement and later lighting calculations, is the watertightness of the available geometry. One of the selected buildings returned a negative response to the watertightness and the simple capping methods within grasshopper returned an error. With a translation from Boundary Representation (BREP) to mesh and back to BREP this specific issue is resolvable, but for this workflow it is opted to take this building out of consideration for further implementation. The buildings selected are visualised in Figure 4-5 building selection and window construction visualised in Figure 4-5.

With the translation between the pixel-based information towards the 3D window construction, the scale between pixels and meters is retrieved from the consistent façade mask height. As follows from Eijgenstein's (2020) information, each façade mask is cut off at a height of 30

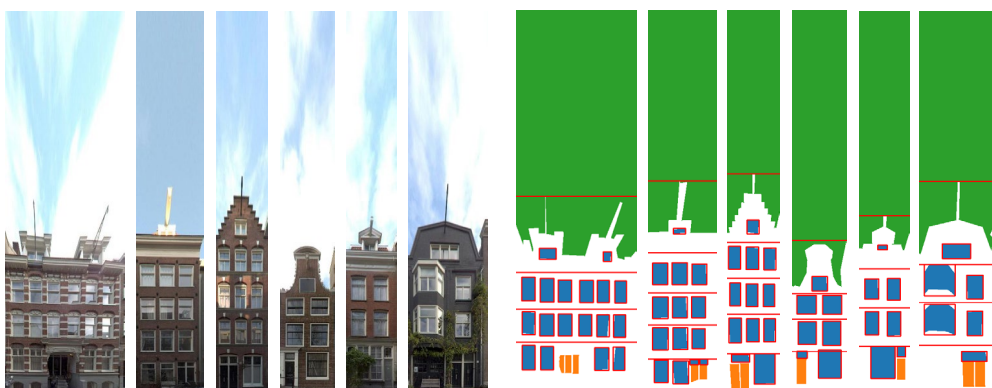


Figure 4-9 comparison of original facade pictures with the façade masks, displaying retrieved window boundaries and estimated floor levels (Eijgenstein, 2020 with adaptations)

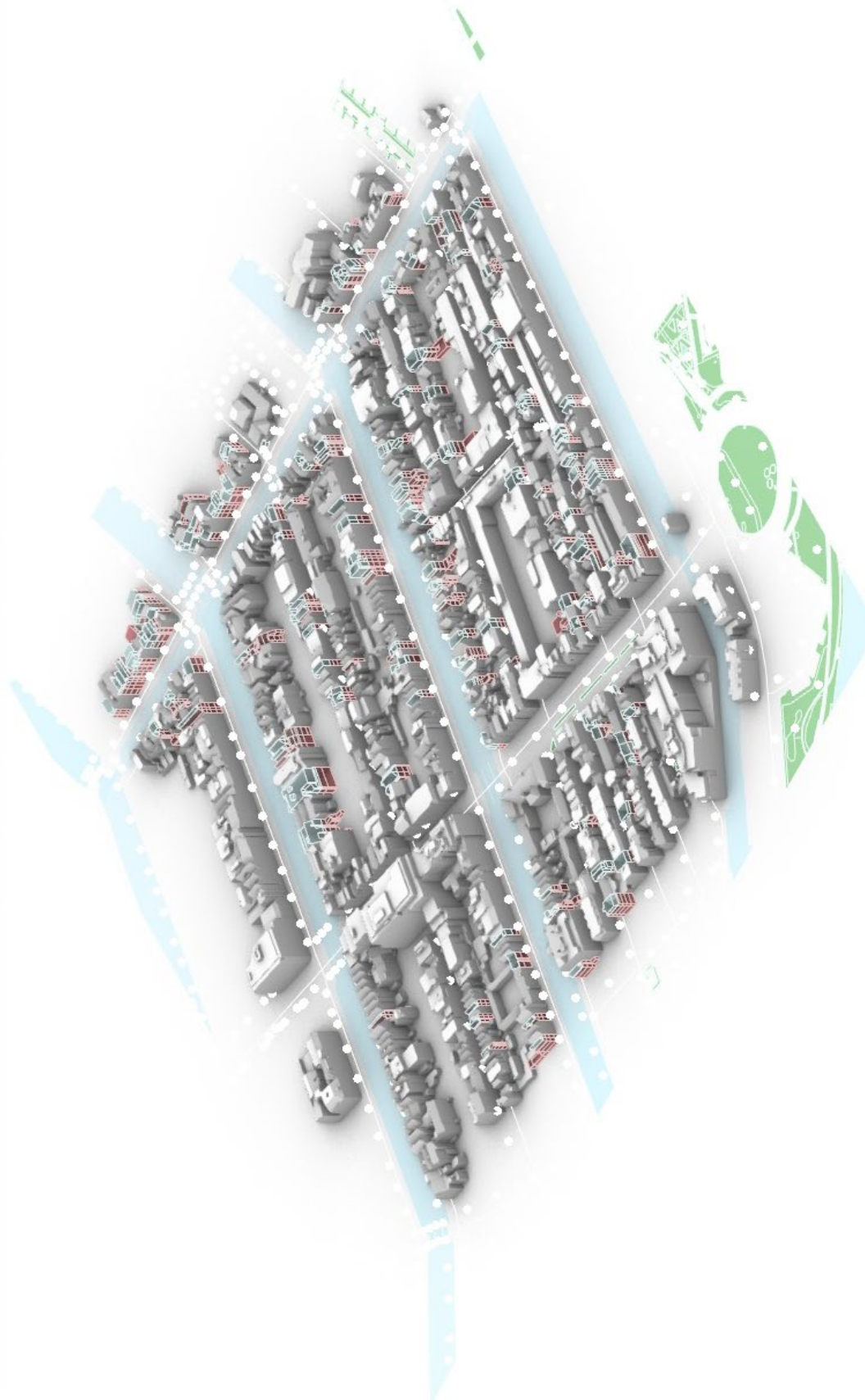


Figure 4-10 large-scale floor level splitting

meters, which corresponds to a pixel count of 900. Using this scaling factor for the masks towards the 3D environment returns high accuracy of 3D window placement.

By projecting both the existing façade elements and the window information onto a plane, thus allocating the overlap between each window and each façade element, a 3D projection of the window information onto all wall surfaces that are within view from the street is made. The original wall elements are then split by the projected window curves, which are grouped into two lists: ‘wall elements’; for the geometries outside of the curves, and ‘window elements’; for the geometries inside of the curves.





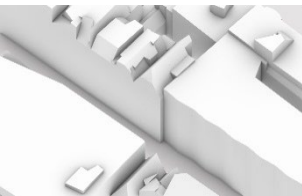
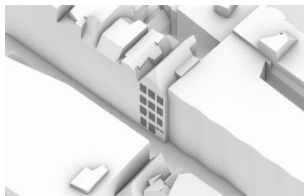

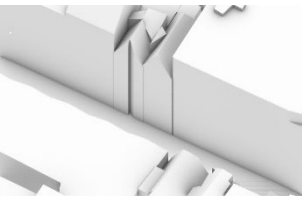
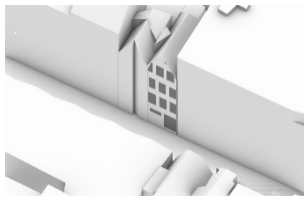

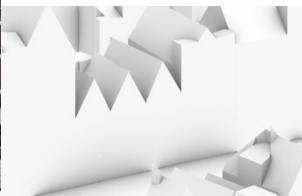
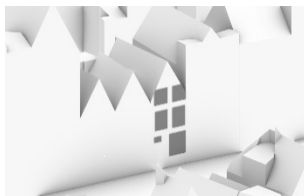

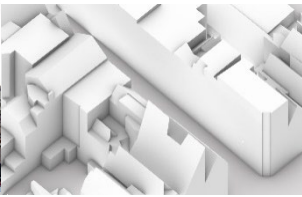

<p>Building 1 Building ID: 36310001217915 1</p>			
<p>Building 2 Building ID: 36310001217952 4</p>			
<p>Building 3 Building ID: 36310001217951 6</p>			
<p>Building 4 Building ID: 36310001218011 2</p>			
<p>Building 5 Building ID: 36310001217919 7</p>			

Table 6 Building selection and window construction visualised (google maps, 2024 and own source)

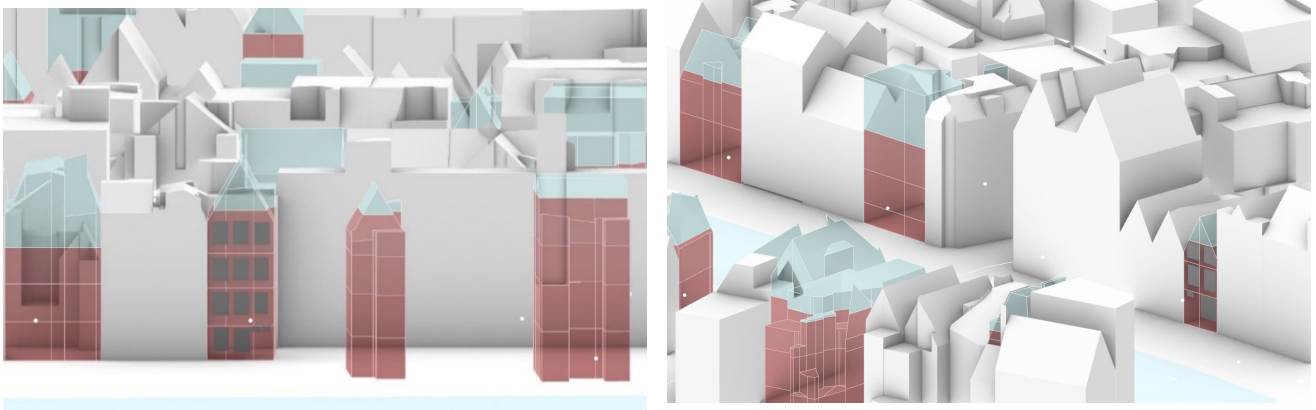


Figure 4-11 Floor level splitting returned similar results for the large-scale assessment as for the 5-buildings

4.3.1. Description of output files

For this phase, the following building elements are retrieved and separated for further analysis. For the workflow of the lighting analysis, the distinction of different material types is relevant, and thus the separation of the following components is made;

- Ceiling: a polygon closing the top of the floor level. In case of the top level of the building, the ceiling returns zero as the distinction between ceiling and wall cannot be made.
- Floor: a polygon closing the bottom of the floor level. For the ground floor level, the horizontal surface closing the geometry on $z=0$ is used.
- Windows: all original building elements that fall within the projection of the window curves.
- Walls: all original building elements that fall outside of the projection of the window curves.

These separations have been executed for the 6 reference buildings.

Rewriting the model for implementing Grasshopper tree structures has been the most effective approach. Although it did not produce the window geometries within the given time, the method successfully adapted geometry on a large scale. Floor-level splitting and façade selection for window projection yielded good results (Figure 4-7). However, for lighting modelling, specific façade-geometries are a minimum, thus the five retrieved geometries will be used for further calculations.

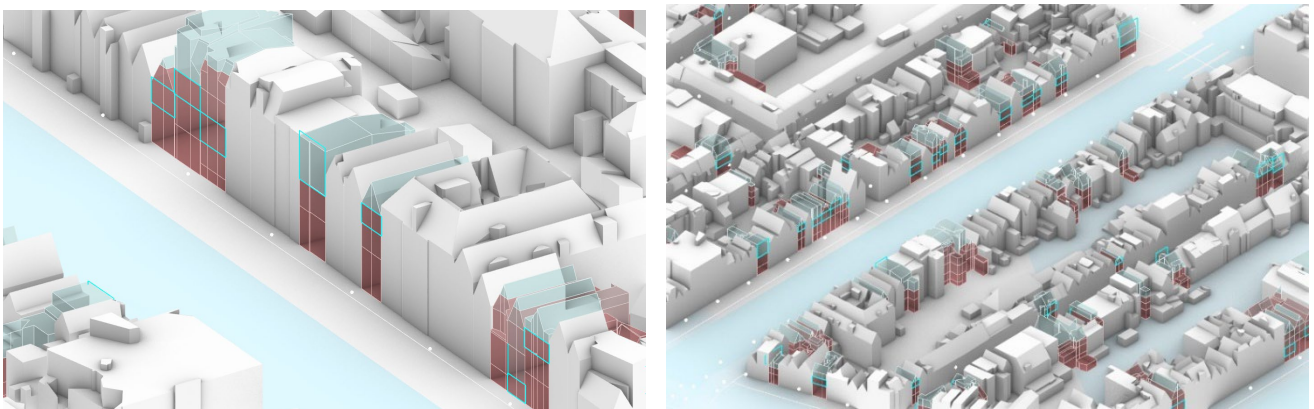


Figure 4-12 Selection of window plane, per floor level (level 3 selected)

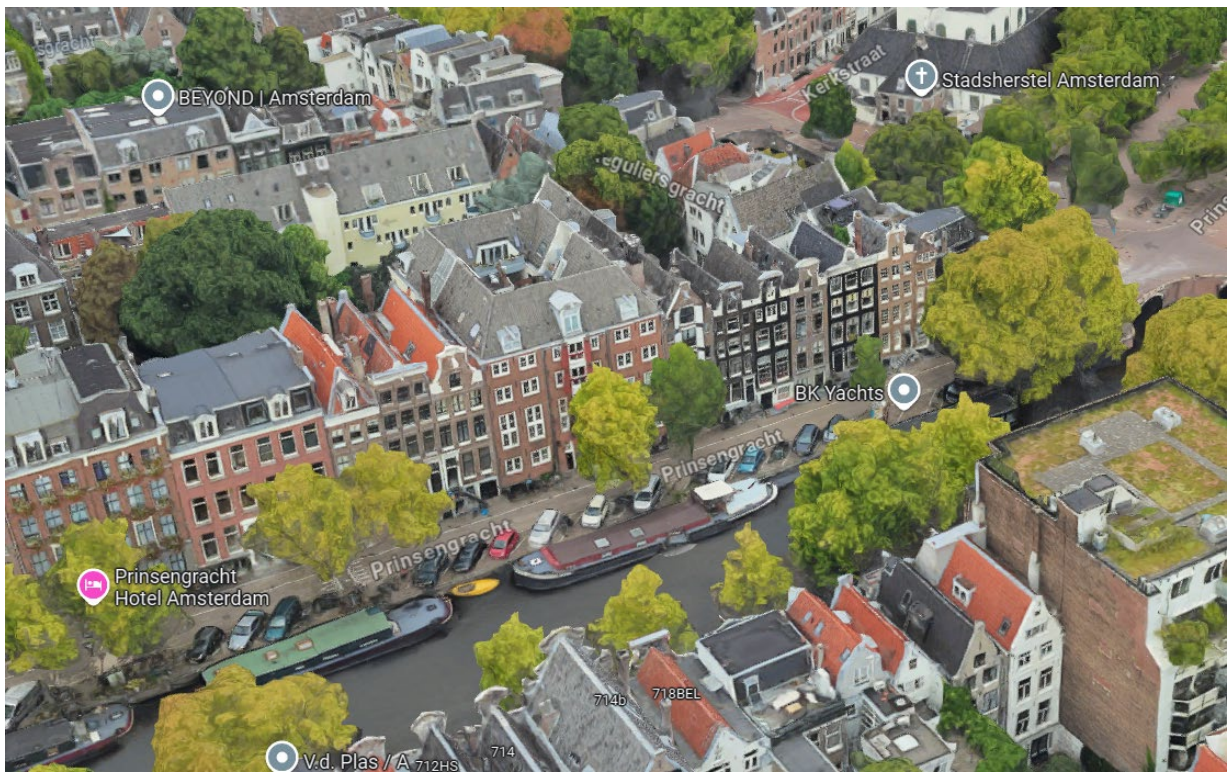
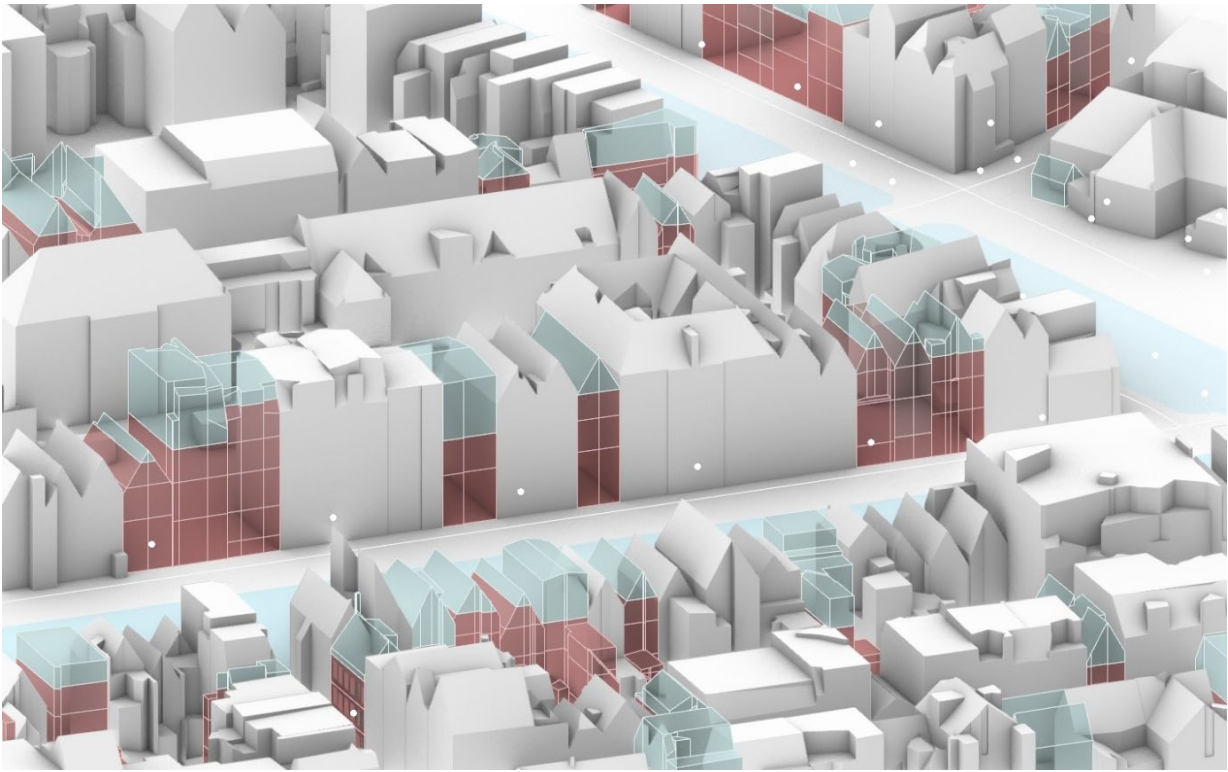


Figure 4-13 Split level buildings, visualized side by side with google maps 3D image (google, 2024)

4.4. Phase 4: Lighting modelling

With the 5 retrieved geometries, lighting analyses are executed in line with the methods described in the methodology. In Appendix 7.6, the results for the five reference buildings are shown in a table format. Before the full-scale lighting analysis, sample analyses are executed for two means:

- To test the accuracy of the measurements;
- To test the impact of the individual design factors on the availability of circadian lighting.

These tests are executed for Building 2, for a single floor or all floors where variations in height could be relevant (visualised in Figure 4-10).

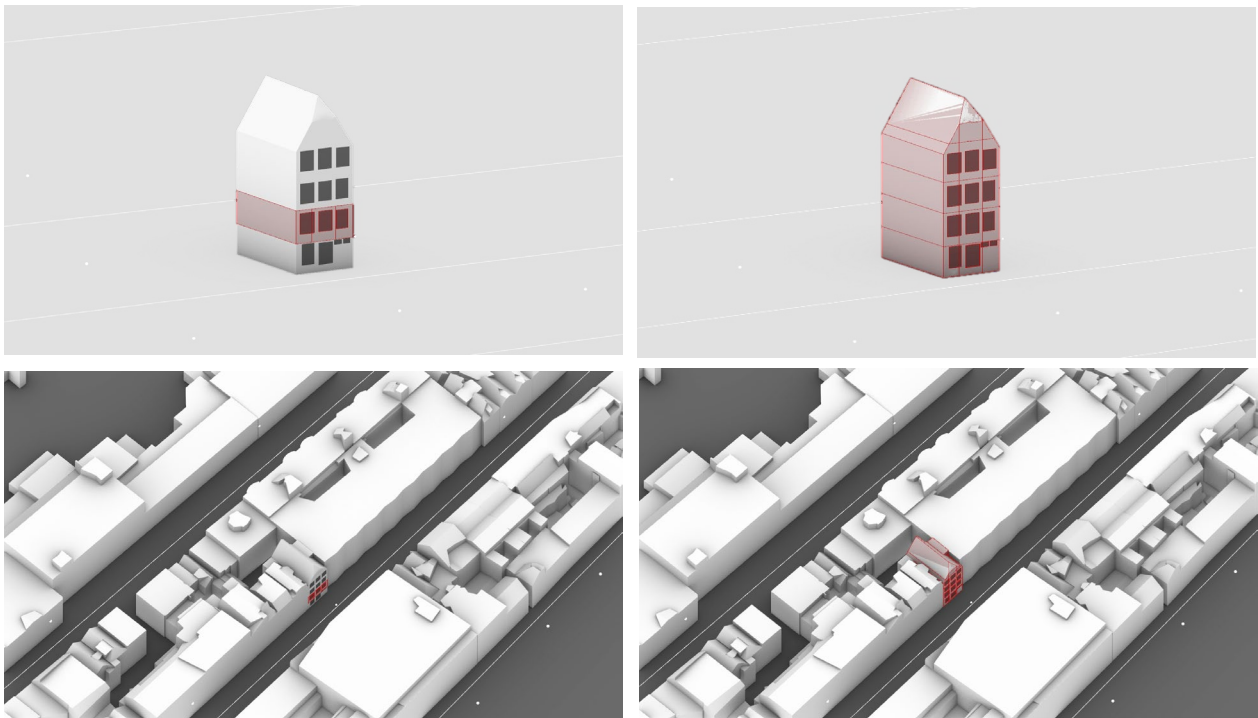


Figure 4-14 Single floor test (left) single building test (right), visualised in their urban context (bottom)

Before, a test run is done to check the impact of the post-processing on the final retrieved m-EDI values (inputs: simulation setup for single floor, IES file 3, LARK SPD). The distributions retrieved from the LARK (2023) post-processing tool, the 9-channel irradiance output and the final Melanopic illuminance are visualised in Figure 4-10.

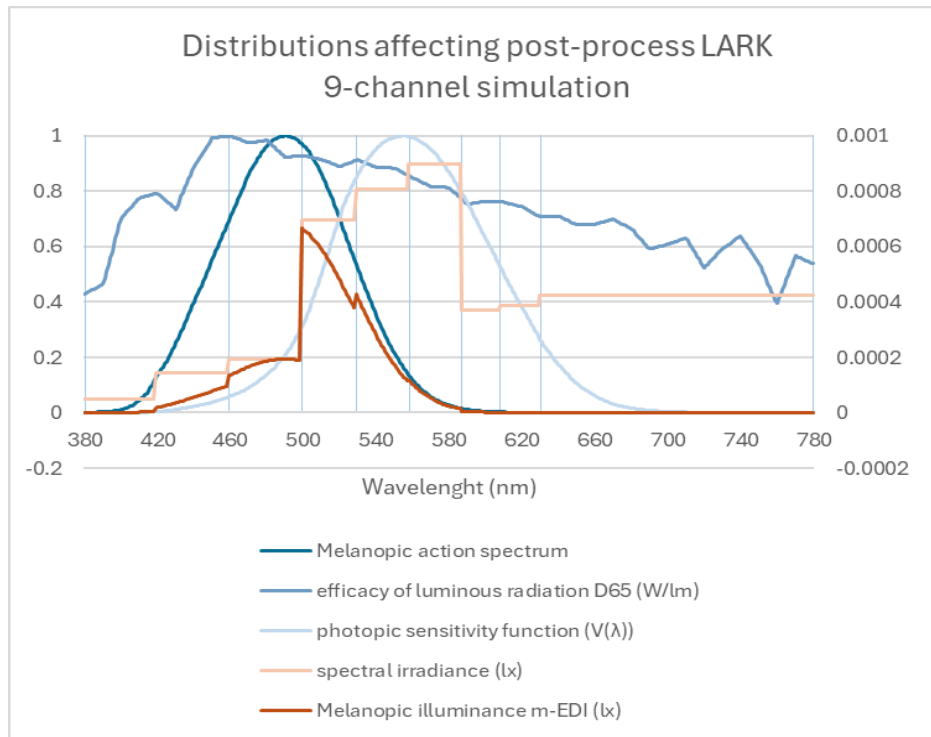


Figure 4-15 LARK post processing

4.4.1. Consistency tests

To check for consistency of the results, 10 runs are executed for a single floor, single point in time (21st of June, 13.00), and results of each of the 9 colour channels are separated. This has been done both for the electric light (3428lm) and the daylight setting. The standard deviation found for each channel is found below 1.1% (Figure 4-15). For electric light, the accuracy is even higher, where the standard deviations per channel fall well below 0.02%. These settings are thus considered adequate, and further analysis is done with these settings. When comparing results of other analyses, this deviation should be considered.

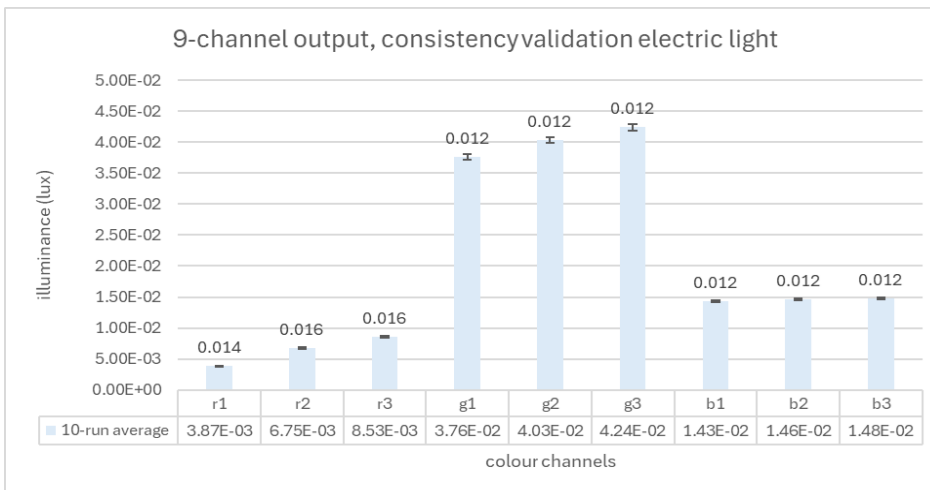
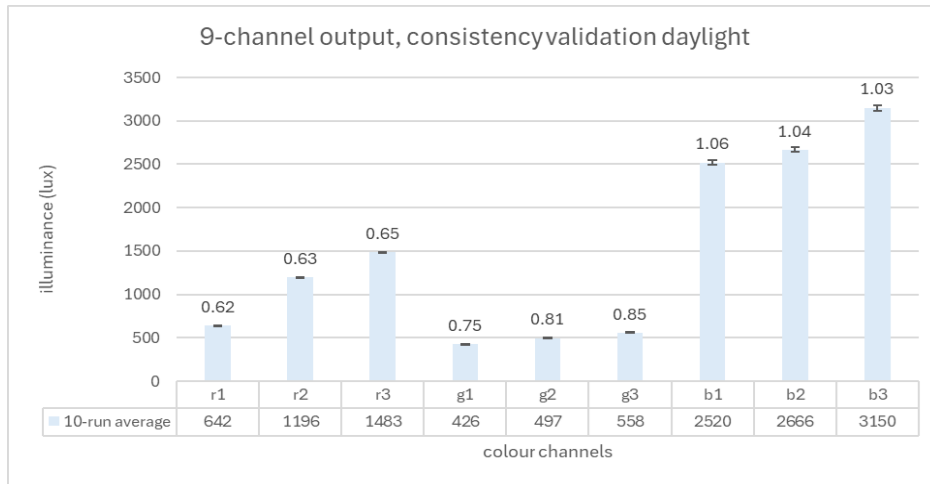


Figure 4-18 Consistency tests of radiance 9-channel calculation (top: consistency test of daylight. Bottom: consistency test of artificial light)

4.4.2. Lighting inputs

4.4.2.1. Light source

The variations in light sources are described in the methods. The scientific parameters that are associated with the light source are intensity, spectrum, timing, duration and contrast. Within the model, the factors that form the input of the light source are:

- The spatial configuration of the light source. This is dependent on the point in time for which the measurement is executed, represented by Hour of Year (HoY) values that summarise the time and date of the measurement. This affects the relative positioning of the sun and the distribution of this light source in the sky. For artificial lighting in this simulation, time is less relevant: the spatial configuration will be consistent and only rely on whether the lighting is turned on or off (depending on the natural lighting availability).
- The SPD: the spectral power distribution of the light source within the scope of visible wavelengths.

Artificial light

With three optically consistent light distributions of various intensities, the results show to be approaching linear correlation between lighting intensity and measured circadian lighting (Figure 4-13). The impact of both the light source and the weighing factors are visualised in Table 7.

In the LARK template file, a 9-bin weighing factor for photopic illuminance is implemented. Jung et al. (2023) suggest a melanopic weighing factor. Both of these weighing factors have been compared with measurements with no weighing factor to find the influence of these factors on the result. These can be found in Figure 4-14.

		light source		
		886 lm	2174 lm	3612 lm
No factor	Level 0	0.05		0.11
melanopic factor		0.04		0.11
template factor		0.04		0.21
No factor	Level 1	1.05		2.47
melanopic factor		1.04		2.48
template factor		1.05		2.47
No factor	Level 2	0.00		0.00
melanopic factor		0.00		0.00
template factor		0.00		0.00
No factor	Level 3	0.00		0.00
melanopic factor		0.00		0.00
template factor		0.00		0.00
No factor	Level 4	0.00		0.00
melanopic factor		0.00		0.00
template factor		0.00		0.00

Table 8 single building test: impact of IES light source and weighing factors

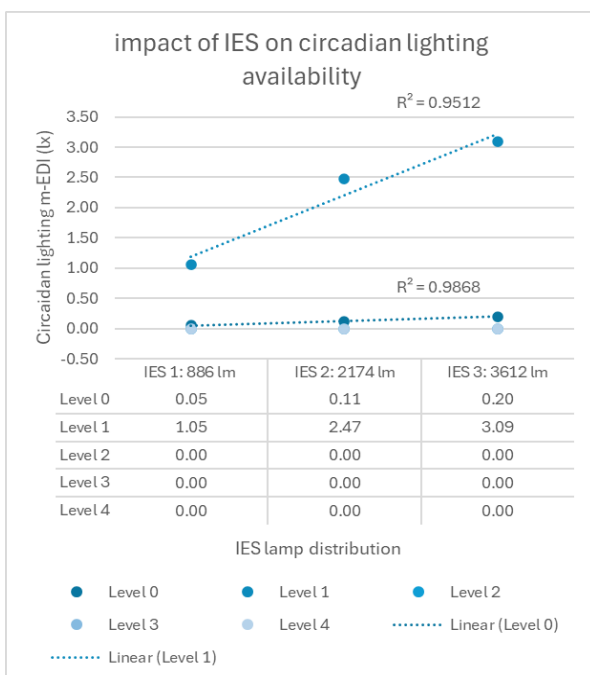


Figure 4-25 The impact of various IES inputs on the circadian lighting availability

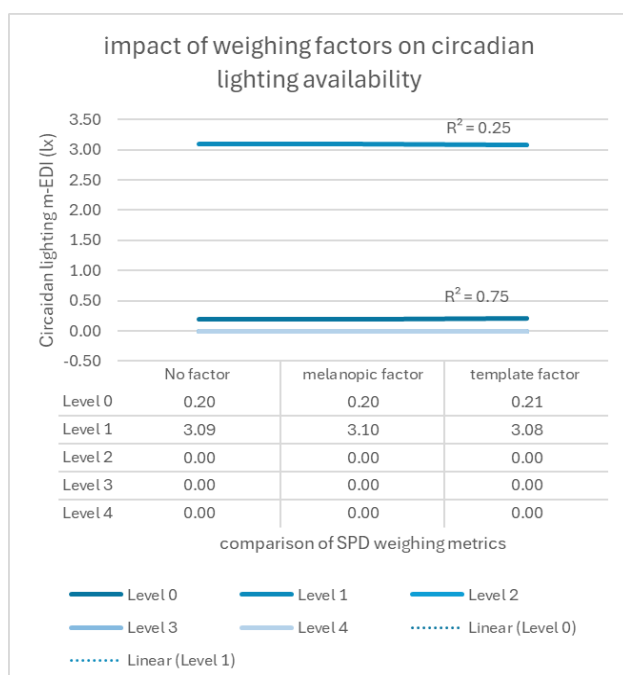


Figure 4-24 The impact of weighing factors on circadian lighting availability

The impact of SPD on circadian lighting is visualised in Figure 4-15 (IES file 3, test single building) What can be seen is that the difference between the three options approaches 0 for all the five floors.

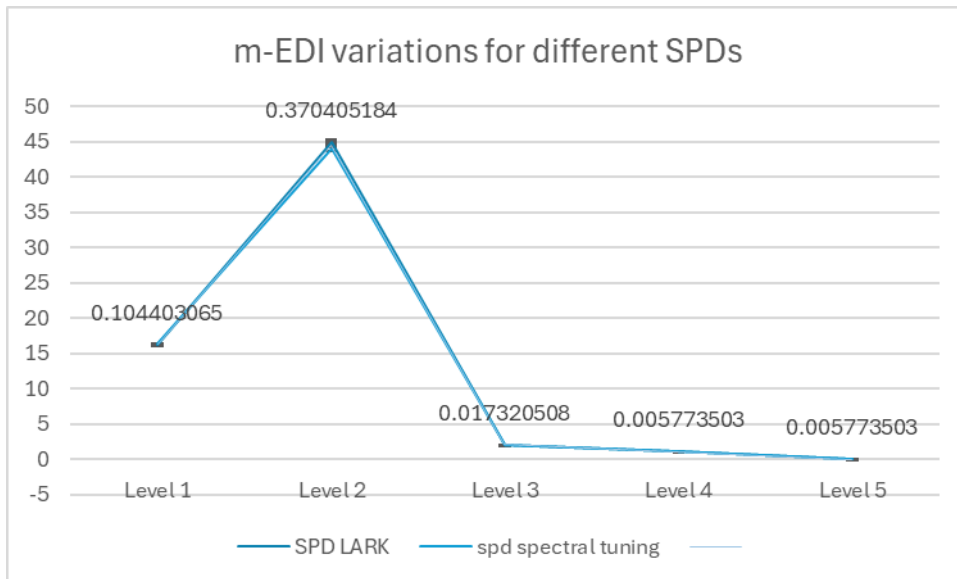


Figure 4-27 m-EDI result variations for different SPDs

To test the accuracy of the light source, a run is executed with the light source 1 meter above the measurement point. As described in the methods, this test is executed to see if the melanopic illuminance values found align with the expected values based on the luminance of the light source (about 1/12th of the luminous flux of the light source).

The results obtained are:

- 326.11 lx m-EDI for light source 3 (estimated around 300lx m-EDI)
- 186.33 lx m-EDI for light source 2 (estimated around 200lx m-EDI)
- 76.23 lx m-EDI for light source 1 (estimated around 75 lx m-EDI)

This variation can be considered minimal, due to the number of factors potentially influencing the measurement (light source direction, light source spatial distribution, light source spectral distribution, material reflectance values, measurement orientation).

Natural light

To test the impact of weather conditions on circadian rhythm, the TAU clear sky calculations are compared with a clouded sky representative, retrieved from the weather file. As described in the methods, using a weather file to find appropriate sky conditions results in different measurement days for each hour of the year measured. The sky conditions retrieved are visualised in Figure 4-16 .

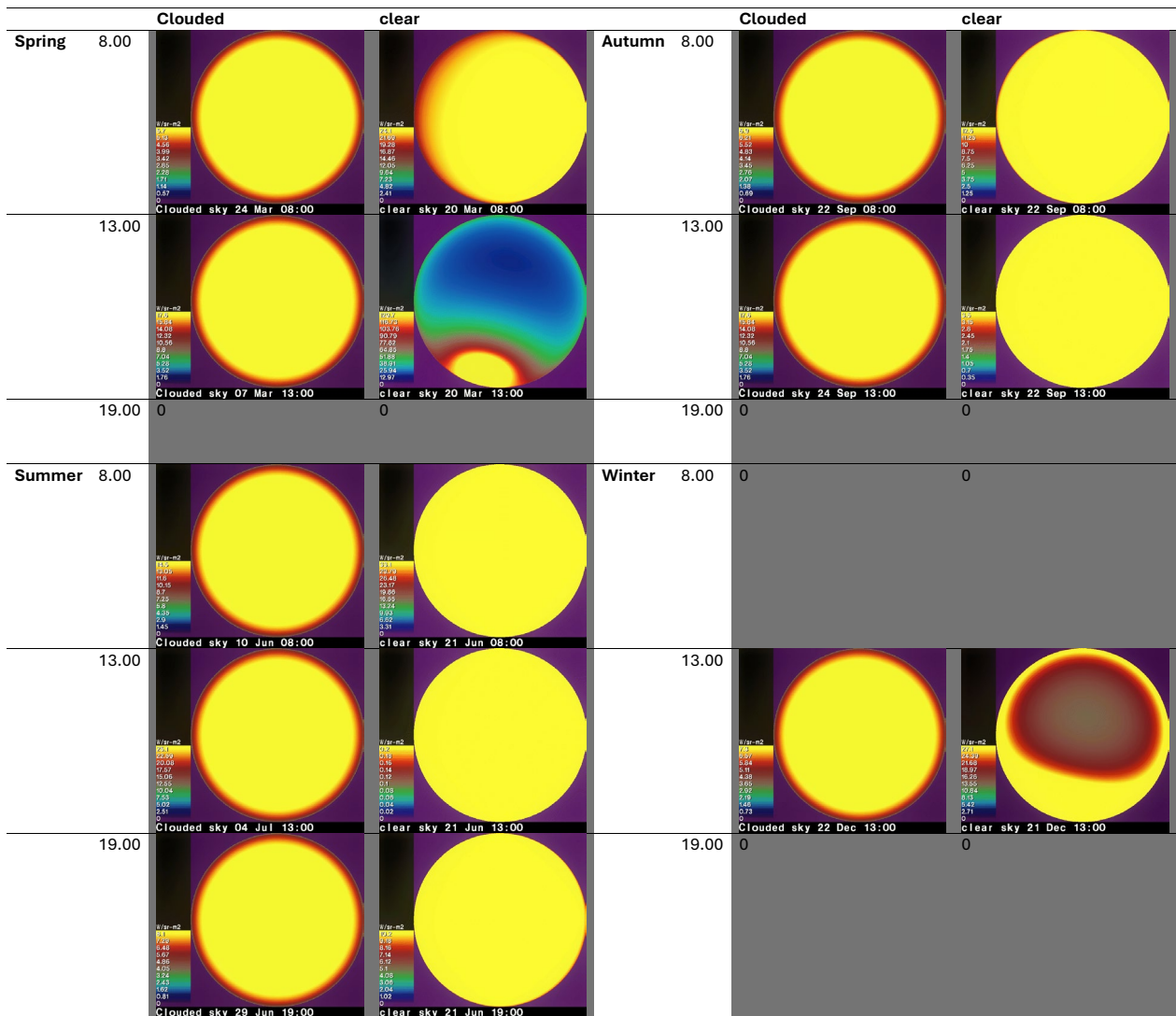


Figure 4-28 Sky visualisations

4.4.3. The role of the design factors on circadian lighting availability

Within a simulation that implements various design factors within one simulation, a general quality of the measured location can be derived, but the impact of individual design factors is still hard to determine. To test what the influence is of these various factors, additional tests are executed where possible for testing each factor individually.

The impact of the façade and the impact of artificial light are tested on the large-scale building model to retrieve an answer on the research question.

The factors of which the direct impact on circadian lighting have been proven by literature and that have thus been implemented as a constant in this simulation are out of this test. These are window characteristics, indoor reflectance and recipients' positioning. Thus, the factors that will be tested are urban building context and urban context reflectance.

4.4.3.1. *Urban context reflectance*

The impact of urban context reflectance is tested by comparing the simulated urban context materiality with a situation of all white context materiality and a situation with all black context materiality. For a single floor test (clear sky, 8.00 21 June) the measurements found are 2236818 lx m-EDI for white context (Macbeth white, SpectralDB, 2024), 2234994 lx m-EDI for black context (Dupont midnight black, SpectralDB, 2024) and 2237526 lx m-EDI for the fully simulated context. The difference with the full context is a reduction of 409 lx m-EDI and 1290 lx m-EDI for white and black context respectively.

4.4.3.2. *Urban building context*

The variations in results between LoD 1.2 and LoD 2.2 are compared for all floors of the test building, to test the effect of context simplification for the daylight analysis. As both the angle of daylight incidence and the elevation of the measurement position affect these measurement results, the validation is run for all levels of the test model, and for all 16 points in time that are defined. The nighttime-results are removed from the analysis, as daylight is not available during this period of time, the results are consistently 0 and thus irrelevant for further analysis.

Presumed is that the setup with LoD 1.2 will return slightly lower values, as due to the uniform heights for each volume, the LoD 1.2 results in higher volumes than the more detailed variant.

As demonstrated in Figure 4-16, this presumption can be confirmed. Especially for higher floor levels, the relative difference between the results with context of LoD 1.2 and LoD 2.2 increase. For comparison over the seasons, a trend in different outcomes cannot be found.

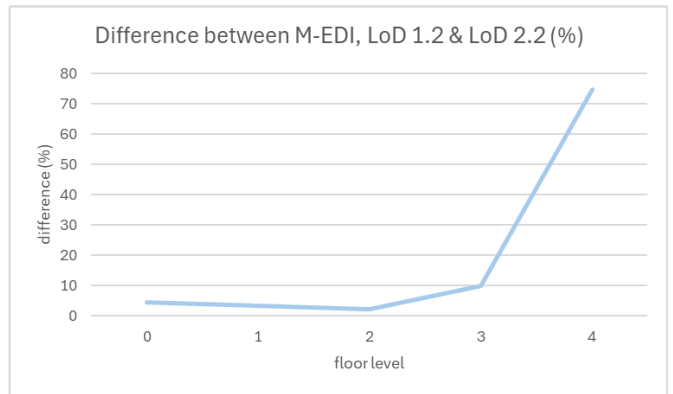
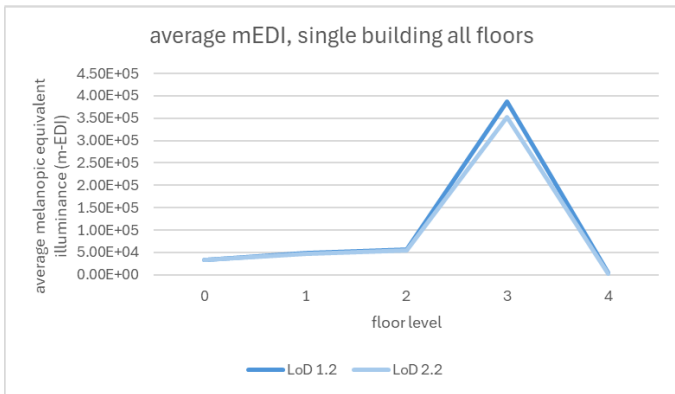
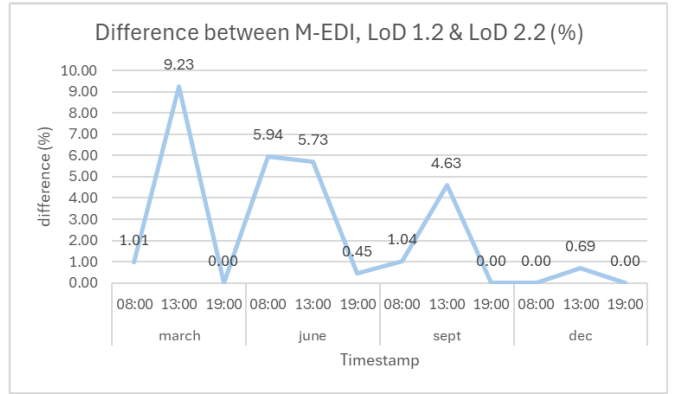
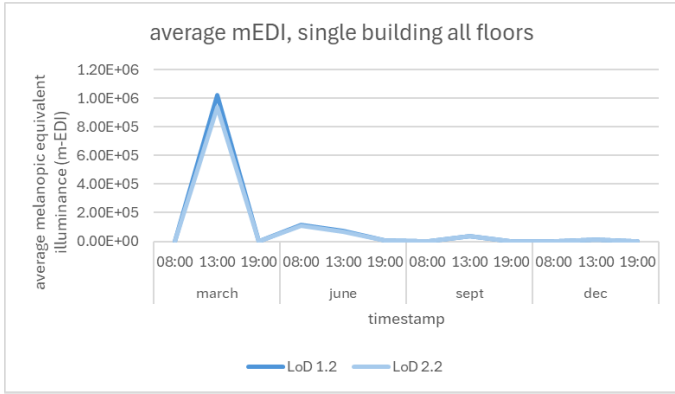


Figure 4-29 Comparison in daylight availability measurements for two contextual levels of detail (LoD1.2, LoD2.2)

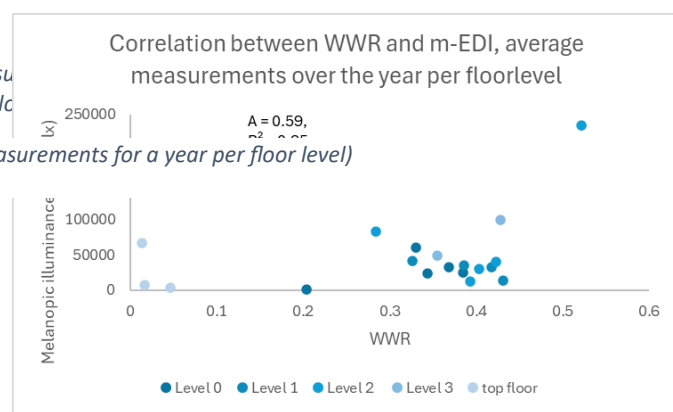
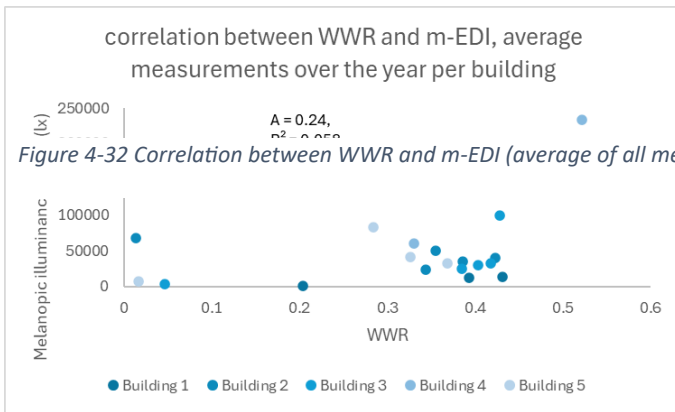


Figure 4-32 Correlation between WWR and m-EDI (average of all measurements for a year per floor level)

4.4.4. General circadian lighting results

To address the impact of façade and artificial lighting design on circadian health in urban contexts, measurements were taken at 16 timestamps for each floor across 5 reference buildings. All measurement results are shown in appendix 7.6.

4.4.4.1. Façade:

The impact of façade design is measured by comparing the full set of results with the WWR values of the façade as calculated in phase 2. With 5 buildings, 3-5 floor levels per building and 16 timestamps, 340 daylight measurements are executed. To find the impact of the façade on these measurements, the average m-EDI result for all 16 timestamps is taken and compared with the WWR as calculated in phase 2. These are grouped per building (reference 1) and per floor level (reference 2). In reference 2, the top floors are taken out of consideration for calculation of the correlation values. Both the sensor placement as the calculated WWR for the top floors are found to have many inaccuracies. This will be discussed in the limitations section.

Building ID	distance between closest street lantern & centre façade	façade orientation (Azimuth ° from North)
Building 1 363100012179197	8	76.1
Building 2 363100012179151	2.3	-103
Building 3 363100012180112	9.6	94
Building 4 363100012179524	30.1	-10.9
Building 5 363100012179516	20.5	9

Figure 4-35 Design factors potentially affecting circadian lighting results

The results show that in general the impact of daylight on circadian lighting availability is found consistently sufficient for mid-day light. Fluctuations that relate with the seasonal fluctuations are more evident.

4.4.4.2. Artificial light at night

Visualised in Figure 4-11 Visualisation of melanopic illuminance (m-EDI) for a selection of buildings is the impact of streetlighting on the indoor Melanopic Equivalent Daylight Illuminance, with the street lighting settings on high intensity (3428lm, 42W).

The results show that the indoor illumination because of street lighting is able to reach undesirable levels of artificial light on indoor environments. With lighting placement near buildings, as shown in the case of Building 1, the artificial lighting values well exceed appropriate levels for m-EDI by night, and even the levels for evening exposure are surpassed in this situation.

A relationship is observed between the proximity of a light source and its impact on circadian light measurements. Specifically, the downward orientation of lamps increases their effect on higher floor levels when positioned closer to a building. Conversely, when the light source is placed farther away, its impact becomes more concentrated on the lower floors. This suggests that both the distance of the light source and its directional orientation play significant roles in determining how light exposure is distributed, with a greater effect on lower floors when the source is positioned farther from the building.

Due to the limited size of the generated circadian lighting results, correlations between various design factors cannot be found with strong significance, and further information is needed to investigate what factors play a role in this.

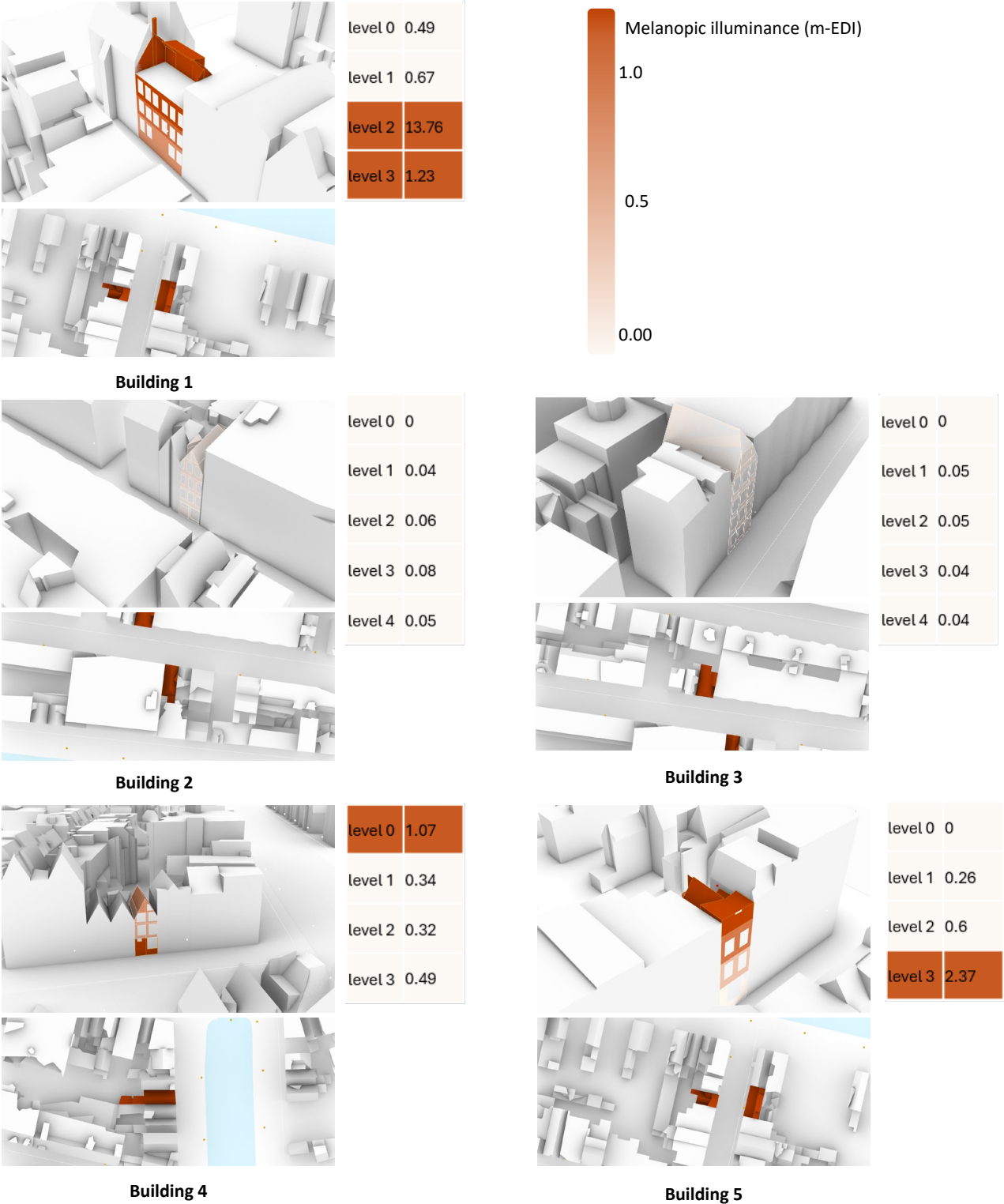


Figure 4-36 Visualisation of ALAN simulated for the selected buildings

5. discussion

In this chapter, the research approach and the findings of the research are discussed and placed in the scope of their design- and academic implications. The results are analysed and compared with literature. Limitations in the methods are discussed and based on these limitations, recommendations for further research opportunities are done. After this, the design implications this research might have on the field of urban planning and architecture are discussed.

First, a short interpretation of the sub-results for each of the phases is discussed, whereafter the final circadian lighting results can be placed into context.

5.1. Interpretation of results

The results of phase one show that the availability of urban level data is high enough to construct a large-scale 3D simulation environment, with a level of detail that encompasses all the distinguished factors influencing circadian lighting availability in the built environment up until the detail level of the façade. These sources are all openly available on the web and cover all The Netherlands, showing the scalability and reusability of this model for different places and cities within this area.

The results of phase two show that the improvement of the level of detail that is available in these large-scale data sources could be enriched with a method with large-scale data coverage. For façade reconstruction, using street-view imaging for enriching building information that is now based on horizontal single-plane data (LiDAR-based height maps for 3D building reconstruction) could enrich the 3D building reconstruction accuracy with information on a vertical plane. With the façade masks derived by Eigensteijn (2020) from Google street imaging, The retrieval of window information that align with the building IDs of 3D BAG has been tested on a limited dataset (810 façade masks, each associated with a different building). The window information forms the basis of the indoor floor level estimation, potentially enhancing the level of detail of the 3D dataset even further.

The results of phase 3 prove the feasibility of implementing this façade- and floor level information in the 3D environment. Splitting the buildings vertically at estimated floor level heights, adding floors and determining which façade has the most potential of being the façade for which window information is available has been proven successful for all buildings tested. Window splitting has been successfully executed for 5 example buildings, as the workflow for façade splitting required an individual building approach. For each individual building, the different façade elements have been labelled with their object type in Rhino Grasshopper.

The results of phase 4 are the measurements of melanopic equivalent daylight illuminance D65 (m-EDI, lx) for all individual floor levels in the example buildings, for 16 times and for a simulation with street lighting, which can be associated with the timeslots where no daylight measurements were found.

Hypothesised is that design factors could have a positive impact on the potential instability of diurnal patterns and compensate for the negative effects of the urbanised built environment on the availability of circadian light. The results are compared with the metric proposed by Brown et al. (2022):

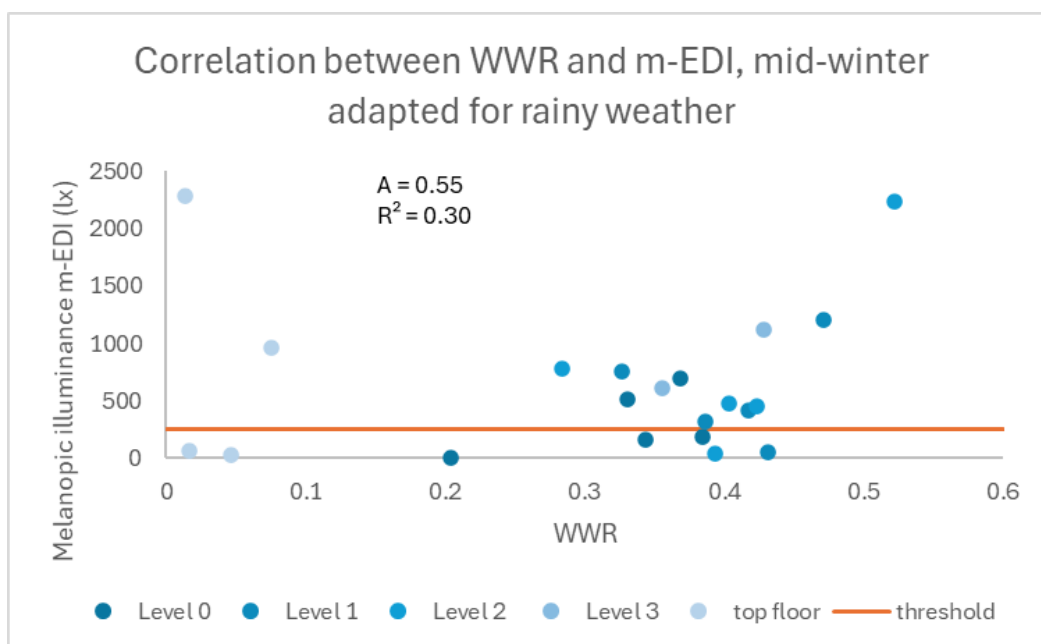
21.00-8.00	8.00-18.00	18.00-21.00
<1 lx m-EDI	≥250 lx m-EDI	<10 lx m-EDI

The circadian lighting results show that indoor circadian lighting availability in urban context is heavily affected by daylight in a clear sky situation, and that the impact of street lighting on indoor circadian lighting can be trespassing the limits described.

The amount of incident light shows to be consistently attaining the mid-day recommendation threshold (250 m-EDI; Brown et al., 2022) for the executed measurements during the full year. This mid-day availability of natural light has shown to have the most effect on the natural dim-light melatonin onset (DLMO; Zerbini et al., 2021). What should be taken into consideration is the scale of variability in daylight availability for clear sky (up to 100 000 lx, reference) to daylight availability for a rainy day (down to 3000 lx, reference): a factor of 0.03. Although this conversion factor is only an indication of the variation that can be found in weather fluctuations, for all measurements on the 20th of December 13.00, this multiplication results in the following values:

Building 1	Building 2	Building 3	Building 4	Building 5
29.3	165.4	184.0	515.7	691.5
515.4	324.1	422.6	1202.7	761.5
453.7	457.6	475.4	2232.9	780.5
x	609.7	1125.1	965.4	66.2
	2283.8	29.2		

For building 1, building 2 and building 3, a lack of circadian lighting on the ground floor level comes forward when compared to the mid-day reference value. Although the measurement values cannot be stated with certainty, this does indicate an effect of the urban building context on the availability of circadian light.



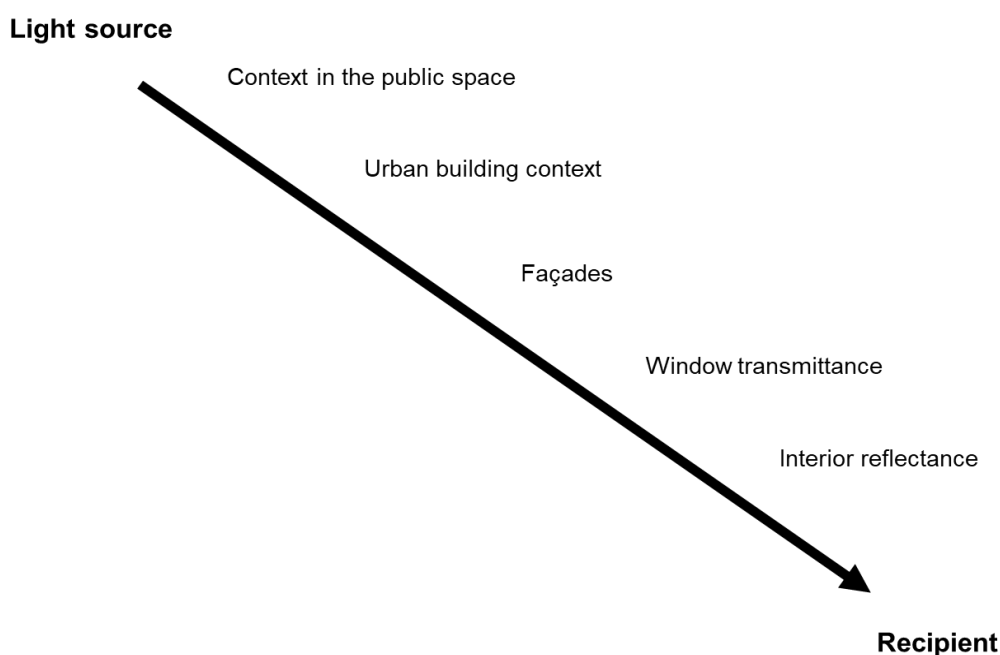
Further, the instability of circadian stimuli due to diurnal patterns has also been shown. This is especially relevant for the morning and evening stimuli, where in summertime, the circadian lighting availability well exceeds the upper limit of the recommended m-EDI, whereas for wintertime, the lighting needs cannot be met in the morning hours. For all buildings analysed, the levels of m-EDI simulated were insufficient for the winter mornings, and were highly surpassing the thresholds in summer evening, when compared to the advisory levels from Brown et al. (2022).

5.1.1. Design factors affecting circadian lighting availability

The factors that have been extracted from the literature affecting the availability of circadian light in homes, from light source to recipient, are:

- Context in the public space;
- Urban building context;
- Façades;
- Window transmittance.

Where façades and window transmittance have been taken as constants for this research. From the theoretical framework, the following scientific parameters have been defined and associated with varying design factors, being intensity, spectrum, timing, duration and contrast.



5.1.1.1. *Urban context reflectance*

The effect of urban context reflectance has shown to have minimal effect on the results of this simulation: affecting the lighting spectrum, the measured variation of reflection is not bigger than the variation that has been found in the 10-time test. The effect of this on the indoor measurements has been hypothesized because earlier research assessing these effects have not been found.

This minimal effect of urban context reflectance on the measured results helps argue that a more detailed representation of the urban context is not necessarily needed for retrieving circadian lighting information on large-scale datasets.

5.1.1.2. *Urban building context*

The effect of the measurements for different levels of detail showed that variations in building shape could especially affect the measurements, and that thus a good representation of the urban context is necessary for executing adequate daylight analyses. Next to that, the five-building analysis shows a first indication of the effect that urban building context can have on the availability of light on lower levels.

Due to the limited scale of executed measurements, a correlation between different urban building design factors and circadian lighting analysis cannot be retrieved. For this, scaling the dataset will be necessary. This could potentially provide information regarding the impact of urban design by street profiles and context building height on indoor circadian light availability.

5.1.2. What design recommendations can be derived from the assessment of the impact of façade design and lighting design on circadian health in urban context?

5.1.2.1. *Light source*

What has been found, is that the design of city lighting is capable of strongly affecting the circadian lighting surplus found in homes. Scientific factors that are affecting the availability of m-EDI inside are all five: intensity, spectrum, duration, timing and contrast. Design factors that are shown to affect the availability of melanopic equivalent daylight illuminance are window size, lamp distance and lamp luminance. From the literature review, a fourth design suggestion is posed and can be associated with street lighting: designing with spectral tuning. With spectral tuning, the SPD of the lamp is adapted to the melanopic sensitivity of humans, without altering the colour temperature or illumination of the visible light. The effect of spectral tuning has been assessed, and although variations in intensity have shown to directly correlate with the measured results, the effect of variations in spectra have not been returning significant differences in results. Eminent is that not only the test for the SPD correlated with lowered melanopic impact has not been found, but that the results were also almost unaffected by the reference spectral power distribution. Further research to the impact of spectral tuning could be done. As the measurements with test persons have been proven to affect the circadian emulation significantly (reference), additional tests with other software would be suggested.

The intensity of the light source has been found to directly affect the availability of circadian light at night and thus potentially disrupting the circadian rhythm of the recipient. For situations where the lamp is close to the façade (building 1) These levels of m-EDI highly surpass the reference values posed by Brown et al. (2022) for the closest floor level to the lamp post. For small streets, the buildings opposite to the lamp post are also within range of returning values exceeding the maximum melanopic illuminance (building 5). The difference in results between buildings with street lighting nearby (building 1, 4 and 5) and buildings of which street lighting

is placed further up in the street (building 2, and 3) is notable. The placement of lantern posts in the street influences the nighttime disruption of inhabitants.

Next to that, the distance to the lamp post affects the floor level at which the highest m-EDI is measured. Having street lighting near your home thus negatively affect the circadian health when you are near the point of measurement in evenings and at night. Municipalities can be kept responsible for this, and solutions can be found in multiple ways:

1. Spectral tuning: Although not proven with this model, real-time measurements have shown that spectral tuning could positively influence the circadian impact of light. This is further to be researched.
2. Lighting orientation: Although this study has taken the lighting orientation as a constant factor, orientation of light fixtures might help for street lighting where the distance to the other side of the street is high (example building 5). For the small streets of Amsterdam, this will not be an option as the power of the light is high enough to disrupt opposites of the street.
3. Lighting placement: The height of the light affects where the light is most disruptive. In situations where sleeping happens on higher floors and living happens on the ground floor, a design suggestion would be to place the light fixtures lower to the ground, as the disruption on the circadian pattern will be minimized.

5.1.2.2. Façade (orientation, window to wall ratio)

Where urban designers have the capability to influence artificial light and even pose rules and regulations on street profile and building height, architectural designers must adapt their design to optimize the influence of natural light, given the situation of the context. This limits the scientific parameters that are within the scope of influence of the designer. Façade design and building orientation can help find the solution to the shortages and surpluses of circadian lighting availability by daylight.

From this thesis, a correlation between the WWR and the availability of incident circadian light measured inside is found. Next to that, high variations between seasons are measured and differences between floor levels and indoor circadian lighting availability is found. To counteract this effect, the results from this workflow can give an incentive to design WWR differently for each floor level to compensate for the light blocking of the urban context. A further development of the 3D window construction method would allow for large-scale data analysis, and thus finding stronger connections between the impact of orientation and window placement on the availability of indoor circadian light.

5.2. limitations

To argue whether the approach of this research has been successful, multiple limitations that affect the quality of the result are described using the four-phase classification as used in the thesis. The limitations have been structured per phase.

5.2.1. Phase 1

Translation between file types & programs:

with no sufficient method to translate data from GIS to Rhino, a simple method has been used: multiple points from the BAG dataset (GIS) and the 3DBAG dataset (Rhino) have been used

as reference points for manually scaling other datasets to the right location. Although this method is considered acceptable, it limits the automation of the workflow and without human interference, accuracy of relative placement can be guaranteed even better.

Quality of source data

This thesis relies on open data, and thus relies on the quality of sources available. For this phase, 3D BAG and BGT is used, two national databases with high accuracy.

3D bag uses multiple sources for generating a high accuracy for their 3D building models. The inputs for LoD 1.0, 1.1 and 1.2 are all retrieved from BAG, where the representation of the building is based on “the outline of the building as the projection of the building as seen from above” (3DBAG, 2024) BAG has a positional data accuracy of 30cm. For the higher levels of detail, 3DBAG relies on airborne laser scanning, with an average point density of 8 per square meter. With these datasets, the 3D models are generated. The accuracy of this building generation is stated in the quality attribute that is assigned per building. The categorical attribute is set to true if the building reconstruction is considered reliable when it:

- shows no overlap with other buildings;
- The Val3Dity validation test returns no errors (Val3Dity “verifies whether a 3D primitive respects the definition as given in ISO19107 and GML/CityGML” (Val3Dity, 2024));
- The point cloud selection is insufficient (outdated or with insufficient data points).

If this quality attribute returns positive, the building is considered of sufficient accuracy. For the scope of this project, the quality of 3DBAG is assumed sufficient, but the mention of the inaccuracy values of their source information is relevant for taking the accuracy of window placement into consideration.

BGT is a collection of 2d surface information within the Rijksdriehoek Coordinate System (EPSG:28992), managed by Kadaster in the automated purveyance (LV). The LV brings together the BGT data supplied by source holders (*BGT Toelichting Controles*, 2023). The supply of data is thus outsourced to unknown parties. The LV follows an extensive list of control factors, but explicit accuracy values are not given. For this thesis, insufficient BGT data could be affecting the results due to reflectance impact, but as contextual reflectance values are assumed constant and their impact is found to be minimal, this accuracy is considered sufficient.

Due to the multi-disciplinary approach of this circadian lighting analysis method, the transition through scales provides accuracy limitations. A false assumption of the geometry close to the measurement point affects the results highly, whereas a rougher estimate of the geometry on further distance is impacting the results barely. Besides that, the impact of decision making by human behaviour significantly alters the level of accuracy when closer to the measurement point (curtains, movement, interior design, and reflectance), which cannot be taken into consideration for this static model. The data uncertainty close to the measurement point should be minimised to find robust data that leaves the impact of human behaviour out of scope.

5.2.2. Phase 2

This phase relies fully on the façade masks derived by Eijgenstein (2020). The accuracy of the façade masks that have been implemented in this thesis is hard to define, as the source information (panoramic imaging) has a large 2-dimensional relative accuracy, but distortion of the image and overlay of obstacles between the building and the camera are hard to recognise (Dang, 2023). Another issue that has not been mentioned in the literature regarding these

masks, is the effect of scale that follows from assigning the 2-dimensional picture to a single plane. When calculating the window area and with this the window-to-wall ratio, the angle of the façade is assumed to be parallel with the photo. What is not considered is how both window shapes and façade elements are distorted if this is not the case, and thus an inaccurate window-to wall ratio is calculated. With projecting the window shapes onto the 3D building elements, this distorted representation of the window is approaching real-time window shapes better than the information of just the 2D data could provide: the convergence of these sources of information generates more information than the addition of individual elements.

The WWR per floor information provides a first good representation of the actual situation, and with the knowledge of window count per floor, the actual situation can be approached quite closely. Still, the actual shapes of the window are not fully predictable, and in case of extreme variation in window shape and size within one floor level, the averages will not represent the actual situation closely at all.

The availability of façade masks is a limit for scalability of the framework. Although the retrieval of the façade masks is automated and thus scalable, errors have been filtered manually, and blemishes in façade pictures make that not all facades are retrievable. This could be improved by running the script on more sets of street images, but a full coverage of data cannot be guaranteed. A second problem that arises with the method of Kingenstein, is the lack of multiple façade masks per building. With this method, only facades that are visible from the street position are retrievable, and even when this regards multiple facades, these have not been taken into consideration.

Making a good estimate of other façades will stay complicated with the limitations of open data. In many cases, the other façade will be oriented towards a private garden. Trying to retrieve this information in other ways (drone imaging, drone LiDAR imaging) might be considered invasive. The information of window placement on street-oriented facades will still be highly relevant. Next to the means this façade information is used for this thesis, this information could also be used for energy estimations, street safety (van Asten, 2021) and urban design decision-making (placement of city furniture, trees)



The window information forms the basis of the indoor floor level estimation. With this, two assumptions are made: there where a window is, there cannot be a floor, and between window two groups of windows, the floor will be at 1/3 of the distance between the window groups, measured from the top of the lower window. As further information regarding floor level placement is lacking, this assumption cannot be checked, but with the accuracy of the data, it can be considered a good estimation.

5.2.3. Phase 3

In this phase, the Grasshopper environment has been used to make adaptations in the 3d building environment. Grasshopper's visual programming interface, while powerful, lacks the same degree of robustness and flexibility seen in traditional coding environments, and it proved to result in serious complexity for elaborate data structures. Small changes to the hierarchy of data trees, such as incorrect path mapping or unintentional changes in list length, can result in unintended outputs, often requiring significant effort to trace and correct. This makes that this method is not so robust when using new datasets. Scaling from single building to multiple buildings has led to consistent errors with data misalignment, where tree structures and CSV data tree hierarchy gets simplified or structured in manners different than needed.

With the window boundary reconstruction, multiple issues were faced to tackle the placement in 3D space. For this, two methods have been elaborately assessed:

- Grouping façade 3D façade elements based on normal direction and closeness to the street;
- Selection of visible facades with the Grasshopper Make2D algorithm, returning visible elements

With clustering the facades based on their normal direction and comparing this with the normal direction from the centre of the building to the street, a high consistency in results was found. A limit was the visible facades from the street that were not parallel to the street, but still visible, resulting in holes in the projection of the facade. This method has thus been considered insufficient.

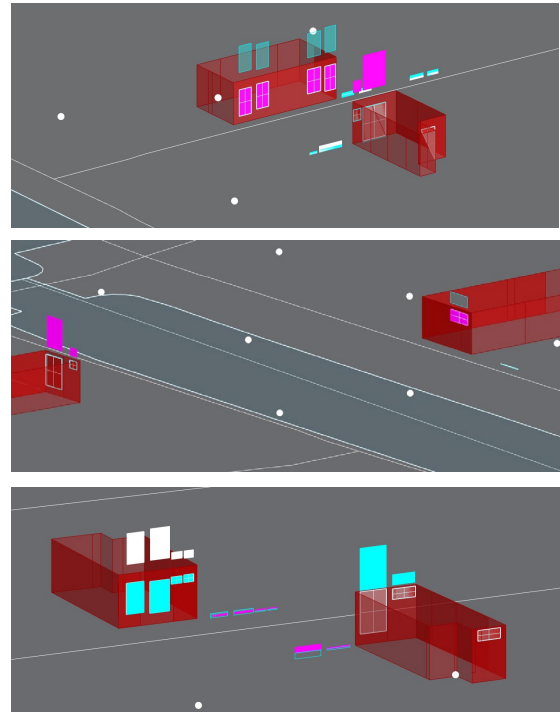


Figure 5-1 Four versions of boundary reconstruction are needed to find correct window placement for different façade orientations

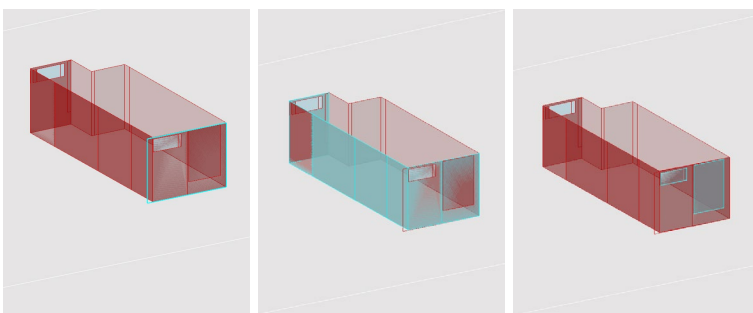


Figure 5-3 When using the make2D algorithm a false façade edge is taken into account.

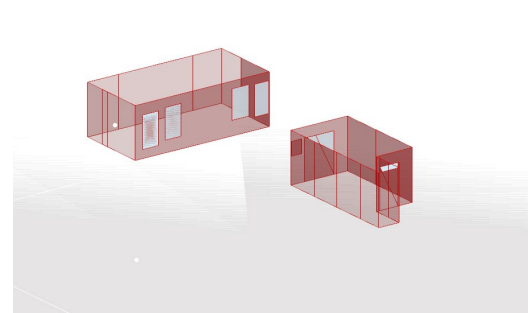


Figure 5-3 Extracting window boundaries shows good results.

The second and final method makes use of the Grasshopper Make2D algorithm. This is an algorithm to project 3d elements to a 2D plane, designed for display. This make2D algorithm simplifies geometries to curves and returns the indices of the curves that are visible from the point of view. With this method, all visible elements from the closest street point could be derived, and a projection of the window boundaries could be executed. One issue that arose with the make2D algorithm is the inclusion of the boundary edges. This tool also includes façade elements when the edge of the element is connected to an element that is visible. This results in too many façade elements being considered, as is shown in Figure 5-4.

The 3D window reconstruction by projection is a method that can reach a high level of accuracy. This method is set up to project the pictured windows onto the 3D shapes, which results in a better approach of window areas on façade elements that are non-parallel to the picture orientation. Four different window plane projection methods are needed to cover the variation in orientation and thus relative vector multiplication, as visualised in Figure 5-14. For extracting the window boundaries, this is no issue as all window planes are outside of each other's range and thus no extraction of duplicate windows is done.

For building 1 (ID=363100012179151), a polygon of the roof geometry is invalidated and removed from the building with the window reconstruction, returning a non-closed polygon. This issue is resolvable with single missing polygons, as the 'cap holes' component can cap all planar holes. With multiple missing polygons, the 'cap holes' component will return negative feedback for succeeding, and the geometry should be eliminated as watertightness is fundamental for further analysis.

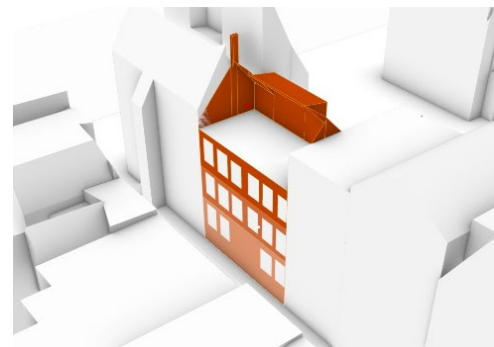


Figure 5-4 invalid geometry

5.2.4. Phase 4

The retrieved circadian lighting analysis show a direction of the impact of the different measures, but due to simplifications in the model and the constants considered, the difference of the values with the real-time situation can vary strongly. For all these variables, a good approach is estimated, but variations of up to 25 percent for indoor reflectance, up to 300% for different weather conditions and variations in window transmittance affect the robustness of the results. Next to that, the strong variation in SPD that occurs with natural light is not included in this model. This is due to a lack of

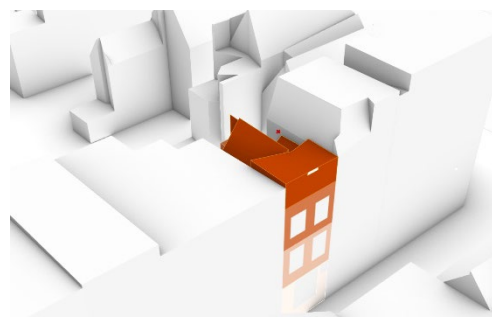


Figure 5-5 measurement point outside of the building

accessible simulation options. This might strongly affect the simulation results, especially around dusk and dawn. Implementation of this daylight SPD variation would be a strong recommendation for further research. Finally, the measurement points and the measurement samples are discussed. The measurement placement resulted in one situation in a measurement point outside of the geometry. This points towards a mistake in floor level placement, as this means that the distance between floor and roof is less than 1.2m.

With the measurements executed, little can be said about the actual impact on the natural rhythm of humans. For this, a full range of measurements should be executed. This is an option within the workflow, but due to calculation time and data management it has been opted to not further investigate the day-to-day impact of circadian light.

5.3. future research

Building on the foundation of this research, several follow-up steps can be suggested of which the most immediate concern is to identify an appropriate method for scaling this workflow. While serial processing with Grasshopper data trees has shown results that prospect large-scale execution to be feasible, a method incorporating parallel processing is strongly recommended to achieve serious improvements in efficiency and complexity of the model.

In terms of scaling the workflow for large datasets, a reliable method has yet to be found. Two approaches were tested—Hops and maintaining Grasshopper tree structures—with mixed results:

- Using the Hops method shows promise as it allows external files, including other Grasshopper scripts, to be referenced. It supports iterative execution and parallel processing, which improves calculation times. The workflow has been tested; however, issues arose when running non-native applications within the referenced Grasshopper script, many of which are fundamental to the workflow. While upgrading from Rhino 7 to Rhino 8 resolved some issues, new problems surfaced since other essential plugins like LARK and RhinoCityJSON have not yet been adapted to the new version.
- Grasshopper's robust data structuring options make using data trees the most straightforward to implement. However, it requires simulations to be executed consecutively, which results in long program freezes during complex calculations. While feasible, the combination of high-level tree structures and long calculation times—especially for geometrical and daylight simulations—has significantly slowed the development process, a limitation that could not be overcome within the time constraints of this research.

Further recommendations include exploring Python integration via Rhino Inside, as well as the Grasshopper Pollination tool for parallel computation. In addition, further research could focus on the following areas:

- **Data Retrieval for Façade Information:** The integration of detailed façade information in 3D modelling could benefit many fields of study. While the current picture-based workflow is robust, it requires further refinement to generate more reliable data. One improvement could involve validating the process using additional images of the same façade, such as by incorporating historical façade images or employing drone scanning for an alternative perspective. Enhancing this workflow is crucial for scaling it to handle larger datasets efficiently.
- **CityGML Compliance:** With further validation, the 3D model generated through this research could be transformed into a richer dataset compliant with the international CityGML standard.
- **Development of a clean method for GIS-3D Model Integration:** Establishing a standard for communication between GIS files and 3D models, particularly for Rhino and Rhino Grasshopper, would greatly facilitate cross-platform compatibility.

For large-scale circadian lighting analysis, the following recommendations should be considered, assuming the necessary geometry is available:

- Spectral Power Distribution Variation: Future research should examine how spectral power distribution varies throughout the day, particularly during the transitions between day and night, which are crucial for circadian rhythm simulation. Capturing these variations more accurately could improve the model's emulation of natural light conditions.
- Time-Specific Analysis: A more detailed analysis around dusk and dawn would also be beneficial. The current research focuses on seasonal extremes, which return expectedly extreme values. However, investigating morning light availability could reveal how lighting conditions vary across the year and how buildings respond to these changes. This could provide insights into urban and façade design by identifying when lighting sufficiency begins to diminish.

Depending on the analysis, different 3D file formats may be more suitable. For some purposes, exporting as an object file or a Rhino 3Dmodel format might be ideal for ease of use. However, for future applications, it is recommended to save these geometries in the CityJSON format, which, according to the literature, offers the cleanest and most comprehensive way to store complex, multi-feature objects.

5.4. design implications

The lessons that can be retrieved from this thesis are aimed at two actor groups that have the ability to affect the circadian light availability, other than the recipient themselves.

5.4.1. urban planning

the literature shows the positive correlation between levels of ALAN and delayed bedtime, and a negative correlation between levels of ALAN and sleep duration, impacting a broad range of health issues (Gaston & Sánchez De Miguel, 2022). With the placement, luminance and possible the SPD of street lighting, the urban planner can affect the impact of circadian disruption in urban context. If there are possibilities at lowering the lamp positioning, lower luminance levels are possible to provide sufficient illumination on street level and less light nuisance will be generated. Further investigation on spectral tuning for street lighting would be suggested, as the literature proved strong correlations between the effect of spectrally tuned lighting and circadian health.

For urban planners, the use of the workflow designed in this thesis could be beneficial. By implementing the wished placement, luminance and SPD in the tool, this workflow could be used to check for the impact of the placement of a light source in urban context on surrounding buildings. Awareness of the effect on health of inhabitants will help prevent negative design consequences.

Next to the placement of street lighting urban planners can learn from the results generated for existing buildings for designing street profiles.

5.4.2. architectural design

For a designer, the information that is gathered on the correlation between window size and indoor circadian lighting analysis can help make design decisions. With an indication that lower floor levels could have more negative effects of urban building context, designers could adapt their window size for different floor levels, with lower levels needing a bigger WWR to attain similar circadian lighting indoors.

For existing buildings, the transmittance of window materials could be adapted to the needs of the different

These two design options are not capable of mitigating the seasonal effects of circadian lighting, but will help attain sufficient circadian lighting values indoors, when daylight is coming short. For mitigating the seasonal effects of indoor circadian lighting availability, balancing building orientation and window size could be an interesting direction. This model has not shown the effect of building orientation due to the limited size of measurements, but for further suggestions an optimal ratio between window size, façade orientation and window transmittance specified for each floor level can optimize indoor circadian lighting.

5.5. Scientific implications

From a scientific perspective, the 3D implementation and the findings of this study contribute to the theoretical knowledge at the intersection of the fields of 3D Geoinformation and Climate Design. It could inspire others to continue in the development of 3D window construction. The methodology that is used has the potential to enrich the current 3D data availability in the field with a new level of detail, which would be of high relevance not only for daylight measurements, but for a broad variety of analyses, of which the urban energy modelling prospects posed by Dang (2023) is one.

6. Conclusion

6.1. Problem summary

Correctly timed lighting availability is essential for human health. In urban context of the Netherlands, the lighting availability on which humans have developed their sleep-wake pattern is adapted due to the place on earth, design factors that limit the availability of natural light and surplus of artificial light, especially at night. These design choices affect individuals in all buildings that are influenced by these design choices, potentially disrupting our sleep-wake pattern. A large-scale circadian lighting analysis is therefore executed to identify and address these issues in the built environment.

To model the lighting availability in the built environment, an enrichment of the current 3D building models is needed, as window information and floor level placement are fundamental for measuring indoor impact. The development of building models from 3DBAG (2024) form a good basis, and a picture-based solution is found for estimating window placement in urban context by Eijgenstein (2020). This method retrieves window placement but lacks integration in the 3D environment.

For analysing the sufficiency of circadian lighting availability, a metric is posed by Brown et al. (2022), as there are no official regulations in practice.

21.00-8.00	8.00-18.00	18.00-21.00
1 m-EDI	250 m-EDI	10 m-EDI

It is unknown how occupants of existing buildings are affected by the impact of urban context on circadian lighting availability in The Netherlands. Urban planning and building design should prioritize natural light access to support overall well-being, and the effect of artificial light at night should be taken into consideration. This was tackled in the present work by developing a simulation tool that compares indoor circadian lighting availability with the above-mentioned metric.

6.2. Key findings

With this thesis, an answer to the following question is given:

How to design a framework for assessing the impact of façade design and lighting design on circadian health in urban context?

6.2.1. Design factors affecting circadian health

To be able to quantify the circadian light availability in urban context, all disruptions from light source to receiver have an impact. These are visualised in Figure 6-1. To quantify the impact of urban context, indoor properties are of lower relevance, and thus for the factors that are variable for each building in urban context, a large-scale open database is needed.

Light source: with variations in illuminance, distribution of light and spectral power distribution the light source heavily effects the circadian light availability within homes. The difference between natural light and artificial light are pronounced but taking actual spectral power distributions of natural light into account, the impact may vary. For artificial light sources, with a constant SPD the strength of the source directly correlates with the amount of artificial light nuisance. For city centres, street lantern design with spectral tuning, specified for lowering the action spectra associated with circadian stimulation, could be a good option to minimise nuisance.

Context: The urban context affects the availability of daylight, but due to the qualitative nature of this research a correlation has not been found, not for context shape (buildings) as for context reflectance (the effect of water or green spaces on circadian lighting availability).

Façade: The impact of façades on circadian lighting availability has shown a direct correlation, both for artificial light and natural light. As the values of natural light surpassed the minimum boundary for the points in time that were measured, more elaborate timestamps should be analysed to further assess the positive or negative effect of façades.

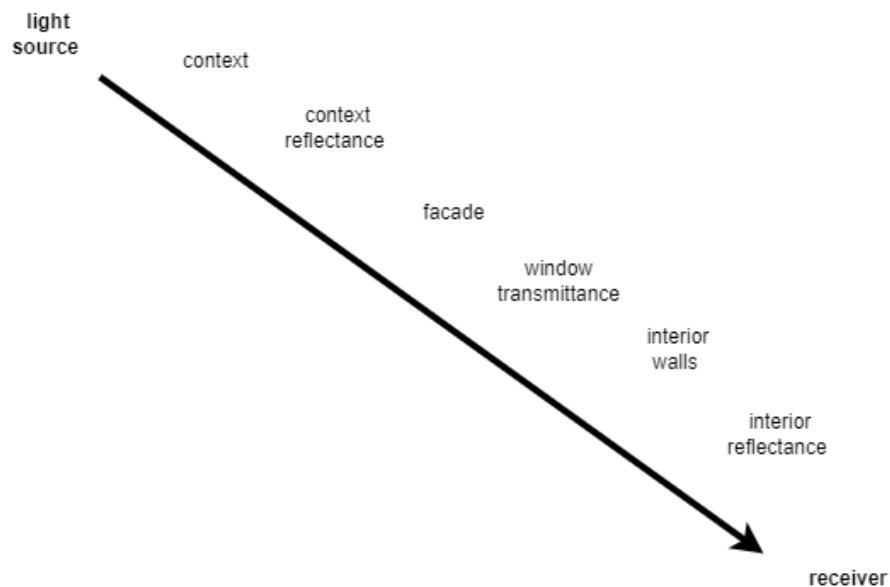


Figure 6-1 factors impacting the circadian lighting availability

6.2.2. Simulating the impact of façade design and urban lighting design

The integration of picture-based data into the 3D environment marks a new step in simulating the impact of façade and urban lighting design on circadian light availability. This method provides a more realistic representation of urban contexts by incorporating actual façade characteristics and window placement. By scaling this process to city- or national-level datasets, the workflow enables accurate analyses of the effect of façades on circadian light exposure. This capability allows for more accurate and context-specific simulations, reflecting variations in building orientation, window-to-wall ratios, and urban lighting configurations. The approach offers flexibility in adapting to different urban scales and typologies, making it applicable to a wide range of urban planning and design projects. The insights gained from this simulation process can support the creation of healthier urban environments by optimizing façade designs and street lighting strategies to enhance indoor circadian light availability across diverse urban contexts.

6.2.3. Design recommendations based on impactful design factors in urban context

It is important for urban planners to consider the non-visual impact of light and opt for lighting with spectral distributions that minimize melanopic effects. The need for street lighting has shown to conflict with limiting artificial light nuisance in the narrow streets of Amsterdam city centre, causing negative health effects on residents. Several types of streetlights have been shown to affect the circadian rhythm, with literature indicating a positive correlation between artificial light at night (ALAN) and delayed bedtimes, and a negative

correlation between ALAN and sleep duration, contributing to a range of health issues (Gaston & Sánchez De Miguel, 2022).

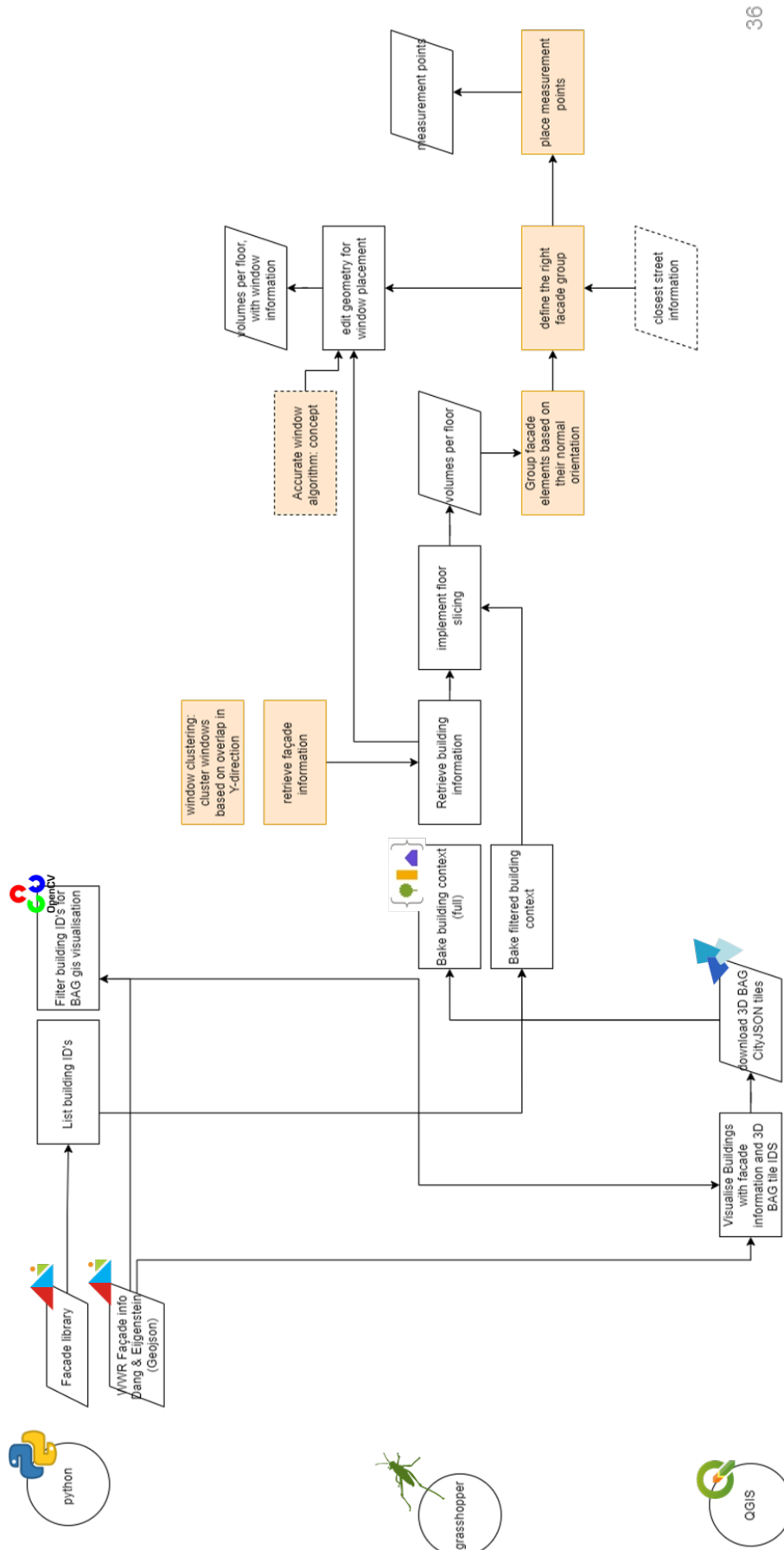
This thesis offers valuable insights for urban planners and architects to design whilst taking circadian light into consideration. Urban planners can influence circadian health by considering the placement, luminance, and spectral power distribution (SPD) of street lighting, an example would be lowering lamp height, which can reduce light nuisance while maintaining sufficient street illumination. Using this thesis' workflow to simulate light source placement can help planners design the street lighting network with minimal negative health impacts on surrounding buildings.

Architects have the possibility to mitigate the effects of urban context on indoor circadian lighting by designing WWR carefully. Within a dense urban context, lower floor levels receive lower circadian lighting. This can be compensated with designing appropriate WWRs for each floor or adapting the transmittance of windows based on floorlevel. These strategies do not address seasonal variations, but implementing the window size, façade orientation, and window transmittance into building design can help design for circadian health.

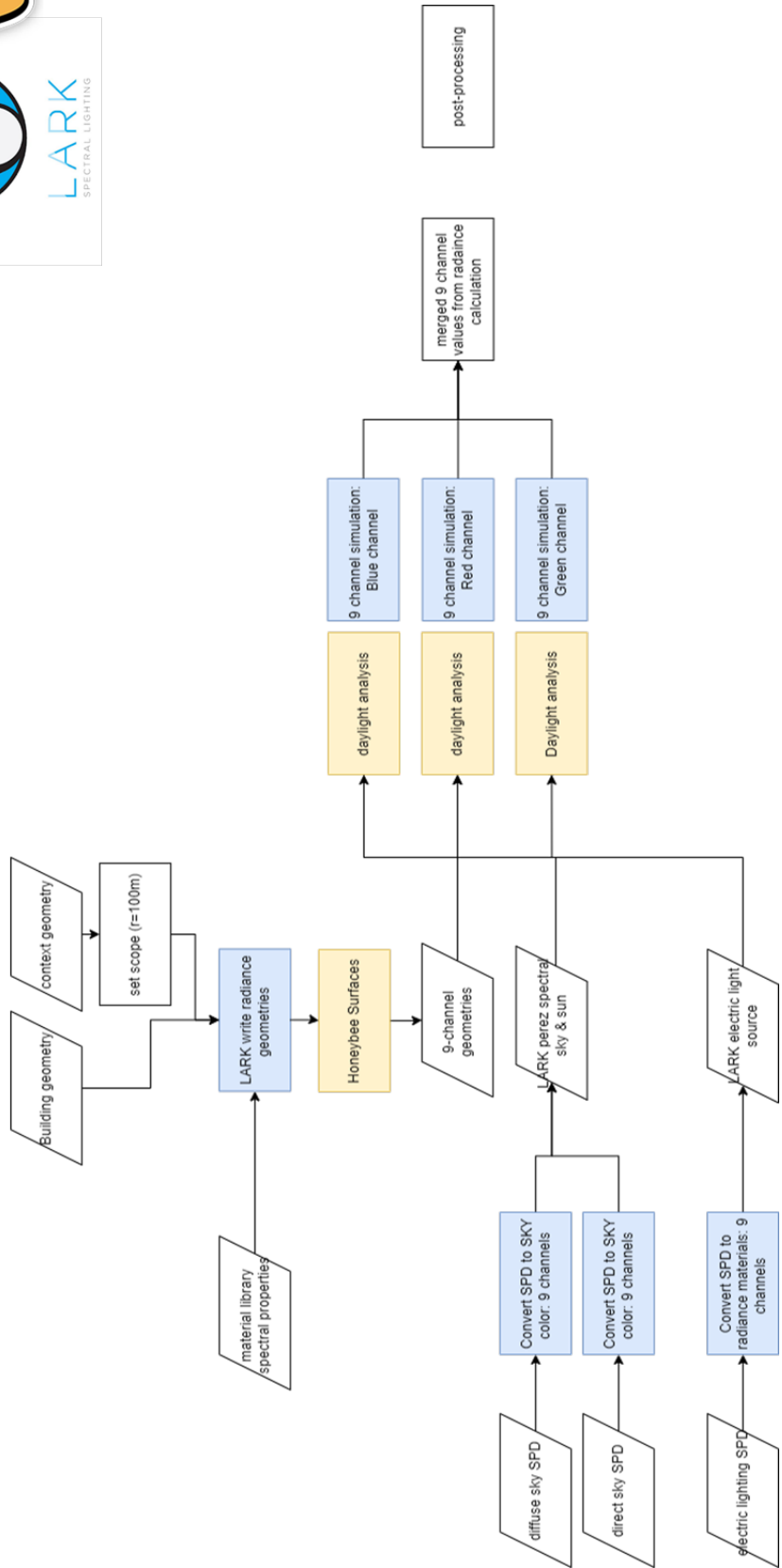
This study bridges 3D Geoinformation and Climate Design, introducing a novel 3D window construction methodology. This can advance not only daylight analysis but also urban energy modelling and other sorts of 3D building analyses, contributing significantly to 3D data availability and future research opportunities.

7. Appendices

7.1. Workflow building preparation (phase 1, 2, 3)



7.2. Workflow circadian lighting analysis (phase 4)



7.3. Material library

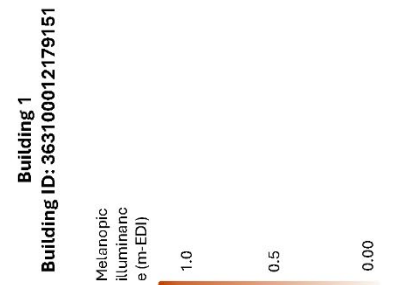
Property	Value	Value	Value	Value	Value	Value	Value
V(λ) Reflectance	12.84%	18.38%	62.96%	88.42%	35.91%	11.96%	10.39%
M(λ) Reflectance	10.53%	17.03%	54.37%	87.47%	25.72%	7.47%	22.14%
M/P Ratio	0.82	0.93	0.86	0.99	0.72	0.62	2.13
Specularity	0.00%	0.27%	0.31%	1.04%	0.00%	0.00%	0.00%
Roughness	0.30	0.20	0.20	0.20	0.00	0.20	0.00
	01137, Dirty brick	01100, Concrete Grey Exterior Floor Tiles	00704, Beige Plaster Wall	00583, White painted ceiling	00434, Wood Maple	01110, Grass	00496, Purplish Blue

Source: SpectralDB (2024)

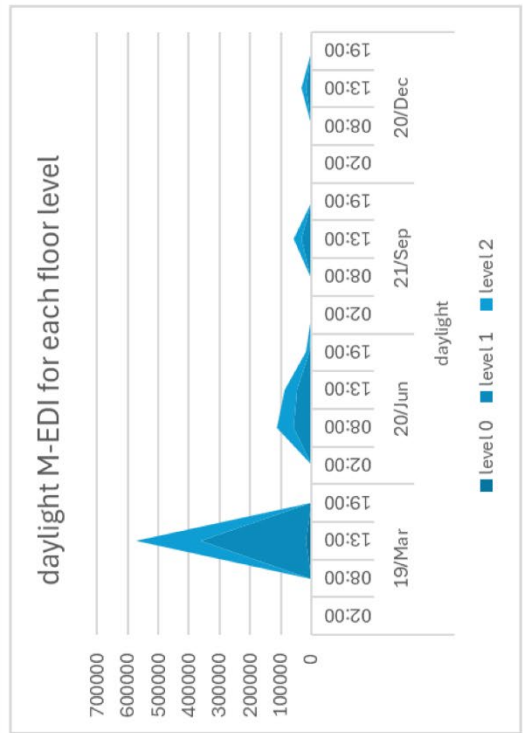
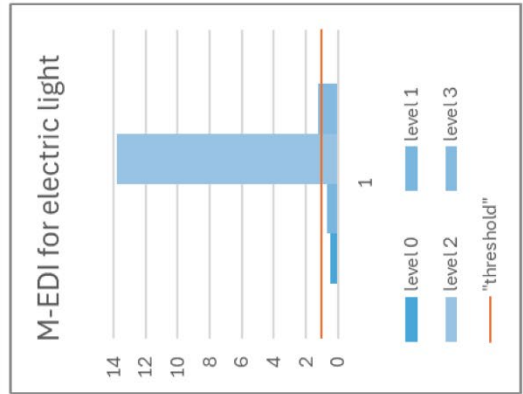
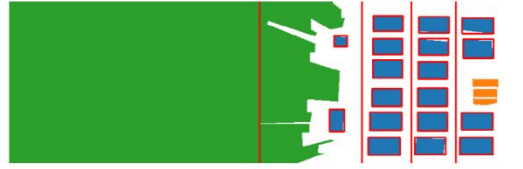
7.4. Example result phase 2

window_ count	indices	boundary	window_placement	avg_win height	floor_ level	ceiling level	floor_ height	avg_sill height	window_ area_ m ²	wall_ area	WWR
4	[0, 1, 2, 3]	[791, 850]	[[183, 797, 33, 53], [226, 795, 27, 55], [57, 794, 30, 55], [14, 791, 30, 58]]	55,25	900	785	115	848.125	6624	32.53 2	0.2036
6	[4, 5, 6, 7, 8, 9]	[712, 772]	[[227, 719, 28, 53], [146, 718, 30, 51], [188, 719, 29, 52], [98, 717, 32, 52], [55, 717, 33, 52], [14, 712, 30, 54]]	52	785	706	78	768	9522	22.09 8	0.4309
6	[10, 11, 12, 13, 14, 15]	[630, 691]	[[230, 639, 27, 52], [189, 638, 28, 52], [148, 638, 32, 52], [98, 637, 31, 52], [56, 633, 32, 56], [13, 630, 31, 56]]	53	706	619	87	687	9664	24.57 3	0.3932
2	[16, 17]	[562, 593]	[[203, 570, 19, 23], [54, 562, 39, 26]]	24,5	619	439.0	180	589.75	1451	50.79 9	0.0285

7.5. Test simulation setup



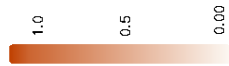
Floor level	WWR	electric		daylight		20 June		21 Sept		20 Dec							
		19 March	20 June	19 March	20 June	02.00	08.00	13.00	19.00	02.00	08.00	13.00	19.00				
0	0.203616	0.49	0	125.64	18242.8	0	0	3319.07	2592.92	423.83	0	87.14	1640.05	0	0	978.17	0
1	0.430902	0.67	0	2413.49	344977.2	0	0	55729.88	43285.44	8257.24	0	1633	29384.05	0	0	17180.3	0
2	0.393275	13.76	0	2503.59	208930.8	0	0	54668.61	40509.63	8724.07	0	1652.91	27860.81	0	0	15122.71	0
3	0.028563	1.23	0	18698.16	983701.7	0	0	238478.5	291248.6	69453.5	0	12840.98	187446.4	0	0	102275.9	0



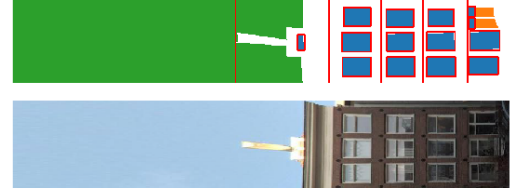
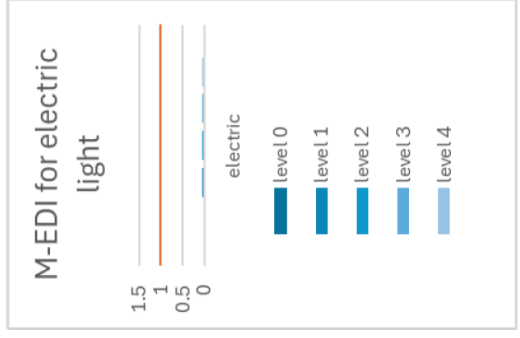
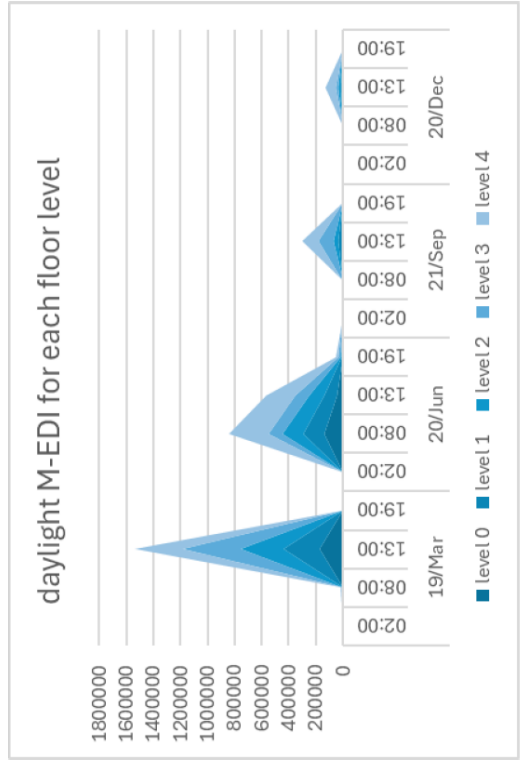


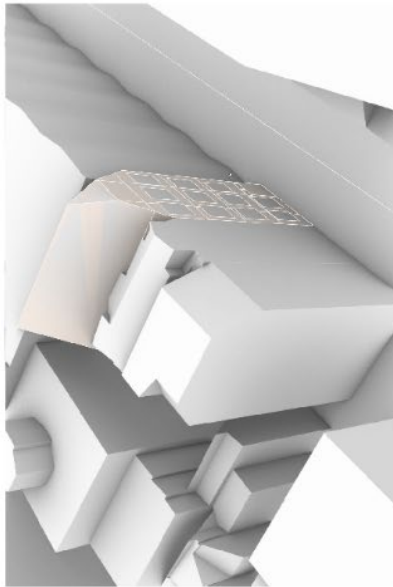
Building 2
Building ID: 363100012179584

Melanopic
 illuminance
 (m-EDI)



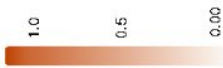
Floor level	WWR	electric		daylight		19 March		20 June		21 Sept		20 Dec					
		02.00	08.00	13.00	19.00	02.00	08.00	13.00	19.00	02.00	08.00	13.00	19.00	02.00	08.00	13.00	19.00
0	0.343463	0	966.03	175508.5	0	0	136093.4	43179.63	3653.86	0	678.34	11831.96	0	0	0	5614.98	0
1	0.366292	0.05	2036.5	253635.1	0	0	155593.6	94377.28	7227.41	0	1380.36	23967.79	0	0	0	10803.27	0
2	0.422829	0.05	2739.47	318462	0	0	154465.8	108760.9	9765.63	0	1837.86	31738.75	0	0	0	15251.63	0
3	0.355169	0.04	3475.84	431336.6	0	0	103305.1	109301.9	12265.52	0	2345.58	111372.7	0	0	0	20324.95	0
4	0.013405	0.04	5454.32	3448936.6	0	0	292389	208667.2	20222.12	0	3696.45	122168	0	0	0	76129.21	0



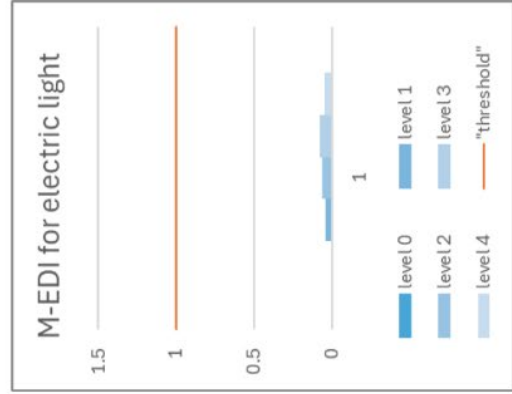
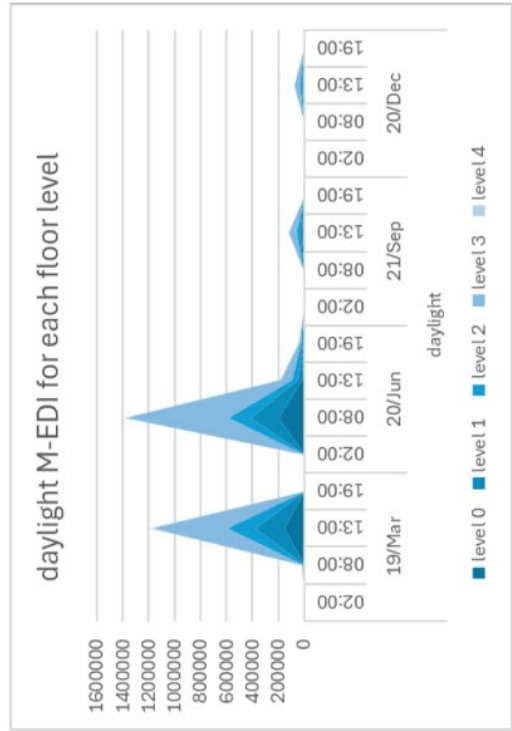


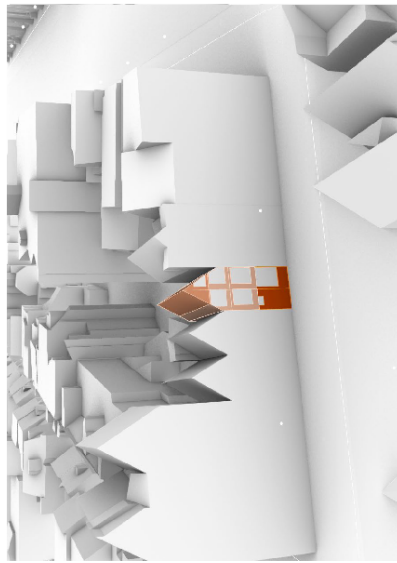
Building 3
Building ID: 363100012179516

Melanopic
 illuminance
 (m-EDI)



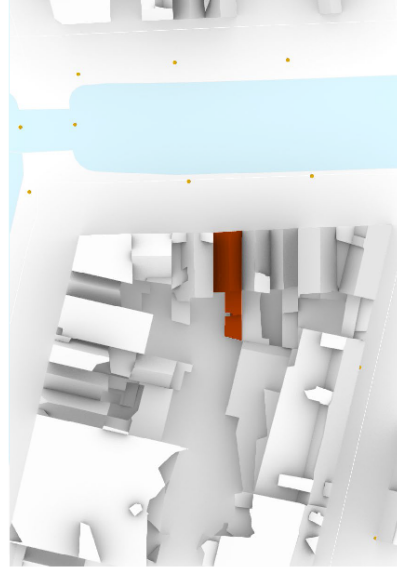
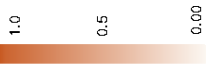
Floor level	WWR	electric		daylight		19 March		20 June		21 Sept		20 Dec					
		02.00	08.00	13.00	19.00	02.00	08.00	13.00	19.00	02.00	08.00	13.00	19.00	02.00	08.00	13.00	19.00
0	0.203516	0.49	125.64	18242.9	0	0	3319.07	2592.92	423.83	0	87.14	1640.06	0	0	978.17	0	0
1	0.430902	0.67	2413.49	344977.2	0	0	58729.89	43285.44	8257.24	0	1633	29384.05	0	0	17180.3	0	0
2	0.393275	13.75	2503.59	208930.8	0	0	54888.61	40509.63	8724.07	0	1652.91	27850.81	0	0	15122.71	0	0
3	0.028563	1.23	18598.16	993701.7	0	0	238478.5	291248.6	69453.5	0	12840.98	187448.4	0	0	102275.9	0	0



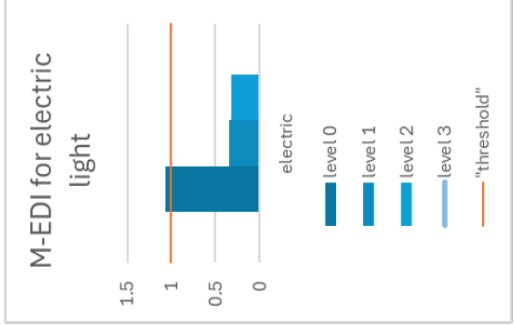
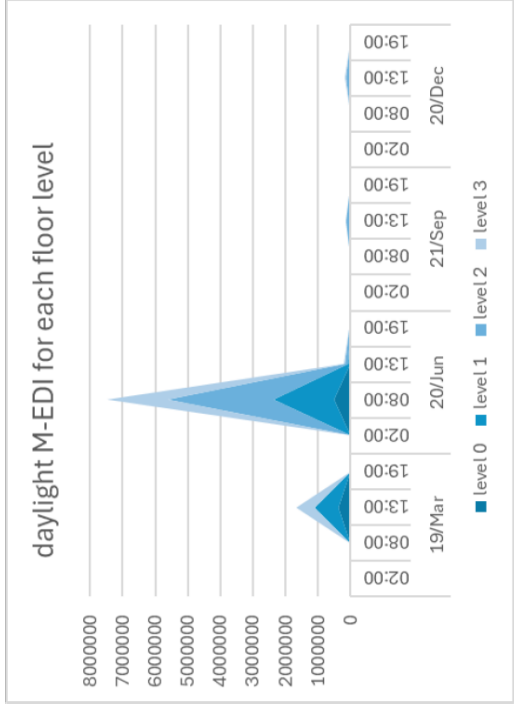


Building 4
Building ID: 363100012180112

Melanopic
illuminance
(m-EDI)



Floor Level	electric		daylight		19 March		20 June		21 Sept		20 Dec		19.00		13.00		06.00	
	WWR		02.00	19.00	08.00	13.00	02.00	08.00	02.00	02.00	02.00	02.00	02.00	02.00	02.00	02.00	02.00	02.00
0	0.330504	1.07	0	0	1400.39	372573.8	0	0	523544.92	25823.99	4579.55	0	0	0	0	0	0	0
1	0.470973	0.34	0	0	3516.47	740420.18	0	0	163156.46	59531.65	11310.67	0	0	0	0	0	0	0
2	0.522152	0.32	0	0	5605.16	129176.46	0	0	325016.46	97629.66	18291.89	0	0	0	0	0	0	0
3	0.075394	0.49	0	0	2011.73	563289.19	0	0	186036.46	36396.18	6769.35	0	0	0	0	0	0	0



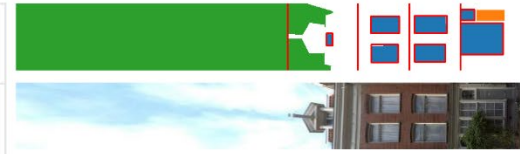
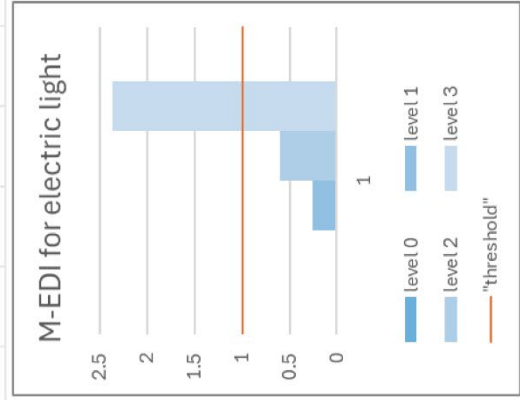
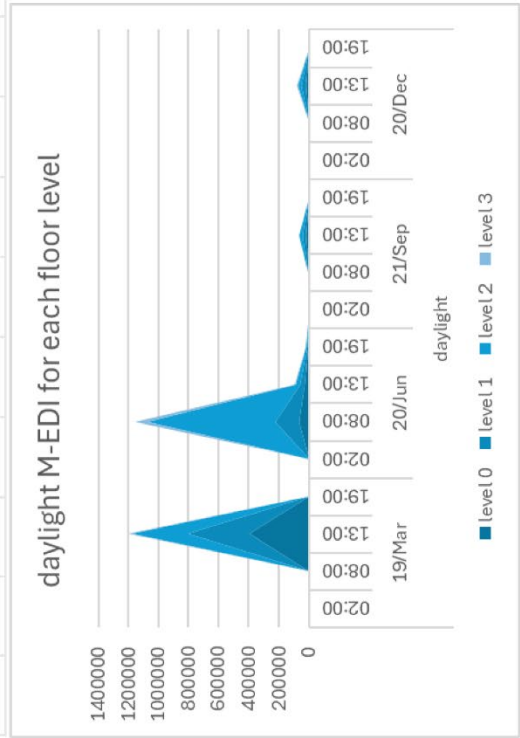


Building 5
Building ID: 363100012179197

Melanopic illuminance (m-EDI)



Floor level	electric		daylight		19 March		20 June		21 September		20 December				
	WWR		02.00	13.00	19.00	02.00	06.00	13.00	19.00	02.00	06.00	13.00	19.00		
0	0.368673	0	0	394275.36	0	62332.38	23796.15	0	4437.29	0	803.64	17047.92	0	23050.08	0
1	0.326225	0.26	0	404321.64	0	162960.08	32057.71	0	6361.54	0	1229.25	21919.13	0	25383.88	0
2	0.284227	0.6	0	2254.72	0	847246.46	34375.59	0	7597.69	0	1495.96	24179.46	0	26015.92	0
3	0.016298	2.37	0	136.56	0	81054.16	2331.83	0	401.52	0	83.41	1492.1	0	2208.6	0



8. Bibliography

- Acosta, I., Campano, M. Á., Leslie, R., & Radetsky, L. (2019). Daylighting design for healthy environments: Analysis of educational spaces for optimal circadian stimulus. *Solar Energy*, *193*, 584–596. <https://doi.org/10.1016/j.solener.2019.10.004>
- ALFA — Solemma. (n.d.). Retrieved 21 October 2024, from <https://www.solemma.com/alfa>
- BGT toelichting controles. (2023). https://www.kadaster.nl/documents/1953498/2770049/BGT_Toelichting_Controlles_v4.03.pdf/13d9988b-5f4a-4ac9-5d52-b22ab52d0b8d?t=1685527790575
- Biljecki, F., Ledoux, H., & Stoter, J. (2016). An improved LOD specification for 3D building models. *Computers, Environment and Urban Systems*, *59*, 25–37. <https://doi.org/10.1016/j.compenvurbsys.2016.04.005>
- Brown, T. M., Brainard, G. C., Cajochen, C., Czeisler, C. A., Hanifin, J. P., Lockley, S. W., Lucas, R. J., Münch, M., O'Hagan, J. B., Peirson, S. N., Price, L. L. A., Roenneberg, T., Schlangen, L. J. M., Skene, D. J., Spitschan, M., Vetter, C., Zee, P. C., & Jr, K. P. W. (2022). Recommendations for daytime, evening, and nighttime indoor light exposure to best support physiology, sleep, and wakefulness in healthy adults. *PLOS Biology*, *20*(3), e3001571. <https://doi.org/10.1371/journal.pbio.3001571>
- Cable, J., Schernhammer, E., Hanlon, E. C., Vetter, C., Cedernaes, J., Makarem, N., Dashti, H. S., Shechter, A., Depner, C., Ingiosi, A., Blume, C., Tan, X., Gottlieb, E., Benedict, C., Cauter, E. V., & St-Onge, M. P. (2021). Sleep and circadian rhythms: Pillars of health—a Keystone Symposia report. *Annals of the New York Academy of Sciences*, *1506*(1), 18–34. <https://doi.org/10.1111/nyas.14661>
- Cai, W., Yue, J., Dai, Q., Hao, L., Lin, Y., Shi, W., Huang, Y., & Wei, M. (2018). The impact of room surface reflectance on corneal illuminance and rule-of-thumb equations for circadian lighting design. *Building and Environment*, *141*, 288–297. Scopus. <https://doi.org/10.1016/j.buildenv.2018.05.056>

- Chellappa, S. L. (2020). Individual differences in light sensitivity affect sleep and circadian rhythms. *Sleep*, 44(2), zsa214. <https://doi.org/10.1093/sleep/zsa214>
- Cie. (2020, November). *CIE User Guide to the alpha-opic Toolbox for implementing CIE S 026*. <https://doi.org/10.25039/S026.2018.UG>
- Circadian emulation | WELL Standard*. (n.d.). Retrieved 31 May 2024, from <https://standard.wellcertified.com/light/circadian-emulation>
- CityJSON Specifications 1.0.1*. (2019, December 9). www.cityjson.org. <https://www.cityjson.org/specs/1.0.1/#city-object>
- Czeisler, C. A., Duffy, J. F., Shanahan, T. L., Brown, E. N., Mitchell, J. F., Rimmer, D. W., Ronda, J. M., Silva, E. J., Allan, J. S., Emens, J. S., Dijk, D. J., & Kronauer, R. E. (1999). Stability, precision, and near-24-hour period of the human circadian pacemaker. *Science (New York, N.Y.)*, 284(5423), 2177–2181. <https://doi.org/10.1126/science.284.5423.2177>
- Dang, M. (2023, January 31). *Estimating Window-to-Wall Ratio for Urban Energy Modelling of Amsterdam centrum by Deep Learning*. <http://amsterdamintelligence.com/posts/estimating-window-to-wall>
- Doorhof, F. (2015). Amsterdam at Night [photo]. <https://frankdoorhof.com/web/2015/04/amsterdam-at-night/>
- Gaston, K. J., & Sánchez De Miguel, A. (2022). Environmental Impacts of Artificial Light at Night. *Annual Review of Environment and Resources*, 47(1), 373–398. <https://doi.org/10.1146/annurev-environ-112420-014438>
- Ghaeili Ardabili, N., Wang, J., & Wang, N. (2023). A systematic literature review: Building window's influence on indoor circadian health. *Renewable and Sustainable Energy Reviews*, 188, 113796. <https://doi.org/10.1016/j.rser.2023.113796>
- Islam, S., & Subasinghe, C. (2022). Denied delights of daylight in density: Optimizing building codes to achieve maximum daylight in apartments of Dhaka, Bangladesh. *Energy for Sustainable Development*, 69, 51–63. <https://doi.org/10.1016/j.esd.2022.04.014>

- IWBI. (n.d.). *Circadian lighting design | WELL Standard—V3*. Retrieved 29 January 2024, from <https://standard.wellcertified.com/v3/light/circadian-lighting-design>
- Jung, B., Cheng, Z., Brennan, M., & Inanici, M. (2023, September 4). *Multispectral lighting simulation approaches for predicting opsin-driven metrics and their application in a neonatal intensive care unit*. 2023 Building Simulation Conference. <https://doi.org/10.26868/25222708.2023.1446>
- Khanh, T. Q., Vinh, T. Q., & Bodrogi, P. (2023). Numerical correlation between non-visual metrics and brightness metrics—Implications for the evaluation of indoor white lighting systems in the photopic range. *Scientific Reports*, 13(1). Scopus. <https://doi.org/10.1038/s41598-023-41371-3>
- Koninkrijksrelaties, M. van B. Z. en. (2018, April 23). *Basisregistratie Grootschalige Topografie—Basisregistraties—Geobasisregistraties* [Webpagina]. Ministerie van Infrastructuur en Milieu. <https://www.geobasisregistraties.nl/basisregistraties/grootschalige-topografie>
- Koster, D. (2023). *Integrating urban context in daylighting simulation: The design consequences in Dutch urban areas, regarding visual & non-visual levels of daylight*. <https://repository.tudelft.nl/islandora/object/uuid%3Aec15c377-36d0-412b-8ace-736db2492a5a>
- Ledoux, H., Arroyo Ogori, K., Kumar, K., Dukai, B., Labetski, A., & Vitalis, S. (2019). CityJSON: A compact and easy-to-use encoding of the CityGML data model. *Open Geospatial Data, Software and Standards*, 4(1), 4. <https://doi.org/10.1186/s40965-019-0064-0>
- Li, S., Zhao, X., Tao, Z., Wei, B., Ding, W., & Dai, Q. (2022). A Simplified Computational Model for Circadian Stimulus Based on Illuminance, Correlated Color Temperature, and Color Rendering Index. *IEEE Photonics Journal*, 14(6), 1–10. IEEE Photonics Journal. <https://doi.org/10.1109/JPHOT.2022.3225427>
- Living Textbook | Spectral reflectance curves | By ITC, University of Twente*. (n.d.). Retrieved 1 September 2024, from <https://ltb.itc.utwente.nl/498/concept/81713>

- López, C. S. P., Sala, M., Tagliabue, L. Ch., Frontini, F., & Bouziri, S. (2016). Solar Radiation and Daylighting Assessment Using the Sky-view Factor (SVF) Analysis as Method to Evaluate Urban Planning Densification Policies Impacts. *Energy Procedia*, 91, 989–996. <https://doi.org/10.1016/j.egypro.2016.06.266>
- Ma, S., Zhou, Y., Gowda, P. H., Dong, J., Zhang, G., Kakani, V. G., Wagle, P., Chen, L., Flynn, K. C., & Jiang, W. (2019). Application of the water-related spectral reflectance indices: A review. *Ecological Indicators*, 98, 68–79. <https://doi.org/10.1016/j.ecolind.2018.10.049>
- Münch, M., Wirz-Justice, A., Brown, S. A., Kantermann, T., Martiny, K., Stefani, O., Vetter, C., Wright, K. P., Wulff, K., & Skene, D. J. (2020). The Role of Daylight for Humans: Gaps in Current Knowledge. *Clocks & Sleep*, 2(1), 61–85. <https://doi.org/10.3390/clockssleep2010008>
- Ohashi, M., Eto, T., Takasu, T., Motomura, Y., & Higuchi, S. (2023). Relationship between Circadian Phase Delay without Morning Light and Phase Advance by Bright Light Exposure the Following Morning. *Clocks & Sleep*, 5(4), Article 4. <https://doi.org/10.3390/clockssleep5040041>
- Paksarian, D., Rudolph, K. E., Stapp, E. K., Dunster, G. P., He, J., Mennitt, D., Hattar, S., Casey, J. A., James, P., & Merikangas, K. R. (2020). Association of Outdoor Artificial Light at Night With Mental Disorders and Sleep Patterns Among US Adolescents. *JAMA Psychiatry*, 77(12), 1266–1275. <https://doi.org/10.1001/jamapsychiatry.2020.1935>
- Releases* · *cityjson/RhinoCityJSON*. (n.d.). GitHub. Retrieved 21 October 2024, from <https://github.com/cityjson/RhinoCityJSON/releases>
- Rights to Light*. (n.d.). GOV.UK. Retrieved 31 May 2024, from <https://www.gov.uk/government/publications/rights-to-light>
- Rijkswaterstaat. (2024a). *Daglichttoetreding: Regels bij nieuwbouw (NEN 2057)* [Webpagina]. Informatiepunt Leefomgeving; Rijkswaterstaat.

- <https://iplo.nl/regelgeving/regels-voor-activiteiten/technische-bouwactiviteit/nieuwbouw/rijksregels/daglichttoetreding-nen-2057/>
- Rijkswaterstaat. (2024b). *Daglichttoetreding: Regels bij nieuwbouw (NEN-EN 17037)* [Webpagina]. Informatiepunt Leefomgeving; Rijkswaterstaat. <https://iplo.nl/regelgeving/regels-voor-activiteiten/technische-bouwactiviteit/nieuwbouw/rijksregels/daglichttoetreding-nen-17037/>
- Souman, J. L., Borra, T., de Goijer, I., Schlangen, L. J. M., Vlaskamp, B. N. S., & Lucassen, M. P. (2018). Spectral Tuning of White Light Allows for Strong Reduction in Melatonin Suppression without Changing Illumination Level or Color Temperature. *Journal of Biological Rhythms*, 33(4), 420–431. <https://doi.org/10.1177/0748730418784041>
- Spitschan, M., Aguirre, G. K., Brainard, D. H., & Sweeney, A. M. (2016). Variation of outdoor illumination as a function of solar elevation and light pollution. *Scientific Reports*, 6(1), Article 1. <https://doi.org/10.1038/srep26756>
- van Asten, T. (2021). *Measuring Natural Surveillance at Scale: An Automated Method for Investigating the Relation Between the 'Eyes on the Street' and Urban Safety*. <https://repository.tudelft.nl/islandora/object/uuid%3A7741ffe9-84f1-4652-8a7b-a26451ddb8db>
- Wirz-Justice, A., Skene, D. J., & Münch, M. (2021). The relevance of daylight for humans. *Biochemical Pharmacology*, 191, 114304. <https://doi.org/10.1016/j.bcp.2020.114304>
- Xu, X., Yuan, L., & Xie, Q. (2022). Circadian Rhythm: Phase Response Curve and Light Entrainment. *Methods in Molecular Biology (Clifton, N.J.)*, 2398, 1–13. https://doi.org/10.1007/978-1-0716-1912-4_1
- Zerbini, G., Winnebeck, E. C., & Meroz, M. (2021). Weekly, seasonal, and chronotype-dependent variation of dim-light melatonin onset. *Journal of Pineal Research*, 70(3). Scopus. <https://doi.org/10.1111/jpi.12723>